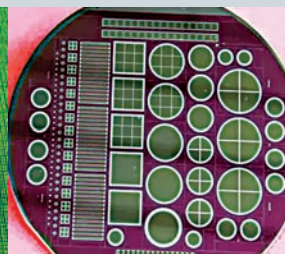
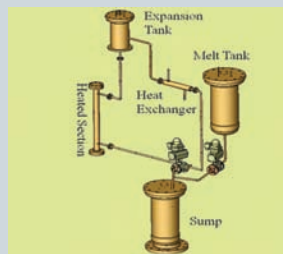




BARC

NEWSLETTER



IN THIS ISSUE

- 62nd Republic Day Address by Dr. Ratan Kumar Sinha, Director, BARC
- Our Gratitude to Dr. Homi J. Bhabha
- Development of Technologically Important Crystals and Devices
- Heavy Liquid Metal Technology Development
- Indigenous Development of Silicon PIN Photodiodes Using a 4" Integrated Circuit Processing Facility
- Development of Room Temperature NH₃ Gas Sensors based on Ultrathin SnO₂ Films
- Development of online radon and thoron monitoring systems for occupational and general environments
- Formal Model Based Methodology for Developing Software for Nuclear Applications
- Development of Digital Radiotherapy Simulator: A Device for Tumour Localization, Radiotherapy Planning and Verification

In the Forthcoming issue

1. **Recent Developments on Radioprotection by Selenium Compounds**
K. Indira Priyadarsini, et al.
2. **Modeling of deformation behaviour of hcp metals using Crystalplasticity Approach**
Apu Sarkar and J.K. Chakravartty
3. **Multi-Detector Environmental Radiation Monitor with Multichannel Data Communication for Indian Environmental Radiation Monitoring Network (IERMON)**
M.D. Patel et al.
4. **Single Phase Flow Simulation of Industrial Scale Agitated Tanks**
K.K. Singh, et al.
5. **Hollow Fibre Liquid Membranes: A Novel Approach for Nuclear Waste Remediation**
S.A. Ansari, et al.
6. **Experiments on reinforced concrete structures; sub-assemblages and components for seismic safety–post installed anchors**
Akanshu Sharma et al.
7. **A Material Transfer System using Automated Guided Vehicles**
R.V. Sakrikar et al.
8. **TB-PCR kit for diagnosis of tuberculosis**
Savita Kulkarni et al.

Contents

<i>Editorial Note</i>	ii
62 nd Republic Day Address by <i>Dr. Ratan Kumar Sinha</i> , Director, BARC	1
Our Gratitude to Dr. Homi J. Bhabha <i>Dr. S.V.K. Rao</i>	13
Technology Development Articles	
Development of Technologically Important Crystals and Devices <i>S.G. Singh et al.</i>	16
Heavy Liquid Metal Technology Development <i>A. Borgohain et al.</i>	28
Indigenous Development of Silicon PIN Photodiodes Using a 4" Integrated Circuit Processing Facility <i>Anita Topkar et al.</i>	34
Development of Room Temperature NH ₃ Gas Sensors based on Ultrathin SnO ₂ Films <i>Sipra Choudhury et al.</i>	39
Development of online radon and thoron monitoring systems for occupational and general environments <i>J.J.Gaware et al.</i>	45
Feature articles	
Formal Model Based Methodology for Developing Software for Nuclear Applications <i>A. Wakankar et al.</i>	52
Development of Digital Radiotherapy Simulator: <i>A Device for Tumour Localization, Radiotherapy Planning and Verification</i> <i>D.C. Kar et al.</i>	63
News and Events	
National Conference on Advances in Nuclear Technology (ADNUTECH 2010): a report	70
DAE-BRNS Workshop on "High Resolution Gamma Ray Spectrometry (HRGS-2010)": a report	72
Workshop on Protection against Sabotage and Vital Area Identification: a report	74
Valedictory function of the Health Physics Training course-15 th Batch: a report	75
National Science Day Celebrations at BARC	77
BARC Scientists Honoured	

62nd Republic Day Address by Dr. Ratan Kumar Sinha, Director, BARC

“Dear colleagues,

My greetings to all of you on the occasion of the 62nd Republic Day of our country. As all of you know, in the year 1950, the Constitution of the sovereign democratic republic of India was adopted and world’s largest democracy was born.

Every year, as a part of this celebration, we salute our national flag. We also remember and salute the members of our armed forces, who provide security to our country.

This function provides us an opportunity to take stock of our achievements during the year. The programmes of our Organisation of more than 15,000 colleagues are extremely diverse and voluminous. Therefore, on this occasion today, I intend to cover only a few representative activities, providing a glimpse of our achievements during the recent past.

Research Reactors

As all of you are aware, last year, two of the research reactors Canadian Indian Reactor (CIRUS) and Dhruva have successfully completed 50 years and 25 years of very productive operation. CIRUS continued to operate at an availability factor of around 87% until December 31, 2010, when the reactor was permanently shut down.

As a part of upgrading the core of the **Apsara**



Dr. Ratan Kumar Sinha, Director, BARC addressing the BARC fraternity

reactor, decommissioning activities of the reactor and reactor systems have already been completed. Demolition of the existing reactor building will commence soon to enable construction of the new building. Detailed engineering of various reactor systems of upgraded Apsara is currently in progress.

Research reactor **Dhruva** has also been taken up for refurbishment and replacement of various equipment and components to ensure its continued high availability.

The Advanced Heavy Water Reactor (AHWR) Critical Facility was operated for various experiments. A mixed pin cluster carrying thorium oxide as well as natural uranium pins was loaded in four different locations of the AHWR Critical Facility. Criticality was achieved with all these loadings and the observed critical height was in close agreement with the estimated critical height. Multiple foils were irradiated to obtain the reaction rates in various energy regions and SAND-II code was used for the spectrum unfolding.

Testing of nuclear detectors in graphite reflector region continued. Moderator level coefficient measurements were carried out and observed values matched with predicted ones. Reactivity measurement due to loading of a cluster containing Thoria and Uranium pins was carried out satisfactorily. Facility was also utilised for large volume sample irradiations for Neutron Activation Analysis (NAA).

The conceptual design of a **High Flux Research Reactor (HFRR)** to be built at our new campus at Vizag, has been completed. HFRR is designed primarily to meet the large requirements of high specific activity radioisotopes and to provide enhanced facilities for basic research in frontier areas of science and for applied research related to development and testing of nuclear fuel and reactor materials.

Advanced Heavy Water Reactor (AHWR)

The AHWR Thermal hydraulic Test Facility (ATTF) is being setup at R&D Center, Tarapur, in collaboration with Nuclear Power Corporation of India Ltd. (NPCIL), to establish thermal and stability margins as well as to test the fuelling machine at prototypical conditions. The various work modules of the project like civil, mechanical, electrical, instrumentation and

control are at an advanced stage of execution.

Thermal hydraulic analysis of AHWR with Low Enriched Uranium (LEU) was carried out to estimate the thermal margin. It was found that adequate thermal margin exists with LEU in the AHWR core. A feasibility study was also carried out for the power uprating of AHWR using pumped circulation with LEU.

In order to reduce the plutonium requirements of the AHWR initial core, various options of partial loading of AHWR initial core were studied. Detailed studies related to AHWR equilibrium core with Th-LEU fuel for a target burnup of 60 GWd/te were carried out. An initial core with LEU fuel has been designed with desirable operational features during refueling and transition to the equilibrium core.

The design of the secondary shut down system of AHWR was modified to have eight injection tubes at two elevations. The jet dynamics was modeled using an indigenously developed methodology and the worths were estimated.

Compact High Temperature Reactor (CHTR) and 600 MWth High Temperature Reactor (HTR) for Hydrogen Production

Solid modeling of CHTR systems and components was completed. CHTR fuel rod simulator costing about 1% of the imported option was developed. Fabrication of molten salt loop and corrosion test facility for high temperature reactor application has been completed.

The challenging task of treating the double heterogeneity effect created by lumping the fuel into particles and those into pebbles has been done using the Reactivity equivalent Physical Transform (RPT) method. The results were compared with reference results from Monte

Carlo simulation of a pebble, in which double heterogeneity has been treated explicitly.

CHTR physics design simulations were performed with new design modifications such as use of thinner control rods for finer control, Reduction in the available locations (18 to 12) for control rod etc. Efforts were made to minimise the single CR worth at criticality by varying the content of burnable poison.

Study of Thorium utilisation in Pressurised Water Reactors

A study of possibility of thorium utilisation in a Pressurised Water Reactor (PWR) was made by considering the (Th-LEU (19.75% U-235))MOX fuel. PWR cores fuelled with thorium using different fissile compositions were studied.

LWR studies

An updated WIMS library in 172 groups has been generated in-house with burn-up chain extended up to ^{252}Cf . This library contains 185 nuclides and resonance integral tabulation for 48 resonant nuclides, including several minor actinides with temperature extended up to 2500°K . This library has performed successfully for the VVER simulations.

Fuel development and supply

BARC has the responsibility of supplying plutonium bearing fuels for the Fast Reactor Programme, including Fast Breeder Test Reactor (FBTR) and Prototype Fast Breeder Reactor (PFBR) (under construction) at Kalpakkam.

For the production of U-Pu mixed carbide fuel pins for FBTR, new technologies like Laser welding for the fuel pin end-plug closure and Laser engraving unit for fuel pin numbering have

been qualified and are being inducted into the production line.

The regular production of Mixed Oxide (MOX) fuel pins for PFBR has started at Advanced Fuel Fabrication Facility (AFFF) and a new fuel pin welding line has been recently commissioned. The experimental PFBR MOX fuel being irradiated at FBTR has now reached a burn-up of 107,000 MWd/T, exceeding the design target burn-up of 100,000 MWd/T.

BARC is also involved in R&D on metallic fuel for the advanced fast breeder reactors with high breeding ratio. Thermophysical properties like phase transition temperatures, solidus temperature and eutectic temperature between U-15%Pu fuel and T-91 cladding has been determined. A glove box train consisting of injection casting, demoulding and eddy current inspection of fuel slugs has been set up at Atomic Fuels Division (AFD)

For the AHWR Fuel Fabrication mock-up facility project, radiation resistance remote viewing system has been developed indigenously for hot cell and shielded enclosure applications for AHWR fuel fabrication.

Based on the post irradiation examination of the thoria-4%plutonia mixed oxide fuel elements, two of the intact fuel elements were certified to be fit for re-irradiation in CIRUS reactor. These two fuel elements, along with fresh fuel elements containing thoria-8%plutonia of AHWR fuel design, manufactured at AFFF, were reconstituted into an irradiation rig and loaded into CIRUS for irradiation. This exercise has helped us to arrive at the procedure for quality assurance for reloading and re-irradiation of experimental fuels in the test loops of research reactor. Both the irradiated pins, despite being

cooled for more than twelve years in the spent fuel storage pool, could withstand the irradiation, till the closure of the CIRUS.

Neutron radiography set-up for irradiated fuel pin at CIRUS was installed and commissioned. After trial runs with unirradiated fuel pin, neutron radiography of irradiated Pressurised Heavy Water Reactor (PHWR) fuel pin and experimental thoria-plutonia MOX fuel pins were carried out. Defects like, fuel cracks, hydriding of clad, and swelling and dislocation of fuel were detected. Details of fuel pin like pellet gap, spring inside the pin at the end were also clearly visible in the neutron radiograph. Decrease in fuel column length was observed in the experimental thoria-plutonia fuel pins having low density pellets. Formation of central void was found in experimental thoria-plutonia MOX high burnup fuel pin.

Detailed post-irradiation examination has been carried out on Zr-2.5Nb-0.5Cu loose fit garter springs, taken out from 10 high flux channels, five each from Kakrapar Atomic Power Station-1 (KAPS-1) and Narora Atomic Power Station-1 (NAPS-1) PHWR reactors. These garter springs were retrieved during the EMCCR operation after around 10.5 Effective Full Power Year (EFPY) of operation.

An indigenous micro-wave heating system (1-6 kW power), adapted and retrofitted to existing hot-cell (without any alteration), was tested. It will be used for the dissolution of irradiated thoria based fuels and materials and also for actinide separation studies of advanced fuels.

Reprocessing and Waste Management

Reprocessing plants at Trombay and Kalpakkam continued to operate safely and satisfactorily. Radioactive wastes generated from nuclear installations both at Trombay & Kalpakkam were

managed safely. In addition, during the year, radioactive wastes generated during partial decommissioning of Apsara was managed quite efficiently.

The development of oblong-shaped metallic melter to achieve higher through-put in waste vitrification process was completed and the unit was commissioned.

As a part of automation programme for plutonium reconversion laboratory, extensive trial runs were taken on rotary vacuum drum filter and continuous screw calciner. Automation of reconversion laboratory, besides increasing the through-put, helps in bringing down the load on operator and man-rem expenditure.

Towards deep geological repository programme, developmental activities were continued. Setting up of an underground research laboratory has been initiated. This laboratory will facilitate conducting various experiments under inactive conditions, such as studying the effect of vitrified waste canister on the host rock, its remote handling aspects, validation of codes for migration of various radio-nuclides, etc.

An incinerator for radioactive solid waste at Radioactive Solid Waste Management Site (RSMS), BARC, Trombay has been refurbished and commissioned. A volume reduction factor of hundred was achieved and the airborne activity during the incineration was below detection limit, indicating effectiveness of air treatment system.

Installation and testing of Resin Fixation Facility for conditioning of spent resins in polymer matrix is nearing completion at RSMS, Trombay. The facility has incorporated the process for immobilisation of spent resins in specific cement also.

At Centralised Waste Management Facility (CWMF), Kalpakkam, a new facility for retrieval, volume reduction and disposal of stored pressure tubes has been designed and a work order has been released after obtaining necessary safety clearances. A facility for melt densification has been in continuous use for treatment of plastic/polythene waste. Based upon the experience gained from the facility, a new scaled up facility with certain modification is being set up.

Feasibility studies have been initiated for vitrification of High Level Waste (HLW) from AHWR and Fast Reactor Fuel Cycle Facility (FRFCF) in sodium borosilicate glass matrix. Irradiation of typical sodium borosilicate glass composition to study long term radiation stability of glass matrix with respect to alpha radiation and recoil damage has been completed. Thermal property of acid and molten glass resistant refractory material has been enhanced by addition of bubble alumina.

Further development work is in progress for Cold Crucible Induction Melting technology for vitrification of HLW. Green heating experiments have been carried out successfully. Model-based design of cold crucible for hull melt densification has been completed.

Separation of useful isotopes such as ^{106}Ru , ^{90}Y etc. was continued for supplying these materials for medicinal use. Techniques for quality control of the recovered ^{90}Y were also developed.

An underground research laboratory is being set up in one of the captive sites of the Department. This laboratory will help in conducting various experiments such as study of the effect of heat generating canister on the disposal environment, development of methodologies for emplacement/retrieval of the canister remotely,

validation of various codes for predicting the migration of activity, mechanical stresses in the host rock due to the digging of the tunnel etc.

Health, Safety and Environment

Environmental Studies

Environmental surveys for the baseline studies of the new uranium mining projects at Tummalapalle (A.P.) and new BARC campus at Vizag are currently in progress. Pre-operational survey at new Nuclear Power Plant sites of Hissar in Haryana and Mithivirdi in Gujarat were also initiated.

Studies on assessment of radiological impact of the proposed uranium tailings pond at Seripalli in Nalgonda district of Andhra Pradesh have concluded that the radiological impact of the proposed uranium tailings pond is trivial up to a period of 2000 years and will be of no concern after this period.

A Cone Beam Optical Computed Tomography (CBOCT) system has been designed, developed and tested for obtaining 3-D dose distribution from advanced radiotherapy equipment using polymer gel dosimeter. The facility for preparing polymer gel dosimeter has also been established. The system will be useful for dose verification in radiotherapy.

There was a need for dosimeters in the dose range of 100 to 1000 Gy for low dose applications of food irradiation, especially for mango irradiation. Accordingly, two new dosimeters were developed in the dose range mentioned using i) Glycine & (ii) Lithium formate. These systems being indigenously developed are cost-effective.

Analysis of the data on the effect of radiation on congenital malformations, such as mental retardation (MR) and cleft lip/palate (CLP), using case control methodology, generated under the three year epidemiological study project, has been completed. The results indicate no statistically significant excess relative risks for the occurrence of these malformations attributable to natural background radiation.

Safety studies

BARCOM Test Model for Ultimate Load Capacity Assessment

The 1:4 size BARC Containment (BARCOM) Test Model simulating the 540 MWe PHWR inner containment was subjected to over-pressure test till the first appearance of crack was realised. This occurred at a pressure of 0.2207 MPa, which is 1.56 times its design pressure. The failure initiation was attributed to inelastic strains developed in the discontinuity regions of Main Air Lock and Emergency Air Lock. The data collected during the pressurisation has been compared with analytical predictions reported by various International Round Robin Participants, including that of in-house code ULCA from BARC.

Cyclic Fracture Tests on Narrow Gap Welded (NGW) SS304LN Stainless Steel Pipes

Cyclic fracture tests were conducted to address the concern about the effect of cyclic loading anticipated during a seismic event. Apart from pipes with cracks in base metal; conventionally welded pipes using Submerged Metal Arc Welding (SMAW) and those welded using Hot Wire Pulsed Gas Tungsten Arc Welding (GTAW), with narrow gap were also tested. The investigation has revealed that the Cyclic Tearing and monotonic fracture resistance of narrow gap GTAW is superior to SMAW, supplementing the

other advantages of GTAW, such as lower residual stress and reduced susceptibility to sensitisation.

A supercritical test facility was set up earlier to investigate heat transfer, pressure drop and stability behaviour of supercritical fluids. The facility was earlier operated with supercritical carbon-dioxide up to 90 bar pressure. The facility was modified for operation with Supercritical Water (SCW) up to 250 bars and 400 °C and experiments are going on.

Channel Heat up Studies for PHWR

Pressure Tube is expected to have a circumferential temperature gradient during flow stratification for a small break Loss of Coolant Accident (LOCA) situation in a PHWR. A trial experiment for asymmetric heating (circumferential) of pressure tube for 220 MWe PHWR at atmospheric pressure has been carried out with a 19 Fuel Pin Simulator.

Seismic Qualification of glove boxes

The seismic qualification tests were performed on different configurations of glove boxes viz. single glove box, glove box train and double module glove box. The studies concluded that the glove boxes could safely withstand a ground acceleration of 0.2 g. Necessary modifications have been identified, which would enable them to withstand higher acceleration.

AHWR safety

As a part of demonstration of safety margins available in AHWR, analyses were carried out to identify plant symptoms generated during Beyond Design Basis Event for “decrease in inventory” category. It was shown that, even for the scenario involving a 200% break at inlet header along with un-availability of Emergency core Cooling System (ECCS) and loss of

moderator as a heat sink, symptoms can be identified and sufficient time is available for well defined operator action to prevent fuel temperature excursion.

Physics

CIRUS Reactor has been used for neutron tomography of hydrogen blister in Zircaloy and for neutron based phase contrast imaging of substances embedded inside dense material.

A high power/high energy Nd:Glass laser system of 20 joules and pulse width 300 – 800 pico second with focusable intensity better than 5×10^{14} watts/cm² has been indigenously developed. This laser system has been used to generate shock pressure exceeding 25 Mega bar in several materials.

The performance of the indigenously developed Folded Tandem Ion Accelerator (FOTIA) has been steadily improving. Recently, the proton beam current from this accelerator has reached a high value of 2 micro amp, one of the best values one can get from a low energy accelerator of this type.

Materials and metallurgy

A process for the separation of rare earths comprising of yttrium as major constituent, along with erbium, holmium, ytterbium as minor components from merchant grade phosphoric acid, employing DNPPA+TOPO as synergistic extractant mixture, was developed by selective scrubbing with 40% sulphuric acid. The scrub solution was further subjected to sodium double sulphate precipitation, followed by re-dissolution and oxalate precipitation and conversion to oxide. The rare earth product was purified to > 99%, with respect to sodium by digesting with hot water. Counter-current tests showed overall 90% recovery.

Production of U-metal ingots was continued and utilised for fuel fabrication for research reactors, proposed Sub-critical Facility at Purnima and specific requirements at Metallif Fuels Division (MFD).

Development of tubular solid oxide fuel cell (TSOFC)

Process has been established to fabricate single SOFC cell of tubular configuration (both in anode and cathode supported) through co-isostatic pressing followed by co-firing. Anode supported cell was found to give a maximum of 62 mW.cm⁻² power density when tested at 900 °C. Work is in progress to improve the performance by addressing the issues related to fuel distribution, sealing and current collection of SOFC cell.

Development of catalyst material for decomposition of sulphuric acid in I-S processes for hydrogen production

A process has been developed for bulk preparation of iron oxide based catalyst pebbles for use in the decomposition of sulphuric acid in I-S processes for hydrogen production. The catalyst showed high (~78%) yield for conversion of H₂SO₄ to SO₂ with long run stability. Bulk preparation is under progress for carrying out pilot test in Chemical Technology Division

The stress corrosion crack growth rates in AHWR simulated high purity water at 288 degree C in a recirculating test facility have been successfully established on the materials proposed to be used in AHWR. SS 304L with addition of 0.08 and 0.16 wt% nitrogen were used in sensitized condition and also in as-received materials with 20% warm working (non-sensitized) conditions. These results on our

materials to be used in AHWR provide important inputs about crack growth behaviour of the materials. Stainless steels have been proton irradiated at FOTIA and at PELLETRON at 4.8 MeV and at a temperature of 300 degree C. The Radiation Induced Segregation (RIS) has been successfully characterised using a new approach of electrochemical and atomic force microscopic characterisation.

Lasers and Accelerators

10 MeV Linear Accelerator (Linac)

The depth dose distribution of the electron beam of the 10 MeV RF linear electron accelerator were measured using B3 Radiochromic films. The electron beam has been employed for demonstrating industrial applications towards cross-linking of poly-ethylene rings (more than 1 lakh pieces), diamond coloration, Teflon degradation and production of photoneutrons.

BARC- ECIL RF LINAC

The 9 MeV cargo scanning RF Linac was operated with beam parameters of 9 MeV, 60 mA, 7 microsecond duration at 250 Hz pulse repetition rate. Experiments on electron beam transport and beam focusing at X-ray target were carried out. X-ray spot size of 2.5 mm diameter on the target and a dose of 24 Gy/minute at 1 meter from the target was measured. The X-ray collimator has been developed and installed.

AVLIS programme

The knowledge of the velocity of atomic beam and thermal ion content is important in various processes involved in our AVLIS programme. The experimental measurements of atomic flux, flow velocity and thermal ion content were carried into a 100kW zirconium evaporator using micro-balance and Langmuir probes.

The measurements carried out up to 3270 K at a height of 400 mm were compared with the estimated values for the thermal velocity, terminal Mach number velocity and velocity due to internal conversion of energy from meta-stable energy levels upto 5000cm^{-1} into kinetic energy.

Demonstration of narrow CPT Resonance

As a part of the ongoing programme on generating an ultra precision frequency reference for atomic clock, a coherent population trapping signal with a width of 14 KHz was achieved through use of a special vertical cavity laser with RF modulation and side band generation.

Test Blanket Module (TBM) development for ITER programme

As a part of Test Blanket Module development for Indian ITER programme, joint MHD experiments at high magnetic fields with BARC-IPR Test-sections at Institute of Physics, University of Latvia (IPUL) have commenced and experimental test-sections made of austenitic steels have been tested.

Development of 15 kV, 6 kW Electron Beam Melting Machine

An indigenous 15 kV, 6 kW Electron beam melting machine was designed and developed. This computer controlled machine will be used for production of high purity Uranium and Thorium alloys in the form of buttons, rings and fingers by EB melting and consolidation.

DM&AG

An Autonomous Guided Vehicle (AGV) based Material Transfer System has been developed, which can be used in manufacturing environments for autonomous transfer or

distribution of materials from a supply point to several machining shops. The same solution can also be used for unmanned transfer of radioactive materials in nuclear installations like Board of Radiation & Isotope Technology (BRIT), Nuclear Fuel Complex (NFC), etc. The system autonomously monitors stock levels at the delivery points and initiates appropriate transfers to maintain uniform satisfaction at all delivery points.

ChTG/RMP

Design, development and manufacturing of a prototype batch of Micro Electro Mechanical Systems (MEMS) based pressure and opto-mechanical pressure sensors using micro-nano engineering technology has been successfully completed.

With the successful criticality crossing of a prototype Advanced Multi-section metallic High Speed Rotor, capacity of producing the separative output of the existing machines will be doubled.

About 1800 acres of land in Challekere Taluk of Chitradurga District has been acquired for setting up of Special Material Facility during the XII Plan.

Prototype Tritium monitors based on Bremsstrahlung technique have been successfully developed.

Computational Analysis Division

A five (5) Teraflop High Performance Computing Facility has been set up at the Facility for Electromagnetic Systems (FEMS), BARC, Visakhapatnam. A variety of in-house codes have been parallelized for efficient use of this system. By end-2011, it is proposed to upgrade

this to a 20 Teraflop system.

An electromagnetic coil-gun, accelerating metallic projectiles weighing 30-50 grams to velocities upto 100 meters/sec, has been set up and in regular operation. A 2-D MHD computer code, developed in-house for modelling this gun, has yielded good agreement with experiments, and is being used for optimization. The gun, which yields reproducible results, will be used for studying high velocity impact and penetration phenomena.

Development of Instrumented and Caliper Pipe Inspection Gauges (PIGs)

In continuation with the development of instrumented pigs and caliper pigs for in-line inspection of pipelines, tools for 24" nominal bore pipelines have been integrated and delivered to Indian Oil Corporation (IOC). They are tested in wet evaluation facility of IOC R&D Centre, Faridabad. The instruments use state-of-the-art digital signal processing (DSP) electronics for acquisition and on-line processing of magnetic flux leakage data. 12" instrumented PIG developed earlier is upgraded and successfully run for 200 km of Allahabad-Kanpur section of IOC pipeline. The defect report has been used for repairing severe defects.

Basic Research in Chemistry

An indigenous synthesis of the ligand, MIBI has been developed and used successfully for the preparation of the heart imaging agent, Tc-MIBI complex. Following the approval by the Radiopharmaceutical Committee, the product is currently being marketed by BRIT and supplied to the hospitals of Maharashtra. This is an import substitute and has reduced the cost of the medicine drastically.

A new pyromethene (PM) laser dye, with significantly improved photo-chemical stability than the commercially available dye has been designed. The new dye shows similar lasing efficacy as that of the commercial one, and is currently being considered for use in the U-enrichment programme.

Using Microwave Plasma Chemical Vapour Deposition (CVD) technique, high quality and highly oriented CVD diamond thin films were grown on silicon wafer (1-5 cm² area) to make alpha detectors, configured in the form of metal-insulator-semiconductor hetero-structure. The detectors were successfully tested for alpha sensitivity in air, using electroplated ²³⁸Pu source.

A granular biofilm based process for denitrification of high strength nitrate-bearing effluents generated in the nuclear industry has been developed. Denitrification of upto 12,000 mg/l nitrate was achieved in lab scale bio-reactors. Effluent nitrate/nitrite levels at the end of 24 h cycle time were less than 10 mg/l, which can be safely discharged to the environment.

A biological process is under development for the removal of sulphate from sulphate-bearing barren effluents, such as those produced at Uranium Corporation of India Ltd. (UCIL), Jaduguda. In this method, a series of three bio-reactors employing sulphate reducing bacteria was used to sequentially bring down sulphate concentration from 18,000 ppm to below 100 ppm. Experiments are being conducted to reduce operational cost by making use of cheap carbon sources for the growth of the SRB.

A fuel cell based hydrogen burner has been developed for burning the deuterium formed during chemical decontamination and the deuterium formed in stoichiometric excess in the moderator cover gas during normal operation.

The method consists of a fuel cell and a heated palladium catalyst column as pre-treatment facility for removing oxygen from deuterium. The catalyst column ensures the removal of oxygen from deuterium and the pure deuterium coming from the catalyst column is allowed to pass through the fuel cell, where it combines with oxygen to form D₂O.

Nuclear Agriculture

A new mungbean variety TM-2000-2 (Pairy mung) with early maturity and disease resistance, suitable for rabi and utera (rice fallow) cultivation conditions has been released and notified for Chhattisgarh State. The total number of Trombay crop varieties released and notified by Ministry of Agriculture, Government of India for commercial cultivation has now reached 39. In groundnut, two simple sequence repeat (SSR) markers were found to be tightly linked with rust resistance gene for use in marker assisted breeding.

Rainwater harvesting facility was developed at agricultural farm of Nuclear Agriculture & Bio-Technology Division (NABTD), BARC, Gauribidanur for breeder and nucleus seed production.

45 Nisargaruna solid waste treatment plants were established in various places in the country under the guidance from BARC.

Technology Transfer and (Advanced Knowledge and Rural Technology Implementation) (AKRUTI) programme

Besides filing three international patents, and one national patent based on in-house R&D activities, seven new technologies in the area of safe drinking water, one in medical electronics and one in solid waste management were transferred to industry successfully.

As a part of development of BARC Centre for Incubation of Technology (BARCIT), civil, electrical, air-conditioning work at the five Technology Incubation Cells are in advanced stages of completion and are likely to start the operation by March 2011, under Phase I of the operation of BARCIT.

Among the ten MoUs signed with different organisations during the year, commercial use of KRUSHAK Irradiator, Lasalgaon by Maharashtra State Agriculture and Marketing Board (Pune) and Barge Mounted Sea Water Reverse Osmosis Plant for Production of Drinking Water, by IREL are noteworthy.

BARC has signed seven AKRUTI Tech Pack agreements for deployment of technologies in rural sector. These include four private companies, 2 NGOS and one woman entrepreneur. Tissue Culture Laboratory at AKRUTI-CARD (Centre for Appropriate Rural Development) in Anjangaon-Surji, Amravati has become operational.

Isotope Hydrology based identification of bore well location has been successfully implemented in AKRUTI-CARD (Community Action for Rural Development), Amravati in a water scarce area. The farmers were asked to drill borehole about 60 m deep at the identified site at Anjangaon village, Amravati district, Maharashtra. The borehole is now yielding ~30,000 Litres of water per hour and is a perennial source of good quality drinking water for 5- 6 villages. Encouraged by the success of the model project, six more projects are underway.

Medical Services

As you all know, our BARC hospital, along with its 12 zonal dispensaries caters to more than 87,000 registered beneficiaries, While every

effort is being made to improve our on-line services, two new machines viz., Radial Fluro X-ray machine and Computerised Radiography System have been installed and are being used for needy patients. The newly renovated ward 4A is now made available, along with 18 normal beds, 6 air conditioned beds and 14 emergency beds to the patients. It is also proposed to introduce new dispensary at Kharghar, Navi Mumbai for the convenience of the beneficiaries of Navi Mumbai. Land for this dispensary has already been occupied, and further work is under progress. It will take 3 years for full functioning of this dispensary.

A multiplex polymerase chain reaction (PCR) protocol, involving two genes for detection of tuberculosis, was standardised and validated. It has been given to BRIT for the formulation of a TB detection kit and its commercialisation.

¹⁷⁷-Lu labeled dotatate synthesised in-house is being used for radiotherapy of neuroendocrine tumors at RMC. With the installation of a new Dual Head Gamma Camera, it has become possible to handle more number of cancer patients in RMC now.

XI Plan activities

We are shortly coming to the close of our XIth plan project activities. In order to formulate our programmes for the XIIth plan project, it is essential to critically review our progress and judiciously extrapolate to decide about closing the projects or, if necessary, continuing under the next plan. This process is currently on through various group Boards. Based on the outcome of this activity, we will be in a position to put up new programmes under the next plan. I earnestly appeal to all of you to timely contribute to this process.

Physical Protection

Physical protection of our Centre and its various installations is of paramount importance. I am sure, all my colleagues will understand that the concern of security has further increased in the present time. I strongly urge our Fire Service personnel to maintain a constant vigil on the various establishments of our centre and strive to improve their coordination with security and the concerned Divisions.

I also compliment all officers and staff of our Centre for extending their cooperation with the security personnel in discharging their duties effectively for implementing the higher level of security procedures. Finally, I urge all my colleagues in our Centre to remain vigilant and alert in the present environment.

The contribution made by the personnel of our Landscape & Cosmetics Maintenance Section is aptly demonstrated by the beautiful ambience of this venue.

Conclusion

My dear colleagues, on one hand, we have committed ourselves to be at the frontiers of science and technology at international level. On

the other hand, we also have a commitment to provide benefits of our knowledge and technologies to the Indian society at large, at all levels. You may know very well that it has been our mandate to develop national capability in all areas associated with nuclear sciences and technologies and our fulfillment of this mandate, inspite of an embargo regime, has been the key to make us strong enough to acquire a pronounced international stature. This spirit of self-reliance and development of indigenous solutions must continue. Currently, we are in the process of formulating our ideas for the XII Five Year Plan period. Let us carry out a rigorous analysis of any residual gaps and vulnerabilities and formulate projects and activities to bridge the gaps indigenously.

I am sure, all of you will continue to put in your efforts so as to sustain our tradition of excellence in the years to come.

Friends, therefore, on this very special day, let us firmly resolve and rededicate ourselves to continue our pursuit of excellence in the frontier areas of nuclear science and technology for the betterment of life of our people.

Jai Hind ”.

Our Gratitude to Dr. Homi J. Bhabha

Dr. S.V.K. Rao

(Retd. Head, Ceramics Section, Metallurgy Divn., BARC)



Dr. Homi J. Bhabha

In 1956, I joined the AEET, Atomic Energy Establishment Trombay, (later renamed BARC) in the Metallurgy Division, operating from the Old Yatch Club (OYC) Building near the Gateway of India. This building housed Dr. Bhabha's office, Administrative, Accounts and Purchase Divisional offices and some Labs including the Metallurgy Lab.

The entire BARC campus, as we see now, was non-existent and it was the vision of Dr. Bhabha and his team which has made it possible.

Through my interaction for some 8 years with the Administrative, Accounts and Purchase Divisional staff and with some of the other

Scientists and Engineers in the OYC building, I could gather my impressions about Dr. Bhabha and how he created such a huge Scientific Establishment at Trombay, in such a short time.

Initially the Honourable Prime Minister Pandit Jawaharlal Nehru invited Dr. Bhabha and asked him to plan the entire developmental process of Atomic Energy for power generation and other peaceful applications for India. Dr. Bhabha was given Carte Blanche to put his plan into action.

Dr. Bhabha himself selected a team of well qualified, experienced and very competent Scientists and Engineers representing all the major Scientific and Engineering fields and gave them full freedom to plan, recruit staff, expand and diversify, and set up their R&D Labs and installations. Several newly appointed Scientists and Engineers were deputed to Canada, USA, UK and France to work there and gain experience in operating power reactors. I was fortunate to have been deputed to the Atomic Energy of Canada Ltd. (AECL), where I had the opportunity to carry out research investigations on the development of Ceramic Nuclear Fuels and their irradiation behavior. Dr. Lewis, the Chairman of AECL, was known to be a great friend of Dr. Bhabha from their Cambridge University days and extended training facilities to a large number of Scientists and Engineers from BARC. The CIRUS Research Reactor at BARC is the outcome of this Indo-Canadian co-operation.

Most of the engineering equipment and installations, for large scale Civil Engineering

constructions and infrastructure and sophisticated scientific equipment were acquired for AEET, through the offices of Dr. Bhabha as Secretary, DAE and Chairman/AEC. This expedited the entire process.

Dr. Bhabha identified reputed and well established large private organizations with proven track records, competence and integrity and gave assignments to them for the execution of the jobs. Thus, by a combination of all these factors, he could build such a huge establishment in such a short time.

Dr. Bhabha wanted the R&D labs of all the scientific disciplines to be under one roof, as it would facilitate carrying out multidisciplinary R&D projects. So we were all asked to design our respective Labs on a modular design basis, so that, each module would have all the service facilities. Thus the Modular Laboratories came into being. Dr. Bhabha was particular that the building should not block the view of the Sea, therefore, he wanted it to be raised on pillars. Our Chief Engineer (Civil) and his staff told me, that they went through tense moments of suspense when Dr. Bhabha came and scrutinized the 3- dimensional scale model of the building. He studied the model for a long time silently and seriously and finally gave his approval. He was very fond of Architecture and wanted all the buildings on the campus to be of different geometrical shapes, so that, they did not look stereotyped and boring. The whole campus was landscaped with lavish lawns, flower beds and gardens and thus provided pleasant surroundings.

One of the major steps that Dr. Bhabha had taken was, to delink the Public Service Commission from our staff recruitment programme. He justified this by saying, that scientific work in Atomic Energy areas was of

a very specialized nature and our multidisciplinary qualified Scientists could take care of staff recruitments. Subsequently, the Training School was started in 1957, which has been providing qualified entry level Scientists and Engineers for various programmes and projects of BARC as well as DAE.

Initially the designations of the Scientific staff, to give a few examples, were Junior Scientific Officer, Scientific Officer, Senior Scientific Officer, Principal Scientific Officer and Chief Scientific Officer etc. Dr. Bhabha wanted to create an atmosphere of equality among the scientific community, which wouldn't be rank conscious. To this end, he changed the designations in such a way, that all were Scientific Officers- SOs with only ascending alphabets within brackets, which showed their seniority. Thus they were changed to SO(SC), SO(SD), SO(SE), SO(SF), SO(SG) etc.

Dr. Bhabha was fully aware of the hardships of lack of accommodation, commuting over long distances, and unaffordable medical expenses of a big-city life for new entrants to our organization. He took care of all these problems. He planned a huge township of staff quarters in Anushaktinagar. As this ambitious plan would take several years to complete, he arranged to purchase outright, any group of newly constructed residential buildings put up for sale, wherever available in the city and suburbs. Such groups of buildings were purchased and converted to staff quarters in many locations in the city and suburbs. From all these widely scattered locations, depending on public transport for commuting to the Establishment in Trombay was real hardship. To solve this, Dr. Bhabha had put forth, that in a large establishment with thousands of employees, in case of a nuclear event, the entire staff would have to be vacated very rapidly. This would require a large fleet of

buses on the campus, maintained in running condition. BARC is thus one of the few R&D centres in Mumbai, which offers transport facilities to its employees.

According to Dr. Bhabha, most of the Laboratories handle radioactive materials in an Atomic Energy Establishment and if the staff members get exposed to radiation, despite all precautions, the treatment would require very specialized medical facilities. Eventually a very large centralized full-fledged Hospital was built and set up, with numerous dispensaries in many locations. The entire medical treatment for the staff and their families is highly subsidized.

I can never forget the unfortunate day, January 24th, 1966. On that day in the evening, we were standing outside, opposite the Modular Laboratory, waiting for our buses. I suddenly saw a couple of cars come rapidly and stop on the Mod Labs side of the road. Across the road, I could see Dr. Bhabha and others getting down from their vehicles. Dr. Bhabha was silently looking at the Mod Labs building which was in an advanced stage of construction, as though taking a last look. After observing for a while, they all went away. None of us standing there realized that it was to be our last glimpse of Dr. Bhabha. That night Dr. Bhabha left by an Air India flight to Paris. Next day we were all shattered to see screaming headlines in the newspapers that Air India Flight AI 101 had crashed in Europe by colliding against the snow clad Mount Blanc peak of the Alps and that there were no survivors. In fact, Dr. Bhabha was to take the same flight exactly one day before the previous night, for which he was booked. But due to a mishap in one of the Technical Physics Labs at South Site, Dr. Bhabha had to visit the site and postpone his journey by a day, only to leave by the fateful flight. It was the hand of destiny. It was a great loss of a person who had

done so much for all of us, and for the whole nation.

Thus, today the staff of BARC are housed in decent staff quarters, commute in BARC buses, and have excellent medical facilities and as regards working environment, all the buildings, Labs as well as offices are centrally air conditioned with a beautiful environment of well maintained green lawns, flower beds and gardens. For the scientists, the legacy of Dr. Bhabha continues, which enables them to work in an atmosphere of equal opportunity, encouragement and recognition of merit. Unlike many other Government Departments, our BARC Administrative, Accounts, Purchase, Stores and Security staff are exceptionally sincere, dedicated and very helpful, consistent with the BARC culture and carrying on the legacy of Dr. Bhabha.

After Dr. Bhabha, successive Chairmen of AEC and Directors of BARC, have taken BARC and all the constituent Units under DAE, to greater heights of achievements.

Now after retirement, whenever I interact with our BARC Doctors and staff, the dedicated care, sincerity, courtesy and commitment they show, reminds me of the legacy of Dr. Bhabha. And occasionally whenever I phone our Administration or Accounts, for some clarification, I find that even very senior officers, unlike in many other Govt. Departments, respond promptly with courtesy and sincerity, reflecting the culture inculcated by Dr. Bhabha.

Even today, 21 years after retiring from BARC, all this makes me to continue to be grateful to Dr. Homi J. Bhabha.

Development of Technologically Important Crystals and Devices

S.G. Singh, M. Tyagi, D.G. Desai, A.K. Singh, Babita Tiwari, Shashwati Sen,
A.K. Chauhan and S.C. Gadkari
Technical Physics Division

Abstract

Device-grade single crystals of technologically important materials for use as scintillators in nuclear radiation detection, lasers and optical devices are grown in Crystal Technology Section of the Technical Physics Division. The expertise has been developed to establish crystal growth processes and design and fabricate crystal growth equipment. In addition, single crystals of new materials to be used in neutron and gamma detection are also being studied and developed currently. The processing, characterization and testing of devices are carried out using in-house facilities as well as in collaboration with other Divisions.

Introduction

Though research on nano-materials is in full swing, single crystals are still on the top in vital areas like radiation detection (γ -ray, X-ray, neutron, IR), solid state lasers, optical windows etc, and even in nano technologies like thin films and quantum dots, the substrates used are invariably made from single crystals. Due to their technological importance and denial by developed countries there is a dedicated facility for single crystal growth in BARC (Crystal Technology Section, T.P.D.). Broadly there are three categories of crystals that are of current interest; (i) Scintillator crystals, (ii) Laser host crystals and (iii) Optical crystals. These are grown from melts using Czochralski and Bridgeman techniques for the single crystal growth.

The materials which convert the energy of high energy electromagnetic radiation (short wave length X-ray, gamma-ray, UV) or particles

(electron, proton, alpha etc) into visible light are called scintillator materials and used in radiation detection. Since the discovery of NaI:Tl doped scintillator crystal in 1948 [1], this field developed very fast and presently many brilliant scintillator materials are in fray. Few important scintillators among these are CsI:Tl, $\text{Bi}_4\text{Ge}_3\text{O}_{12}$ (BGO), PbWO_4 (PWO), PbMoO_4 (PMO), CdWO_4 (CWO), ZnWO_4 , Lu_2SiO_5 (LSO), $\text{Lu}_2\text{Si}_2\text{O}_7$, $\text{LaBr}_3\text{:Ce}$, $\text{Li}_6\text{Gd}(\text{BO}_3)_3$ (LGBO), $\text{Li}_2\text{B}_4\text{O}_7$ (LBO), $\text{NaBi}(\text{WO}_4)_2$ (NBW) etc [2-4]. Among these crystals CsI, LGBO, LBO, PMO and NBW are presently being grown in our lab while NaI, PWO and BGO have been grown in the past.

Some oxide and halide crystals doped with rare earth elements (Nd, Yb, Ho etc) are important solid state materials for generating laser light in visible to infrared region. Important among these are $\text{Nd:Y}_3\text{Al}_5\text{O}_{12}$ (Nd-YAG), $\text{Al}_2\text{O}_3\text{:Cr}$ (ruby), double tungstates $\text{NaY}(\text{WO}_4)_2$ (NYW),

$\text{NaGd}(\text{WO}_4)_2$ (NGW), $\text{NaLa}(\text{WO}_4)_2$, NBW, $\text{KY}(\text{WO}_4)_2$, $\text{KGd}(\text{WO}_4)_2$ etc. [5]. Currently, we are involved in the growth of Nd doped NYW and Yb doped NGW crystals. These crystals will be used in the diode-pumped high power q-switched lasers due to their broad absorption and emission bands arising from their disordered structures.

Optical window is a piece (mostly circular but sometimes rectangular, optically flat and parallel disc) of a transparent optical material that allows light (for a wavelength range of interest) into an optical instrument isolated from vacuum or other medium. Highly transparent optical windows in deep UV and IR region are technologically important. The materials to be used in these applications should have large band gap, isotropic and of good mechanical properties. Most popular materials used in optical windows are CaF_2 , LiF, BaF_2 , ZnS etc [6]. At present we are involved in the growth of former three crystals.

Other crystals that have been grown in our lab in the past are lead germanate, Al_2O_3 , YAG, KCl, NaCl and KBr etc.

Crystal Growth Techniques and Instruments

The crystal growth process involves a change of phase, where the molecules of the material gradually, uniformly and continuously lose their random character (in liquid form) and achieve crystalline solid character. Single crystal growth proceeds on a seed crystal (may be of same material) that provides a nucleation center for the growth. In the absence of a seed crystal, it is necessary for a system to super-cool or to attain a certain degree of super-saturation. Such super-saturated solutions are in the metastable states. Due to thermodynamic fluctuations, tiny solids called nuclei emerge when the critical size

of the solid favors the reduction of free energy. This process is known as “nucleation”. Once the system (vapor, melt, or solution) is in thermal equilibrium with its nucleus, the latter is capable of growing by attaching more and more material to it, and this process is termed as “growth”.

There are various methods for the growth of single crystals e.g. melt growth, high temperature solution growth, low temperature solution growth, vapor deposition growth, hydrothermal growth etc. [7]. Nearly 80% of all the single crystals are grown by melt growth techniques. Due to relatively faster growth rates the melt growth is suitable for large scale production. Different techniques employed for the melt growth, are mainly (i) Czochralski technique, (ii) Bridgman technique, (iii) Float Zone technique and (iv) Verneuil technique. Among these Czochralski and Bridgman techniques were used to grow most of the halide and oxide single crystals for materials study as well as for the industrial production. A brief description of these two popular single crystal growth methods is given here.

Czochralski Technique

This technique was first developed by Jan Czochralski (after which it was named), a polish chemist, in 1918 [8]. The Czochralski technique (Cz) is a popular method of crystal growth because it can produce large, dislocation free crystals at a relatively faster rate. In Cz technique crystal is grown by slow pulling of a seed/wire/capillary from the free surface of a melt contained in a crucible. A growth station, to contain crucible and minimizes heat losses (by conduction and radiation), is made using appropriate ceramic tubes, felts, and wools. Material to be grown is melted in the crucible by heating it in a suitable furnace (resistive heating, RF heating, Arc heating). A seed is lowered in

to the melt, and then pulled (at a rate 0.2-5 mm/h) along with rotation (5-25 rpm) at a slow rate after achieving dynamic equilibrium at the solid-melt interface. After the completion of crystal growth with desired length, the process is terminated by suitably adjusting pull rate and temperature at the solid-melt interface. The grown crystal is, then, cooled down to room temperatures at a slow cooling rate suitable for the material.

During the growth the melt temperature is nearly constant in normal conditions (no stoichiometric deviation due decomposition and dissimilar evaporation of melt components). The shape of the crystal can be determined by controlling the diameter of the growing crystal through the manipulation of the melt temperature and pull rate depending on properties of the material under consideration.

Theoretically, every material that melts congruently and does not undergo any phase transition during cooling, can be grown by this technique but there are some practical restraints which put some limits on the material properties which can be grown by this technique [7]. These limits are:

- i) Suitable crucible material (should be unreactive, withstand high temperatures, easy in cleaning, easy in fabrication, e.g. Pt, Ir etc).
- ii) Material should have a low vapor pressure. (Though there are modified methods for the growth of such materials but not very convenient)
- iii) Thermal conductivity of the material should be high (to conduct away the heat released from crystallization at the solid-melt interface).
- iv) Materials in crystalline form should not have pronounced cleavage planes.

Bridgman Technique

This method is based on the work of Bridgman in 1925 [9]. This is a popular technique to grow single crystals of various halides. In this method temperature gradient moves slowly relative to a crucible (vertically or horizontally) until the melt in the crucible solidifies. The main economic advantage of the method is simple basic apparatus, and little operator attention. Disadvantages arise from the contact between container and melt/solid which can give spurious nucleation, sticking of the crystal ingot inside the crucible and consequently generating thermal and mechanical stresses. Therefore to choose appropriate crucible material and its proper processing and design are important considerations. The system consists of two heating zones controlled independently and separated from each other using a baffle to increase the temperature gradient and minimize temperature fluctuations (Fig.1). A crucible containing the material is kept in the upper zone (hot zone) for complete melting then it is slowly lowered (1-5 mm/h) to the lower zone (cold zone) through an optimized temperature gradient until complete solidification.

A modified form of Bridgman method and probably simplest method for directional crystallization is gradient freeze technique. In this method freezing isotherm is moved by slowly reducing the power input to the furnace. The main advantage lies in absence of any movement of either furnace or crucible which eliminates any possibility of vibration or other mechanical problems. Though it is difficult to keep a constant growth rate throughout the crystal growth process due to a relatively small temperature gradient (otherwise temperatures at the top of the furnace will be out of limit), though in some cases it is achievable by a segmented cooling program in accordance with the temperature gradient to keep the rate of movement of freezing

isotherm constant.

Fluorides crystals are grown in vacuum Bridgman furnace which consists of vacuum chamber containing a graphite heater. Electrodes and translation mechanism are isolated from vacuum chamber by different types of sealing. The growth usually commence under high vacuum conditions.

Growth of Single Crystals

Scintillator Crystals

There are two categories of scintillator crystals that are grown at present namely (i) halides (CsI, NaI) and (ii) oxide crystals (PWO, PMO, ZWO, BWO, NBW). Halide crystals are generally grown by Bridgman technique while oxide crystals are grown by Czochralski technique.

Alkali Halide Scintillator Crystals

High quality single crystals of alkali-metal halide material are important as optical elements and as scintillation crystals in various types of radiation detectors. Among these sodium iodide (NaI) and cesium iodide (CsI) activated with thallium occupy important place in gamma-ray spectroscopy and high energy particle detection. Scintillation properties and radiation hardness of these crystals are highly sensitive to crystal growth condition and post growth treatment.

These crystals are generally grown in crucibles of noble-metals (platinum, platinum-alloy, iridium etc.), silica glass or ceramic employing the Bridgman technique. While the noble-metal crucibles are very expensive, the silica glass and ceramic crucibles have several inherent problems such as crucible contamination and the grown crystals adhering to the crucible. Extraction of grown crystals is very difficult and invariably requires an inversion of the ampoule

at high temperatures [10]. Here we describe the growth of cesium iodide crystals up to size of 40 mm diameter and 40 mm length employing two different methods

(i) Using graphite crucibles by vertical Bridgman technique:

Single crystals of cesium iodide were grown in the resin impregnated graphite crucibles [10]. To demonstrate the use of the present method, a graphite crucible that had polished inner surfaces was loaded with the high purity anhydrous CsI (having 0.2% Tl) material and placed in a silica glass ampoule. The ampoule was evacuated and sealed under a pressure of 10^{-2} mbar. A home-built Bridgman crystal growth system (Fig.1) was used that has a three zone furnace operating in the normal ambient conditions by two independently controlled heater elements.

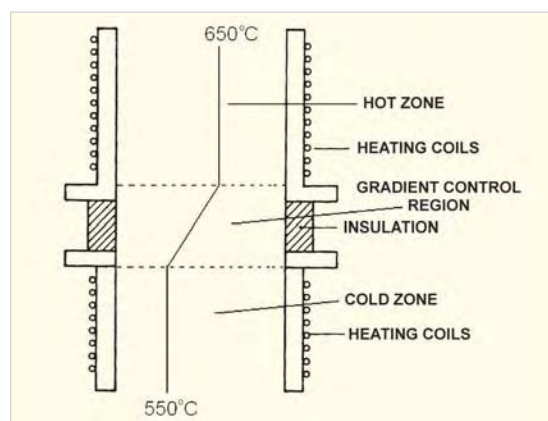


Fig. 1: Schematic of Bridgman furnace for growth of alkali halide crystals.

The crucible sealed in the silica glass ampoule was located in the upper zone and the temperature was raised to about 650°C to melt the material. After attaining equilibrium the ampoule was lowered at a rate of about 1.5 mm/h through a temperature gradient of about 20°C/cm. The lowering was stopped when the crucible in the silica glass ampoule reached the lowest zone and held here at about 550°C for 2 h before

finally cooling down to the room temperature at a rate of about 50°C/h. The silica glass ampoule was cut open and the grown crystal could be easily removed from the graphite crucible. Both, the ampoule and the crucible were reusable for the next several experiments.

(ii) Using carbon coated silica by gradient freeze technique:

A crystal growth furnace has been designed to have a positive temperature gradient from top to bottom. Plot 'a' of Fig. 2 shows the gradient of the furnace with a blank crucible. Temperature profile in the melt is shown in plot 'b' in the figure. Silica crucibles of one inch diameter and having conical bottom were used for the growth. Carbon coating on the inner surfaces of the crucible was carried out by cracking of organic solvents at high temperatures

in an inert ambient. As-coated crucible was then transferred in a vacuum furnace and annealed at 1100°C. High pure (99.995%) and dry CsI and Tl (0.2 mole%) were taken in the carbon coated crucible and sealed under 10^{-3} mbar running vacuum at 200°C. Crucible was then placed inside the furnace on a growth station and temperature of the furnace was raised so that the bottom of the crucible was at 640°C (about 20°C higher than the melting temperature of the CsI). The melt was kept at this temperature for about 4 h and then the furnace was cooled at a rate of 4°C/h until complete solidification of the melt into single crystal. Photograph of a polished CsI:Tl single crystal is shown in Fig. 3.

Though both the methods yielded good quality crystals, the later one is simpler and is more suitable for production of the crystals at industrial levels.

Characterization of grown crystals was done by recording transmission and photoluminescence spectra. Typical transmission and luminescence spectra are shown in Fig. 4. Scintillation properties were tested on a homebuilt gamma spectrometer. Linearity of the pulse height response of a detector fabricated using the grown crystal was checked up to 1332 keV gamma photon. A calibration curve for the detector is shown in

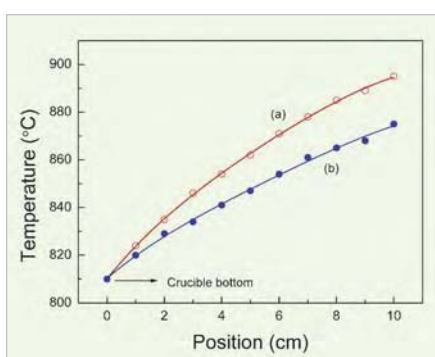


Fig. 2: Temperature gradient of gradient freeze furnace with blank crucible (a) and with crucible containing melt (b).



Fig. 3: Photograph of a polished single crystal of CsI:Tl grown by gradient freeze technique in carbon coated crucible.

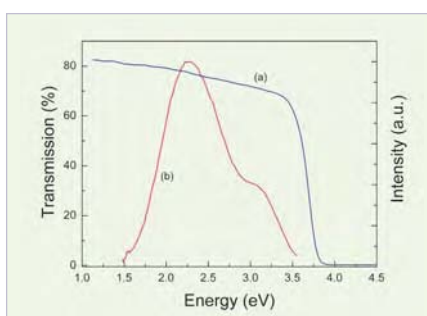


Fig. 4: Transmission (a) and luminescence spectra of CsI:Tl shown in Fig. 3.

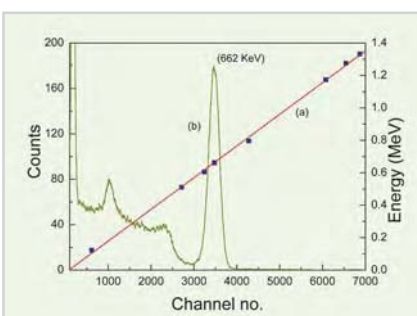


Fig. 5: Calibration line (a) of gamma detector fabricated using crystal shown in fig.3 along with typical gamma spectra of ¹³⁷Cs (b).

Fig. 5 and a typical ^{137}Cs gamma spectrum is shown in the same figure exhibiting an energy resolution of $\sim 7.8\%$ at 662 keV which is comparable to or better than reported values.

Oxide Crystal Scintillators

High density, ultra radiation-hard luminescent oxide crystals are forerunners in the fray for applications in high energy particle detection in ultra high energy particle accelerator like LHC. Search for an ideal scintillator crystal having high density, ultra radiation-hardness, fast decay time, inert to ambient and high light output is going on for the past half century. $\text{Bi}_4\text{Ge}_3\text{O}_{12}$, PbWO_4 , PbMoO_4 , CdWO_4 , ZnWO_4 , $\text{Lu}_2\text{SiO}_5:\text{Ce}$, $\text{Lu}_2\text{Si}_2\text{O}_7:\text{Ce}$, $\text{Li}_{2(1-x)}\text{Y}_{2x}\text{SO}:\text{Ce}$, and $\text{NaBi}(\text{WO}_4)_2$ are a few crystals which fulfill most of the, if not all, properties of an ideal scintillator. Among these $\text{Lu}_2\text{SiO}_5:\text{Ce}$, $\text{Lu}_2\text{Si}_2\text{O}_7:\text{Ce}$, $\text{Li}_{2(1-x)}\text{Y}_{2x}\text{SO}:\text{Ce}$ are the most prominent candidates owing to their high light yield and fast decay constant but their growth is relatively difficult due to their high melting temperatures ($> 2000^\circ\text{C}$). Another drawback is their high cost due to the use of lutetium which is very rare. On the other hand $\text{Bi}_4\text{Ge}_3\text{O}_{12}$, PbWO_4 , PbMoO_4 , and $\text{NaBi}(\text{WO}_4)_2$ are materials that are relatively cheap and have all properties of ideal scintillator except their low light yield which is not a crucial parameter in the high energy physics. These crystals are relatively easy to grow and are very much cost effective therefore can be produced at large scale to be used in large size detector systems.

These crystals are grown by the Czochralski growth technique. For the crystal growth, synthesized polycrystalline material or constituent oxides was taken in a platinum crucible (typically 50 mm diameter and 50 mm height) and was placed inside a growth station. Heating was carried out at a rate of about $100^\circ\text{C}/\text{h}$ until complete melting of the material. The molten material was allowed to soak for 1-2 h at the temperature $30\text{-}50^\circ\text{C}$ above the melting point.

To start the growth process, a seed crystal or a platinum wire in absence of a seed crystal, is used. Seed crystal/Pt wire is slowly lowered to touch the melt surface and allowed there for some time to attain thermal equilibrium with the melt. After that, pulling is started according to predetermined parameters using crystal growth software though initially few changes have to be made manually. The grown crystals are cooled down to room temperatures at a uniform rate (typically $30\text{-}50^\circ\text{C}/\text{h}$) depending on the material.

Various studies have shown some aspects of the complex relation between the crystal growth parameters and the resultant optical properties [11, 12]. The most severe problem during growth is stoichiometric variation due to decomposition of the material at elevated temperature and selective evaporation of the constituent oxides. Coloration, frequent cracking, inclusion, core formation in the grown crystals are the consequences of the stoichiometric variations during the growth. Other reason of the coloration in the crystals could be extrinsic impurities. Growth parameters, related problems and their remedies of individual crystals are as follows.

(i) PbWO_4 (PWO)

Single crystal of lead tungstate grown under normal conditions turned yellowish showing an absorption band at 420 nm. The yellow coloration of PbWO_4 crystals may arise due to the stoichiometric deviation and/or presence of trace impurities in the starting material. In lead tungstate PbO evaporates selectively and single crystal deficient in PbO has various defects related to Pb centers. To compensate for the PbO losses from the melt a known amount of PbO is added in the initial charge. But by conducting several growth runs it was established that stoichiometric deviation is not the only factor responsible for the coloration. It is, thus, apparent

that the coloration is caused by other defects/trace impurities too. Studies have shown that growth ambient also had a pronounced effect on the coloration. Using already crystallized charge and oxygen rich ambient colorless crystal could be grown. A gradual change in color of single crystals from yellow color to colorless in successive experiments is shown in Fig. 6. Cracking problem of this crystal is highly depended on the after-growth cooling rates. A detailed study showed that cracking could be prevented (for crystals having diameter >20 mm) only if the cooling rate was less than 20°C/h. Further, it was found to be independent of the growth direction. We believe that cracking problem in $PbWO_4$ is due to the cleavage planes, which for this crystal is (101), known to get cleaved by application of a very little force.

(ii) $PbMoO_4$ (PMO):

The single crystal growth was carried out by the Czochralski technique, using an automatic diameter-controlled crystal puller (Cyberstar model: Oxypuller). For the growth of 20mm diameter and 50 mm long crystals, a pull rate of 2 mm/h and a crystal rotation rate of 20 rpm were employed [12]. Seed crystal used for the growth was oriented along the c-axis. Cracking and coloration are the major problems faced with the Czochralski growth of PMO crystals. Apart from the cooling rate and orientation the main reason behind cracking of this crystal was found to be the stoichiometry variation during the growth. In lead molybdate, unlike PWO, the selective evaporation of MoO_3 took place which makes crystal Mo deficient.



Fig. 6: Color transformation from yellow to transparent in $PbWO_4$ crystals.

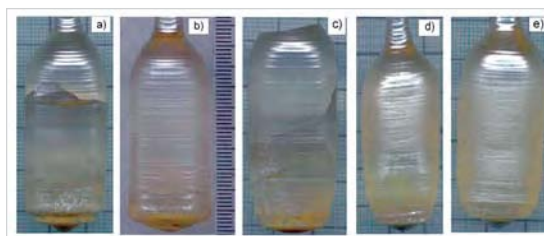


Fig. 7: PMO crystals grown using different stoichiometric starting charges under different ambient: (a) stoichiometric/air, (b) stoichiometric /Ar, (c) 1wt% Pb excess/air, (d) 1wt% Mo excess/air, and (e) 1wt% Mo excess/Ar.

Therefore to grow crack-free crystals one has to take utmost care to compensate for the MoO_3 stoichiometry. Fig. 7 shows the photographs of crystals grown under identical conditions but using starting charges of different compositions and under different ambient viz., (a) stoichiometric/ in air (b) stoichiometric/ in argon, (c) 1% excess of PbO / in air, (d) 1% excess of MoO_3 / in air and (e) 1% excess of MoO_3 / in argon. The photographs show clearly that the crystal having excess of PbO like (a), and (c) shows high density of microcracks. On the other hand, crystals grown using charges of stoichiometric composition in argon ambient (b) or those from charges having an excess of 1% MoO_3 (d) and (e) did not crack either during growth/annealing or on subsequent handling and

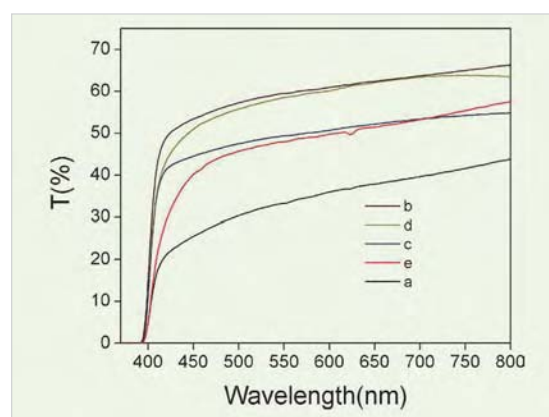


Fig. 8: Transmission spectra of PMO crystals grown using different stoichiometric starting charges: (a) stoichiometric/air, (b) stoichiometric /Ar, (c) 1wt% Pb excess/air, (d) 1wt% Mo excess/air, and (e) 1wt% Mo excess/Ar.

also showed superior transmission characteristics as shown in Fig. 8.

The results show that the crystals grown from charges containing slightly excess of MoO_3 are more resistant to cracking, whereas an excess of Pb promotes the generation of microcracks. This is an important result from the point of crystal cracking which shows that to obtain a crack-free crystal the starting charge must be slightly rich in MoO_3 .

(iii) $\text{NaBi}(\text{WO}_4)_2$ (NBW)

Single crystals of NBW were grown in air by the Czochralski technique employing automatic diameter controlled Cyberstar crystal pullers, having a 50 kW induction heater in Oxypuller model (axial gradient $60^\circ\text{C}/\text{cm}$) and 12 kW molybdenum silicide resistance furnace in TSSG model (axial gradient $6^\circ\text{C}/\text{cm}$). A uniform pull rate of 2 mm/h and a rotation of 15 rpm were employed for growing crystals of 20 mm diameter from the melt contained in 50 mm diameter platinum crucibles. A uniform post growth cooling rate of $40^\circ\text{C}/\text{h}$ was employed in the regular crystal growth experiments. Two types of initial charges were used for the crystal growth; (i) material synthesized by sintering of constituent oxides at 750°C for a total duration of about 100 h, in multiple segments involving grinding and mixing after every 24 h, (ii) transparent crystal chunks of previously grown crystals [13]. Typical photographs of three crystals referred as A, B and C, grown from the two differently prepared starting charges under two different temperature profiles are shown in Fig. 9.

It can be seen that diameter of A-type crystals grown from sintered charge under low gradients ($6^\circ\text{C}/\text{cm}^{-1}$) is not well controlled along with yellow coloration. Though the use of a high temperature gradient was helpful in the precise

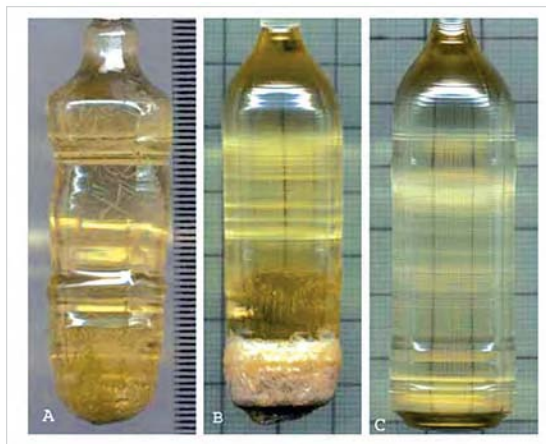


Fig. 9: Photographs of $\text{NaBi}(\text{WO}_4)_2$ crystals grown from 'A': sintered charge under $6^\circ\text{C}/\text{cm}$ gradient, 'B': sintered charge and 'C': re-crystallized charge under $60^\circ\text{C}/\text{cm}$ gradient.

diameter control (crystal B) but coloration still persists in the crystal. Also the segregation of an impurity phase material can be seen at the bottom suggesting the presence of other impure phases along with NBW. This problem was solved by using a charge refined by multiple crystallization and large temperature gradient (crystal C). The C-type crystals show better radiation hardness as compared to the other two types crystals [4].

(iv) BaWO_4

The growth process is somewhat similar to that discussed above for the growth of PbWO_4 crystals. But the problem in this case is the high melting point i.e. 1475°C of the material which is close to softening temperature of the Pt-crucible. The pulling rate was initially fixed at 4 mm/h and a fixed rotation rate of 15 rpm was used. After the growth, crystals were cooled down to room temperature at a constant rate of $30^\circ\text{C}/\text{h}$. The grown crystals were colorless, and did not show any major influence of the ambient i.e. air or oxygen. However, the cracking of crystals, as shown in Fig.10, was frequently observed, and was a matter of concern. In order to investigate this problem, thermal expansion measurements were carried out on the grown crystals [14]. Sample for these measurements

was prepared by carefully cutting the crystal into a rectangular piece of dimension 6.5mm x 4.5mm x 4.0mm having faces parallel to (100), (010) and (001) crystallographic planes. Measurements were carried out using a dilatometer (model-TMA/92 Setaram, France) with a silica probe, in the temperature range 30-1000°C employing a heating rate of 10°C/min in high pure Ar ambient. The results of experiment show that expansion coefficient is quite high in <001> direction compared to that in other two directions i.e. <100> and <010>. Therefore <001> direction was selected for the growth in order to allow maximum expansion in the growth direction and thus keeping isotropic expansion directions in the rotation plane. The cracking was successfully avoided in this manner.

(v) LBO/LGBO

Lithium tetra borate and lithium gadolinium tri borate have elements like Li, B, Gd that have high neutron capture cross-sections and hence can be effectively used in neutron detection and dosimetry. Being low-z materials these are also gamma transparent which is a crucial property for materials to be used as a neutron detector in high gamma background, like reactors. These materials are mostly grown by the CZ method.

LBO has a tendency to go into a glassy phase during the cooling which limits its growth rate.

To avoid the glassy phase a very slow pull rate has to be employed (typically 0.2-0.5 mm/h) therefore to grow a 20 mm diameter and 20 mm length crystal it takes about a week. Another growth related problem in the case of LBO is the core formation which is due to decomposition and selective evaporation of LBO at elevated temperatures.

LBO crystals doped with Cu and Ag were also grown by the Cz method. The doped LBO crystal is an excellent dosimetric material (thermally stimulated as well as optically stimulated luminescence dosimetry) [3]. Typical photographs of doped and undoped crystals are shown in Fig.11.

LGBO is a new material and has potential to be used as a scintillation detector for neutrons when activated with Ce. Its growth is relatively easy compared to LBO. But due to the presence of cleavage planes, cracking in a large size crystal is still an unresolved problem. We have grown crack-free transparent crystal having 12 mm diameter and 40 mm length, as shown in Fig. 12. Research is going on in order to increase the dimensions further

Laser Crystals

Oxide materials like YAG, Al₂O₃, NYW, NGW KYW, KGW are a few of the excellent laser

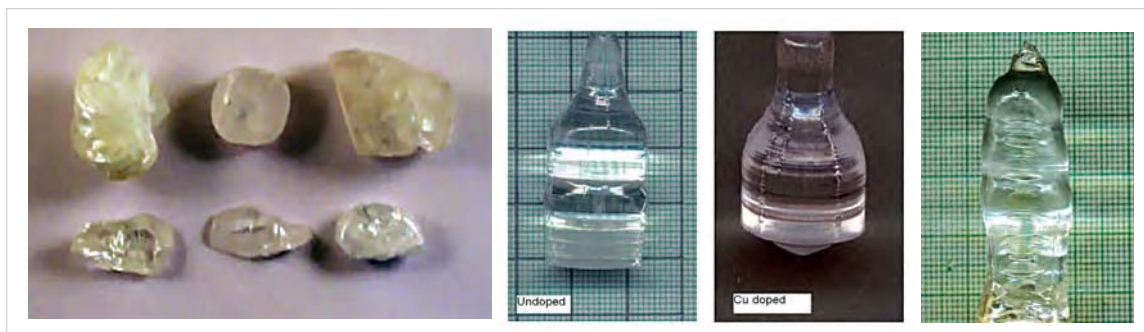


Fig. 10: Photograph of BaWO₄ crystals showing cracks.

Fig. 11: Photographs of LBO single crystals (as-grown).

Fig. 12: Photograph of as-grown single crystal of Li₆Gd(BO₃)₃.

hosts. Here in crystal technology lab we have grown single crystals of NYW, NGW doped with Nd and Yb, respectively. These crystals are grown by the Czochralski techniques (CZ). Growth details and problem encountered during the growth of these crystals are as follows:

(i) $\text{NaY}(\text{WO}_4)_2$ (NYW)

Single crystals of NYW are grown by the CZ technique. The occurrence of compositional changes during the growth of NYW crystals causes instabilities in the mass growth rate and increases the vulnerability of these crystals towards development of cracks. Analysis of different regions of grown crystals and post growth residual charges revealed the presence of excess Y_2O_3 in the upper portion of ingots and excess of Na_2O in the residual charge, in the form of binary compounds of sodium tungstate. Phase purification through recrystallization, as achieved in another double tungstate crystal $\text{NaBi}(\text{WO}_4)_2$, was not effective in NYW, due to a lack of segregation of all foreign components into the melt and decomposition of the material.

The phase diagram of the Na_2WO_4 - $\text{Y}_2(\text{WO}_4)_3$ pseudo-binary system shows that there exists a congruent melting composition corresponding to a 1:1 molar ratio in this systems. However, crystal growth from a congruent melting composition did not yield a good quality crystal and suffered from the above mentioned problems. In our recent work on this material, several off-stoichiometric compositions were prepared along with a stoichiometric compound using a solid-state route and characterized for their thermal and structural behavior using DTA and XRD measurements. Based on results of this study, a suitable composition rich in the $\text{Y}_2(\text{WO}_4)_3$ for the growth of NYW crystal was suggested [15]. Furthermore, crystal growth experiments were carried out on NYW by the

Czochralski technique employing the starting charge rich in $\text{Y}_2(\text{WO}_4)_3$ that rectified all the growth related problems except those which may arise probably due to the anisotropy in thermal properties of the crystal. A polished disc from the grown crystal (undoped) is shown in Fig.13 which shows a good transparency.

(ii) $\text{NaGd}(\text{WO}_4)_2$ (NGW)

Yb doped $\text{NaGd}(\text{WO}_4)_2$ single crystals are important for applications in high power tuned laser sources in the near-infrared region due to their relatively smaller stock-shifts and broad absorption/emission bands. Single crystals of 4% Yb doped $\text{NaGd}(\text{WO}_4)_2$ (NGW) were grown from stoichiometric charges using the Czochralski technique under normal ambient conditions. The grown crystals were transparent with a slight greenish tinge. The coloration of the grown crystals was increased when the same charge was used in the following growth runs by replenishing the drawn amount with an equivalent amount of the fresh charge. After many growth run the leftover charge was analyzed and it was found that it was rich in foreign phases like sodium tungstates and $\text{Na}_5\text{Gd}(\text{WO}_4)_4$. Annealing studies revealed that the oxygen related defects were the main cause behind the coloration. Based on these feedbacks a recrystallized charge was used that yielded less



Fig. 13: Photograph of as-grown single crystal of $\text{NaY}(\text{WO}_4)_2$ (left) and polished disc.

colored crystals. Crystal growth experiments with different ambient are also planned in order to minimize the coloration. Photographs of as-grown crystals and polished disc and cubes are shown in Fig. 14.

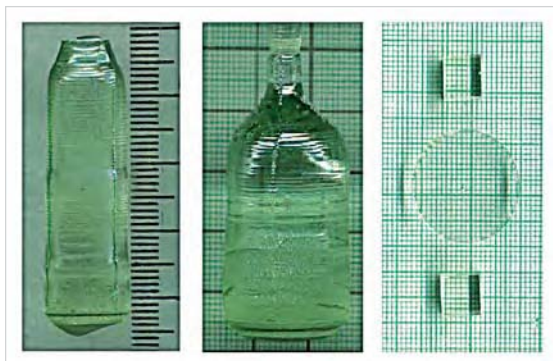


Fig. 14: Photographs of as-grown crystals and polished disc and cubes of $\text{NaGd(WO}_4)_2$.

Transmission and absorption spectra were recorded at room temperatures employing a spectrophotometer in the 200-1100 nm range. The absorption spectrum of Yb was fitted in multi Gaussian peaks centered around 936, 954, 964, 975, 981, 996 and 1010 nm that matched well with the theoretically predicted values [16]. This result also confirmed the quasi three level nature of the $\text{Yb } ^2\text{F}_{7/2} \rightarrow ^2\text{F}_{5/2}$ system.

Optical crystals

Fluoride optical crystals CaF_2 , BaF_2 , LiF are grown using the vacuum Bridgman furnaces. A graphite heater is used for the resistive heating of graphite crucibles containing the material. Lowering mechanism is coupled with the crucible using a Wilson seal. All the systems including growth chamber, electrodes, pulling mechanism are cooled using a complex heat exchanger mechanism.

The growth of these materials is relatively easy though there are few problems which had to be conquered. Even after high vacuum of the order of 10^{-5} mbar, contamination of oxygen during the

growth is the most serious problem in growing high quality device grade fluoride crystals for applications in optics. The oxygen scavenger like PbF_2 that does not affect other optical properties of crystals is used to minimize the oxidation of materials during the growth. Dehydration and proper fluorination are also necessary steps to grow high quality crystals. Fluorination of the material is done in a special furnace which is resistant to HF. Typical photograph of 80 mm diameter LiF (as-grown) and a 50 mm polished disc of CaF_2 is shown in Fig.15.

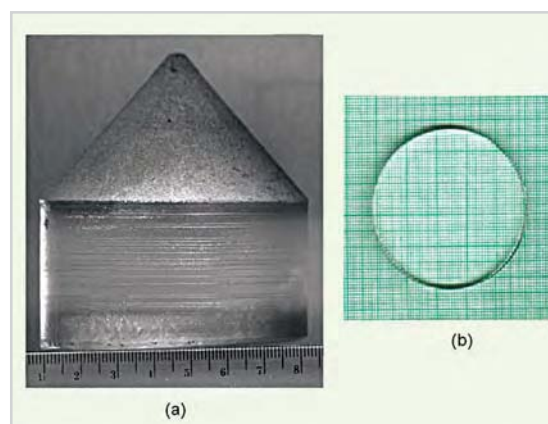


Fig. 15: Photographs of (a) LiF as-grown crystal and (b) polished disc of CaF_2 .

Crystal growth and characterization facilities at CTS

Under the single roof of the crystal technology building, there are several sophisticated crystal growth facilities equipped with advanced Czochralski crystal pullers and indigenously developed high temperature vacuum Bridgman furnaces in the clean-room environments. Photograph having panoramic view of Czochralski pullers and vacuum furnaces are shown in Fig.16 and Fig.17, respectively. In addition, there are various instruments for characterization of grown crystals including powder X-ray diffraction instrument, X-ray fluorescence instrument, photoluminescence spectrometer (200-900 nm), differential thermal



Fig. 16: Photograph of Czochralski crystal puller lab.



Fig. 17: Photograph of vacuum Bridgman furnace lab.

analyzer (50-1750°C), thermo-mechanical analyzer (50-2400°C), in-house developed gamma-ray spectrometer for scintillation testing and thermoluminescence reader and spectrometers. Results of these experiments are used as feedbacks in successive growth runs to develop the device-grade crystals.

References

1. Robert Hofstadter, *Phys. Rev.* 75 (1949) 796-810.
2. S.E. Derenzo, M.J. Weber, E. Bourret-Courchesne, M.K. Klintonberg, *Nucl. Instr. and Meth. A* 505 (2003) 111-117.
3. Babita Tiwari, N.S. Rawat, D.G. Desai, S.G. Singh, M. Tyagi, P. Ratna, S.C. Gadkari, M.S. Kulkarni, *J. Lumin.* 130 (2010) 2076 – 2083.
4. S.G. Singh, Mohit Tyagi, A.K. Singh, S.C. Gadkari, *Nuclear Instrum. Methods In Phys. Res. A* 621 (2010) 111-115.
5. Alexander A. Kaminskii, *Phys. Stat. Sol. (a)* 200 (2003) 215-296.
6. www.globalopticsuk.com
7. J.C. Brice, “*The Growth of Crystals from Liquids*”, North-Holland Publishing Co., 1973.
8. J. Czochralski, *Z. Phys. Chem.* 92 (1918) 219-221.
9. P.W. Bridgman, *Proc. Amer. Acad. Arts Sci.* 60 (1925) 303-383.
10. K. Chennakesavulu, S.G. Singh, A.K. Singh, S.C. Gadkari, *Proc. NSGDSC, BARC, (2009), India.*
11. K. Nitsch, M. Nikl, S. Ganschaw, P. Reiche, R. Uecker, *J. Crystal Growth*, 165 (1996) 163-165.
12. Mohit Tyagi, S.G. Singh, A.K. Singh, S.C. Gadkari, *Phys. Status Solidi A* 207 (2010) 1802-1807.
13. S. G. Singh, M. Tyagi, A. K. Singh, and Sangeeta, *Cryst. Res. Technol.* 45 (2010), 18 – 24.
14. A.K. Chauhan, *J. Crystal Growth*, 254 (2003) 418-422.
15. R.G. Salunke, S.G. Singh, A.K. Singh, D.G. Desai, S.W. Gosavi, A.K. Chauhan, S.C. Gadkari. *American Institute of Phys.: Conf. Proc. 1313 PEFM* (2010) 397.
16. S.G. Singh, M. Tyagi, D.G. Desai, A.K. Singh and S.C. Gadkari, *14th National Seminar on Crystal Growth, NSCG-XIV, VIT University, Vellore* (2010).

Heavy Liquid Metal Technology Development

A. Borgohain, N.K. Maheshwari, P.K.Vijayan and R.K. Sinha

Reactor Design & Development Group

Abstract

Liquid metal is increasingly getting more attention as the coolant for advanced reactor systems. This article deals with the activities performed on coolant technology for high temperature reactor applications. A lead bismuth natural circulation loop has been set up, for thermal hydraulics, instrument development and material related studies relevant to the Compact High Temperature Reactor.

Introduction

Many reactor designs based on heavy liquid metal as coolant have been envisaged by various countries for high temperature process heat applications such as hydrogen production by thermo-chemical processes. Heavy liquid metal systems are excellent spallation targets for Accelerator Driven Systems (ADS). Liquid metal especially lead-lithium is also considered for the blanket in the International Thermonuclear Experimental Reactor (ITER). Natural circulation of liquid metal coolant is being considered as the normal core cooling mode in some advanced reactor designs including the Lead cooled Fast Reactors (LFR) being developed by Generation IV International Forum (GIF) [1]. Presently, technology development for a small power Compact High Temperature Reactor (CHTR) capable of supplying high temperature process heat at 1273K is being carried out in BARC.

Attributes of Lead Alloys as a Reactor Coolant

Lead and lead alloys have extremely high boiling temperature at atmospheric pressure (1943-2023K). This facilitates an ambient pressure

primary system- a safety hall mark of liquid metal cooled reactors, which essentially precludes the loss of coolant accident initiator. Very high coolant boiling point precludes boiling induced voiding. This holds when the properties of the lead alloys are exploited to raise core outlet temperature in a range (1173-1273K) suitable for hydrogen production missions. This margin allows room for passive safety strategies to work. Lead and lead alloys are used as a coolant because they do not react vigorously with air and water. Neutronically, lead (and lead alloys generally) exhibit low neutron absorption and low neutron slowing down power. Lead alloys are excellent gamma ray shields. Activation of the coolant is significant for Pb-Bi alloy and is significantly less for pure lead. The long-term activation which might affect decommissioning waste streams exceeds that of sodium. Their ability to corrode iron-based structural materials requires a regime of rigorous coolant chemistry control to maintain protective surface layers on the structural members.

R&D Scope and Challenges

Lead alloy cooled thermal reactor concepts will require several years of “technology focused” R & D in order to establish some of the

fundamental data and understanding required beyond the pre-conceptual design. Research and development required for reactor design and development to use lead alloy as a coolant in the field of analytical chemistry and engineering application is listed below and it would later be followed by more extensive development to actually bring a product to use.

Material compatibility at high temperature

In the CHTR [2], beryllia and graphite are extensively used as reactor core materials. The compatibility of lead alloy coolant with these materials is required to be assessed. Furthermore, issues have been raised concerning the possibility of leaching out of alloying agents from structural materials containing very hot flowing lead and lead-bismuth. The compatibility of materials are first to be assessed separately and then in combinations. The coolant additives or high temperature coatings may result in acceptable material compatibility at high temperature and is required to be assessed from corrosion chemistry and integrity point of view.

Oxygen control and measurement

The amount of dissolved oxygen in liquid lead alloys should not increase beyond a limit to avoid the contamination of the liquid system by lead and bismuth oxides and should not be less than a certain limit which may cause dissolution of alloying element of the structural material. Therefore the oxygen level must be constantly monitored and kept within a certain range [3]. The development of robust oxygen sensor for online measurement of dissolved oxygen is also an important requirement for safe operation of the system.

Solid impurities control

Impurities enter the coolant during reactor

operation by corrosion of metal surfaces, diffusion of metal constituents through the metal and via maintenance operations involving access inside the system. The monitoring of the impurities is essential for online detection up to a very low level.

Coolant activation

In lead bismuth eutectic, the generation of radioactive polonium (Po-210, $t_{1/2}=138.3$ days) resulting from an (n, γ) reaction with ^{209}Bi and subsequent beta-decay is an issue. Polonium-210 is very toxic and troublesome in the event of leakage owing to its tendency to scatter through the available volume. The methods for effective removal of polonium from contaminated surfaces and from the atmosphere are required to be developed and tested.

Thermal hydraulics

Systematic studies on the degradation of heat transfer due to oxide formation on heat transfer surface are needed for design of reactor coolant circuit and heat exchangers. The studies on behaviour of liquid metal during natural circulation under various transients are rare. For 3-D thermal hydraulic analysis of reactor systems involving natural circulation, CFD codes are found to be very useful. But proper validation of the codes for liquid metal application is essential before using it for the actual system analysis. Another area of importance is the coupling of the system codes with 3-D CFD codes. This will help in coupled 1-D and 3-D analysis of the whole reactor system accurately and economically.

The liquid metal systems using lead (Pb) or lead-bismuth eutectic (LBE) require measurement technologies especially adapted to them. Instruments for measurement of pressure, pressure drop and low flow rate for high

temperature application are required to be developed.

Activities on Lead Bismuth Coolant Technology Development

Lead-Bismuth test loop

A lead-bismuth natural circulation loop has been set up, for thermal hydraulics, instrument development and material related studies relevant to CHTR. Steady state and transient studies are carried out in the loop. Fig. 1 shows the isometric view of the loop and a photograph. More details of the loop and experimental studies can be found in [4]. The loop mainly consists of a heated section, air heat exchanger, valves, various tanks and argon gas control system. All the components and piping are made of SS316L. The LBE ingots are melted in a melt tank and then transferred to the sump tank. The LBE coolant in the sump tank is then pressurized by argon gas system. Due to pressurization molten LBE flows into the loop and subsequently fills up the loop. After filling, the loop was isolated from the sump tank by a valve. Natural circulation of the coolant takes place in the loop due to heating of the coolant in the heated section and cooling in the heat exchanger. Air is used as the secondary side coolant in the heat exchanger. After losing heat in the heat exchanger LBE enters the heated section through 15mm Nominal Bore (NB) pipeline.

Oxygen measurement and control

An oxygen sensor was developed to measure dissolved oxygen level in LBE. The oxygen sensor consists of a one-end closed YSZ tube. Bismuth and Bismuth oxide is used as reference electrode. The sensor has been tested in a separate test set up [5] before installation in the loop. Fig. 2 shows the oxygen sensor used in the

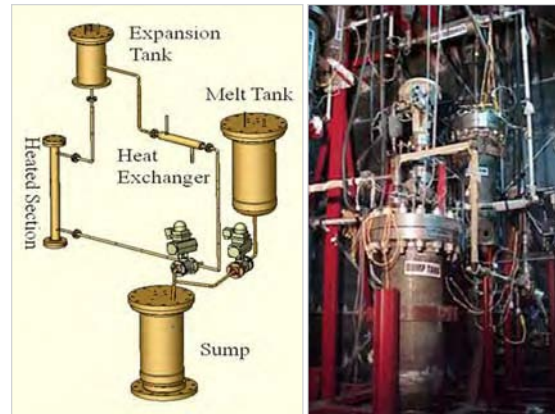


Fig. 1: 3D view of the main loop and photograph

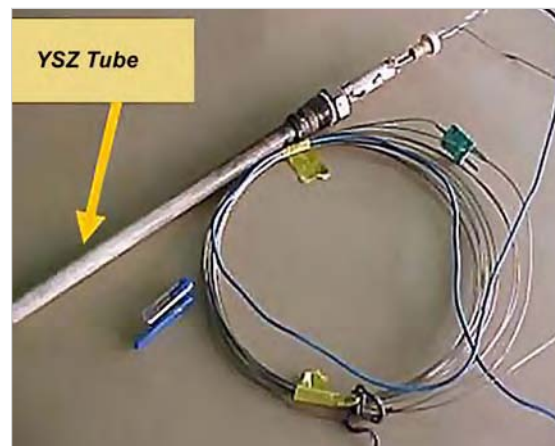


Fig. 2: In-house developed oxygen sensor

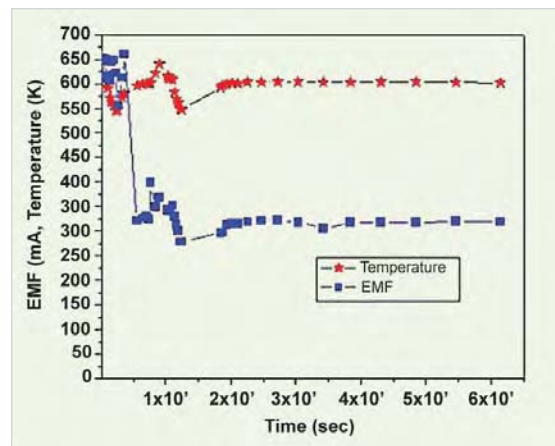


Fig. 3: Variation of temperature and EMF with time

loop. Fig. 3 shows the variation of *emf* of the sensor during operation of the loop.

Material testing in Lead-Bismuth environment

Material compatibility related studies with lead bismuth coolant at high temperature are in progress. Fig. 4 shows the micrograph of graphite sample tested at 1123K in LBE medium for 500 hrs. No significant corrosion or penetration of LBE into the graphite material is observed after the test. Material compatibility studies on stainless steel and graphite in LBE medium have also been carried out by other researchers [6, 7].



Fig. 4: Micrograph of graphite after 500 hrs operation in LBE at 1123K

Computer code development and its validation

A computer code, LeBENC (Lead Bismuth Eutectic Natural Circulation) is developed to study the steady state and transient behaviour of liquid metal natural circulation in a closed loop. The code can handle uniform and non-uniform diameter piping in the loop, different working fluids (water and LBE) and accounts for axial conduction in the fluid and pipe wall. The details of the code can be found in [3]. The code was first validated [8] with experimental data on natural circulation in water.

Validation in the Lead-Bismuth loop

Steady state and transient experiments were carried out. In transient studies start up of the natural circulation, loss of heat sink and loss of heater power were studied. For all the experiments, the computer code was run with

the same inputs as initial conditions in the test loop and results obtained were plotted for comparison. Fig. 5 shows the steady state results at various heater powers and the comparison of the prediction of LeBENC code. Fig. 6 shows a comparison of theoretical results with experimental data for start up of natural circulation from stagnant condition with heater power of 1800W in the loop.

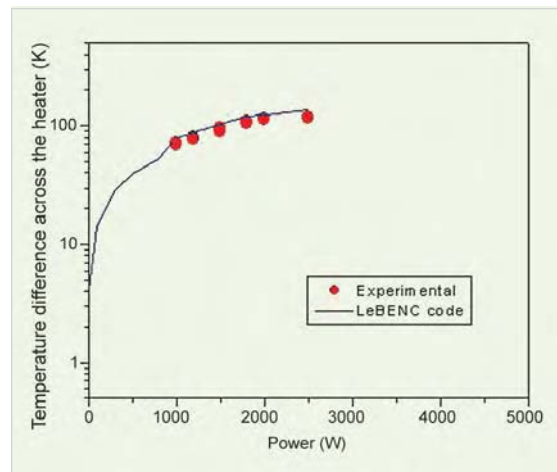


Fig. 5: Steady state natural circulation results at different power levels

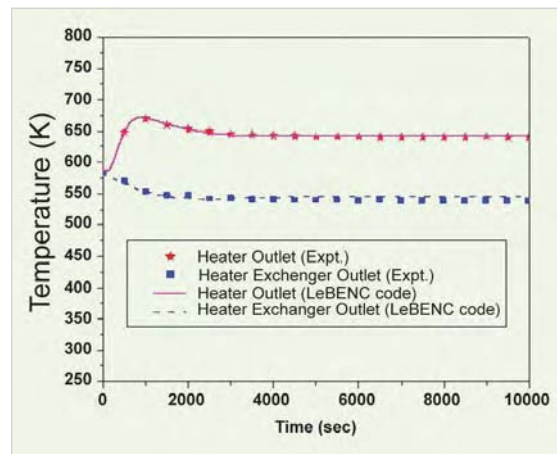


Fig. 6: Start-up of the loop from stagnation condition, heater power 1800W

CFD analysis

Computational Fluid Dynamics (CFD) is used for the 3-D thermal hydraulic analysis related to CHTR. PHOENICS, a general purpose CFD

code is used for the analysis. The code has been assessed for liquid metal heat transfer analysis [9]. Based on the assessment 3-D thermal hydraulic analysis of the CHTR core [2] is carried out. The full-scale reactor core has been modelled in PHOENICS. Natural circulation of the coolant is modelled with Boussinesq approximation. Fig.7 shows the 3D temperature distribution in the core for normal operating condition. The average flow velocity of the coolant in the fuel tube is found to be 3.3m/min. CFD analysis on the lead bismuth loop has also been carried out. Fig. 8 shows the steady state 3D temperature distribution of the loop with heater power 2000W.

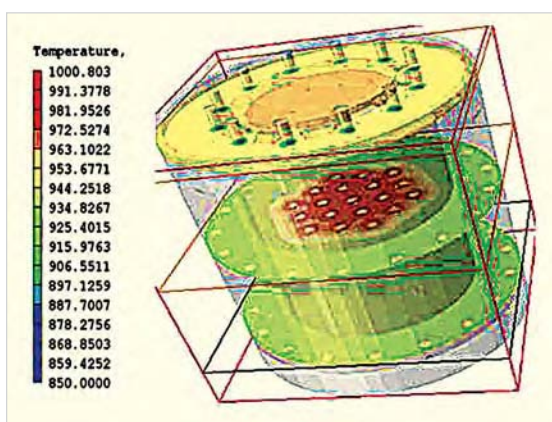


Fig. 7: Temperature Distribution in the CHTR core.

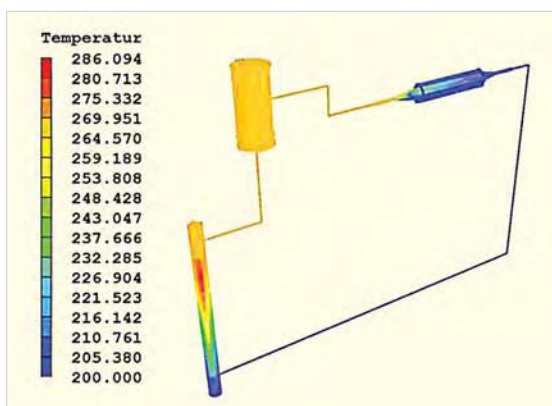


Fig. 8: Temperature distribution in the loop, heater power 2000W.

Concluding Remarks

Steady state and transient studies have been carried out in the Lead-Bismuth loop. Sensor for online measurement of dissolved oxygen in LBE at high temperature was developed and tested in the loop. A computer code is developed and results are compared with the experimental data. The development of instruments for liquid metal application and material testing are in progress.

References

1. Annual Report-GIF, 2009, <http://www.gen-4.org/PDFs/GIF-2009-Annual-Report.pdf>.
2. I. V. Dulera and R. K. Sinha, 2008, "High Temperature Reactor", *J. Nucl. Materials*, 383 1-2, 15, 183-188.
3. X. Wu, J. Ma, Y. Jiang, B. Fu, W. Hang, J. Zhang, and N. Li, 2006, "Instrumentation of YSZ Oxygen Sensor Calibration in Liquid Lead-Bismuth Eutectic", *IEEE Explorer*, accessed at: <http://ieeexplore.ieee.org/stampstamp.jsp?tp=&arnumber=1464945&userType=inst>.
4. A. Borgohain, B. K. Jaiswal, N. K. Maheshwari, P. K. Vijayan, D. Saha and R. K. Sinha, "Natural Circulation Studies in a Lead Bismuth Eutectic Loop", *J. Nucl. Progress* (accepted for publication).
5. A. Borgohain, N. K. Maheshwari, P. K. Vijayan, D. Saha and R. K. Sinha, 2008, "Development of High Temperature Oxygen Sensor for Lead Bismuth Eutectic", Proc. Discussion meet on Electro Analytical Techniques & their applications", ISEAC Munnar, Kerala, Feb 25-28.

6. C.M. Das and R. Fotedar, "Experiences on Lead-Bismuth Loops", 2008, Workshop on Steel and Fabrication Technologies for Fusion Programme (WSFT-08), Institute for Plasma Research, Ahmedabad.
7. A. K. Sengupta, R. K. Bhagat, A. Laik, G.B. Kale, T. Jarvis, S. Majumdar and H.S. Kamath' 2006, "Out of Pile Chemical Compatibility of Pb-Bi Eutectic Alloy with Graphite", *International Journal for Materials Research*, 97, 834-837.
8. B.K. Jaiswal, P.K. Vijayan, N. K. Maheshwari, A. Borgohain, 2008, "Development of a Computer Code to Study the Steady State and Transient Behaviour of Liquid Metal Natural Circulation Loop", 19th National and 8th ISHMT-ASME heat and mass transfer conference, JNTU Hyderabad, India.
9. A. Borgohain, N.K. Maheshwari, P.K. Vijayan, D. Saha and R. K. Sinha, 2008, "Heat Transfer Studies on Lead-Bismuth Eutectic Flows in Circular Tubes", Proceedings of 16th International Conference on Nuclear Engineering (ICONE), May 11"15, Orlando Florida.

Indigenous Development of Silicon PIN Photodiodes Using a 4" Integrated Circuit Processing Facility

Anita Topkar, Arvind Singh, Bharti Aggarwal and C.K. Pithawa

Electronics Division

and

A.S. Rawat

Laser & Plasma Technology Division

Abstract

A wide range of single element silicon PIN photodiodes and 16-element PIN photodiode linear arrays have been indigenously developed using the 4" integrated circuit processing facility of Bharat Electronics Limited, Bangalore. The photodiodes show low dark currents and good optical performance in the visible range. The overview of this technology development activity is presented in this article.

Introduction

Silicon PIN photodiodes feature high speed, low series resistance, low dark current and low junction capacitance resulting in low noise and fast response time of the order of a few ns. Compared to photomultiplier tubes, silicon photodiodes offer specific advantages such as low operating voltage (<100V), high quantum efficiency, insensitivity to magnetic fields, and small sizes. As a result, PIN photodiodes are now being used extensively in wide range of applications involving radiation monitoring, nuclear physics (for medium-energy charged particle detection) and particle physics experiments (electromagnetic calorimeters). These devices are widely used in laser based metrology applications (measurements of diameter, surface roughness, projectile velocity, distance and vibration) and beam parameter measurements (power, temporal profile, pulse energy). As scintillation detectors, major

applications of PIN photodiodes are in the arena of security systems such as X-ray baggage scanning and cargo scanning, industrial tomography and medical imaging systems. The technology for the production of PIN photodiodes for the above mentioned applications was not available in our country resulting in dependency upon the foreign commercial suppliers for these devices. Therefore, indigenous development of these devices was taken up.

Fabrication Technology

Considering the range of applications of silicon photodiodes as mentioned above, indigenous technology development of silicon PIN photodiodes has been carried out using a 4" processing line of Bharat Electronics Limited (BEL), Bangalore. The silicon photodiodes have been fabricated using silicon IC fabrication technology. A planar process which combines oxide passivation with ion implantation gives

better device properties compared to diffused junction devices, and hence this process has been adopted for fabrication of the photodiodes. Oxide passivation over the surface is useful for reduction of leakage currents whereas ion implantation allows accurate control of junctions. N Type, <111>, 4-6 k Ω -cm high purity silicon wafers of 300 μ m thickness are used as starting material and the subsequent process steps have been optimized so that the generation of defects is minimized. The front P⁺ region has been obtained by boron ion implantation while phosphorous has been used to obtain a N⁺ region at the back. Several process steps have been incorporated to reduce the dark current. The breakdown voltage has been tuned to enable operation in full depletion mode so as to get a minimum terminal capacitance. Silicon dioxide has been used as an anti-reflection layer over the active region and it has been tuned for the wave length of CsI scintillator. Initially, process runs have been carried out using a test-mask to optimize the required electrical and optical performance. Subsequent to process development, another mask was designed to incorporate different types of photodiodes. This design incorporated photodiodes with sensitive area ranging from 0.5mm²-150mm², quadrant detectors and 16-element linear arrays of photodiodes. The main fabrication steps used for the fabrication of photodiodes are given below:

- Initial oxidation
 - P⁺ lithography
 - Screen oxidation
 - P⁺ implant of boron
 - P⁺ drive-in and anneal
 - Back N⁺ implant of phosphorous, drive-in and anneal
 - Contact opening, metallization and passivation on the front side
 - Dicing and packaging
- Subsequent to wafer fabrication, the photodiodes

are packaged in different types of packages such as metal TO (Transistor Outline) packages with glass window or flat package using ceramic substrates. The packages were custom developed at BEL, Bangalore.

Fig.1 shows the photograph of fabricated wafer incorporating various types of photodiodes.

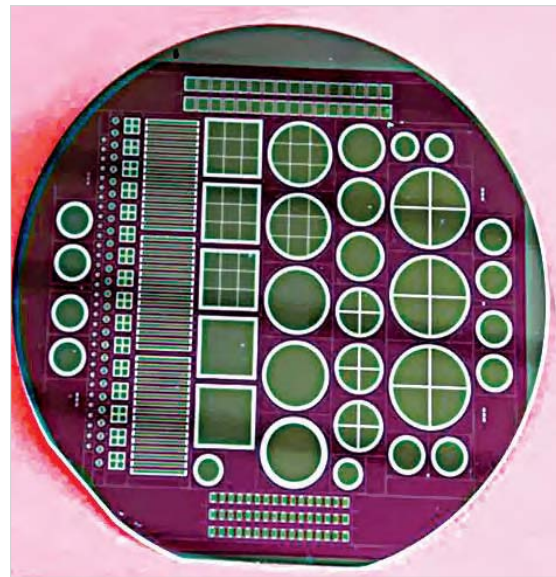


Fig. 1: Fabricated wafer showing various types of PIN photodiodes

Performance of Photodiodes

The characterization of the photodiodes has been carried out by measuring the dark currents and reverse capacitance at different bias voltage using automated measurement setups. The typical dark currents at different bias voltages for a number of photodiodes of area 100mm² are shown in Fig. 2. The dark currents at voltages exceeding full depletion voltage are about 3-5nA/cm². The typical capacitance vs voltage characteristics for photodiode with area of 100mm² is as shown in Fig. 3. As can be seen, the capacitance at full depletion voltage is about 45 pF/cm².

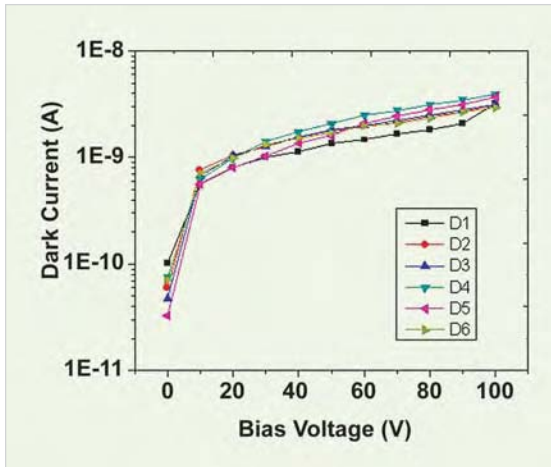


Fig. 2: Typical dark current vs voltage characteristic for photodiodes of area 100mm²

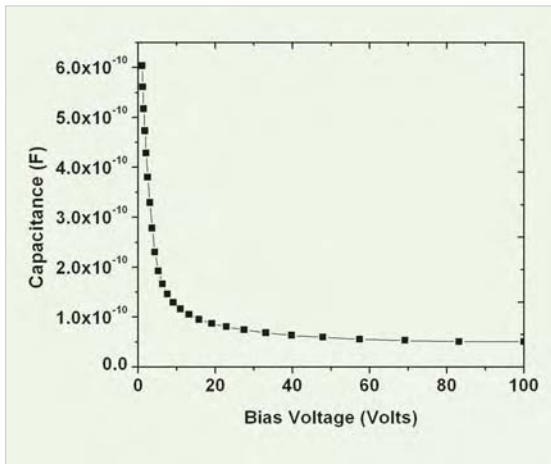


Fig. 3: Typical capacitance vs voltage characteristic of photodiode of area 100mm²

The optical characterization has been carried out by measuring the responsivity at different wave lengths of light in the visible range. The responsivity has been measured at 543nm, 632nm and 940nm wavelengths using laser/LED. During these measurements, the optical power of incident light on the photodiode was measured using a power meter. The current generated due the incident photons in the photodiode was measured using a trans impedance amplifier. The diodes were used in photoconductive mode and the output voltage was measured to calculate the photocurrent.

The optical response of the photodiodes was compared with commercially available photodiodes of similar specifications. The spatial uniformity of the optical response and linearity at different input optical powers was also measured.

The optical performance of the photodiodes has been observed to be as good as that of imported commercial photodiodes (Fig.4).

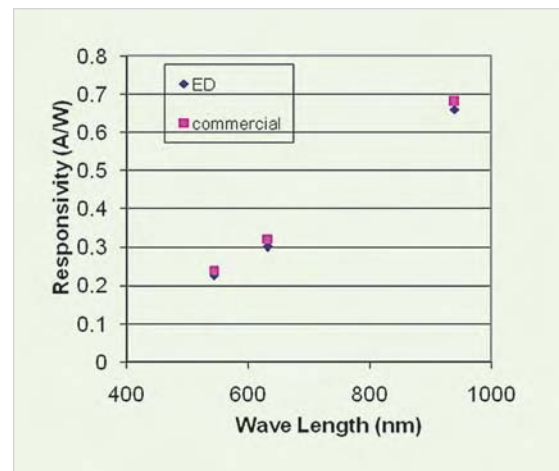


Fig. 4: Responsivity of photodiodes at different wavelengths in the visible range

The spectroscopic performance of indigenously developed CsI-photodiode detector assembly for different gamma energies was investigated by coupling the photodiode to CsI scintillator. The CsI scintillator was grown at TPD, BARC. A CsI scintillator with dimensions of 10x10x15 mm³ was coupled to a photodiode of 10mmx10mm geometry for carrying out these measurements. Fig. 5 shows the response of CsI:PIN photodiode detector assembly for different gamma-ray energies over a range of 511keV to 1275keV [1].

The CsI-photodiode detector shows a good linearity in the 511 keV -1275 keV range. The detector shows energy resolution of about 16% at energy of 662 keV.

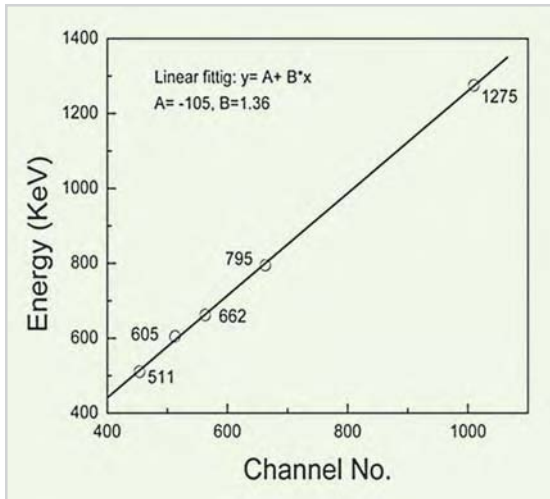


Fig. 5: Response of CsI:PIN photodiode detector assembly for different gamma-ray energies [1]

Types of Photodiodes Developed

Various types of photodiodes which have been developed include single element diodes, quadrant detectors and 16-element linear arrays. Some of these photodiodes are shown below:



PIN photodiode with active area of 0.2 mm² (0.5mm dia.) and with a mini-lens window

PIN photodiode with active area of 0.78 mm² (1mm dia.) and with a mini-lens window

Quadrant detector with each element of 1.3mm x 1.3mm, 0.1mm gap and with a glass window

PIN photodiode with active area of 25 mm² and with a glass window



Quadrant detector with total active area of 150/50mm² and with a glass window

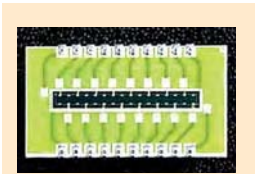


PIN photodiode with active area of 50/100mm² and with a glass window

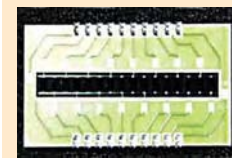


PIN photodiode with a square geometry, with active area of 100mm² and with a glass window

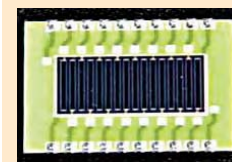
16-element PIN photodiode linear arrays for X-ray imaging with scintillator



Element geometry of 1.57mm x 1.22 mm and pitch of 1.57mm



Element geometry of 2.5 mm x 2.15mm and pitch of 2.5mm



Element geometry of 10 mm x 0.8mm and pitch of 1.3 mm

Summary

Various types of PIN photodiodes have been indigenously developed using the 4" integrated processing facility of BEL, Bangalore and their performance has been evaluated. The photodiodes have been observed to have

performance comparable to that of commercial photodiodes. As this technology development was carried out using the foundry facility of BEL, the photodiodes will be commercially available from BEL, Bangalore. Using the technology developed, it would be also possible to tune the specifications such as geometry, types of segmentation, spectral response, etc., for specific applications.

Acknowledgement

The authors would like to thank Mr. G.P. Srivastava, Director E&IG, Dr L. M. Gantayet, Director, BTDG, Mr. R.K Patil, Associate Director (C), E&IG and Dr A.K. Das, Head,

L&PTD for their support in carrying out this work. The contribution of Dr S.C. Gadkari, TPD and Mr. S.G. Singh, TPD, BARC in investigating the gamma response of CsI-photodiode detector is acknowledged.

References

1. S.G. Singh, Arvind Singh, Anita Topkar, S.C. Gadkari, "Performance of indigenously developed CsI(Tl)-photodiode detector for gamma-ray spectroscopy", presented in 55th DAE-Solid State Physics Symposium (DAE-SSPS 2010), Paper *in press* in AIP Conference Proceedings.

Development of Room Temperature NH₃ Gas Sensors based on Ultrathin SnO₂ Films

Sipra Choudhury, C.A. Betty, K.G. Girija
Chemistry Division

Abstract

Ultrathin SnO₂ film deposited by Langmuir–Blodgett technique showed high sensitivity (< 3 ppm) for NH₃ gas at room temperature with fast response (<1 min) and 90% recovery within half-an-hour. The sensitivity remained the same and was reproducible even after one year indicating the long term stability of the sensor. The sensor was highly specific to NH₃ in presence of the other reducing gases - H₂S, SO₂, CO, H₂ and CH₄. In the presence of H₂S and SO₂, the film conductivity increased whereas it decreased with ammonia. There was no response with other reducing gases.

Introduction

The current era of high technology and advanced industry has produced an incredible rise in living standards. However, this has also been accompanied by a variety of serious environmental problems, for example, the atmospheric release of various chemical pollutants, including NO_x, SO_x, HCl, NH₃, CO₂, volatile organic compounds (VOCs) and fluorocarbons from industries, automobiles, and homes. These polluting gases result in serious global environmental issues, such as acid rain, greenhouse effect, sick house syndrome and ozone depletion. To prevent or minimize the damage caused by atmospheric pollution, monitoring and controlling systems are needed that can rapidly and reliably detect and quantify pollution sources within the range of the regulating standard values. Till now, air pollutant measurements have been carried out with analytical instruments using optical spectroscopy, gas chromatography or mass spectrometry.

Although these instruments can give a precise analysis, they are time-consuming, expensive, and can seldom be used in real-time in the field. Therefore, a gas sensor that is compact and robust with versatile applications and low cost, could be an equally effective or better alternative.

Gas sensors for detecting air pollutants must be able to operate in a stable manner under deleterious conditions, including chemical and / or thermal attack. Therefore, solid-state gas sensors would appear to be the most appropriate ones in terms of their practical robustness. There are several solid-state gas sensors currently available for gases such as O₂, H₂O, H₂S, LPG at relatively high concentrations [1]. However, the range of air pollutant concentrations that is to be detected reaches as low as few ppm in combustion exhaust control or indoor monitoring and few ppb in atmospheric environmental monitoring. Therefore, the development of more sensitive and selective gas sensors than the conventional ones is still required. Over the past

few decades solid state gas sensors based on polycrystalline SnO_2 thin films have become predominant for gas alarms in domestic, commercial and industrial premises. These sensors are usually operated at temperature $>200^\circ\text{C}$ to achieve reversibility and fast response and they are mainly used for H_2S , CO and H_2 sensing. Sensors operated at high temperature, though specific to a particular gas at that temperature, suffer from shorter life-time and high thermal budget. Besides, in an explosive environment, the high-temperature operation of these oxide sensors is not favorable. Evidently, room temperature operation is preferable, however, in the case of polycrystalline thin films the bottleneck for room temperature operation lies in the dominant grain boundary barrier resistance (Schottky diode). This can be readily overcome by exploiting nano-scale structures of SnO_2 . Very small grain size and high surface-to-volume ratio associated with the nanocrystallites allow the sensors to be operated in the most sensitive, grain-controlled mode, having a completely depleted space charge region.

Depending on the degree of nonstoichiometry (SnO_{2-x}) of the film, exposure to oxygen leads to some of the oxygen being adsorbed at surface defects. The adsorption passivates the surface vacancies, drawing electrons from the bulk and localizing them on the chemisorbed / ionosorbed oxygen, thereby creating a space charge region of positively charged ions near the surface. The effect of grain size and grain boundary barrier on carrier density modulation (Δn_c) is schematically shown in Fig. 1 (n_c vs. film thickness l), for micro

and nanogranular films. The two cases are scaled using Debye length L_D in SnO_2 film for a given temperature. Fig. 1(i) and (ii) (upper part) show the top view of the polycrystalline interconnected micrograins and nanograins respectively without any amorphous phase in between. The distance between the grain boundaries to the dotted line indicates the Debye layer thickness L_D created by the charge transfer with the surface adsorbed species. With the film thicknesses $l > 2L_D$, band bending due to oxygen chemisorptions exists only near the surface [2] (the band diagram is shown later in Fig.6). The corresponding electron density plot (lower part of Fig. 1 (i)) shows that there is no effect on the bulk electron density except on the grain boundary due to the adsorbed species. In contrast, the effect of adsorption on nanostructures ($l < 2L_D$) is to deplete the nanograin completely of the charge carriers (Fig. 1(ii) upper part). This in turn changes the location of the Fermi level (which is proportional to Δn_c) within the band gap of the nanostructure (Fig. 1 (ii), right bottom panel) causing an appreciable conductance drop. In order to exploit the above

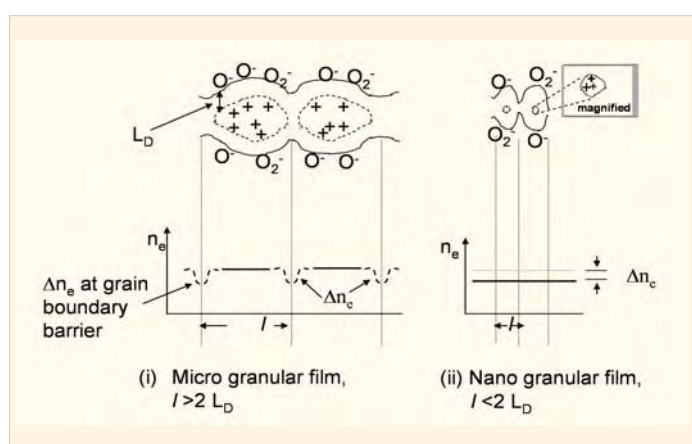


Fig.1: Schematic diagrams of space charge formation at the grain boundaries (upper part) and carrier density modulation (lower part) due to surface adsorbed species (O^- , O^{2-}) on micro and nano granular film. The continuous lines (upper part) represent grain boundaries. L_D is the Debye length, l is the grain size, n_c is carrier density, Δn_c change in carrier density. (+) indicates the charge on Sn atom inside the grain.

mentioned nanostructure properties in gas sensor design we have deposited ultrathin films with $L_D > l/2$ by controlling the thickness of SnO_2 films using Langmuir–Blodgett technique. Gas sensors fabricated using these ultrathin SnO_2 films have been successfully demonstrated for their room temperature response to NH_3 detection with high sensitivity and fast response.

Deposition of ultra thin SnO_2 film

Ultrathin SnO_2 film was deposited by Langmuir-Blodgett (LB) technique, which provided highly ordered thin films of SnO_2 . This technique of depositing thin tin oxide film has advantages over other methods as it does not require vacuum and needs only moderate temperature. It also

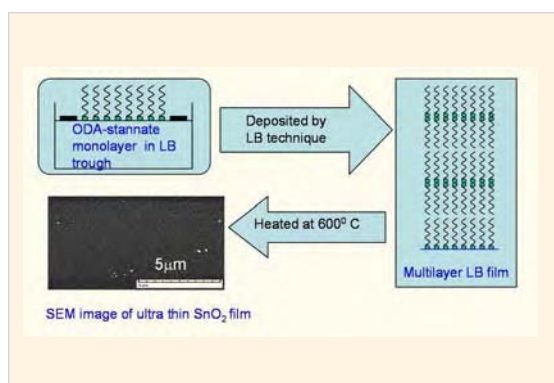


Fig. 2: Flow chart of the preparation of ultra thin SnO_2 film from LB film precursor

provides very good control of film thickness and uniformity of the ordered multilayers. Multilayer LB films of the anionic tin complexes with octadecyl amine (ODA) deposited on various substrates (Si, quartz and glass) were decomposed at 600°C (2 hours) for desorption of long hydrocarbon chain. In the presence of oxygen, the tin ions formed oxides on the substrates (Fig. 2). SnO_2 films of 15-20 nm were formed on various substrates from 120 layers of octadecyl (ODA) stannate LB film [3,4]. Surface morphology in SEM examination appeared to be non-porous (Fig. 2).

XRD pattern of the decomposed LB film showed peaks that are characteristic of cassiterite structure of SnO_2 (Fig. 3(i)). Using the Scherrer equation, analysis of $\langle 110 \rangle$ peak of cassiterite gave an approximate crystallite size of 8 nm. In the XPS spectra, peaks were observed at 486.6 and 495 eV (Fig. 3(ii)a) with full width at half-maximum of 1.6 eV representing one oxidation state of Sn. Two oxygen peaks (Fig. 3(ii)b) are observed at 530.1 eV and 532.2 eV. The lower binding energy peak is attributed to lattice oxygen in the SnO_2 crystal structure. The shoulder peak at higher binding energy in O1s spectrum of the SnO_2 film corresponds to adsorbed oxygen at the surface [3].

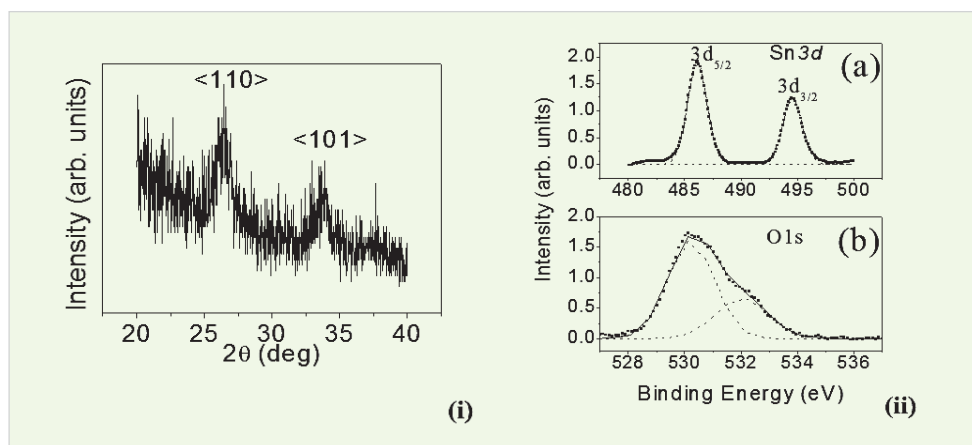


Fig. 3: XRD pattern (i) and XPS spectra (ii) of Sn 3d (a) and O1s (b) of ultrathin SnO_2 film.

Gas sensor fabrication

Inter-digitated gold electrodes were deposited by physical vapour deposition using shadow mask on the SnO₂ ultrathin film grown on quartz substrate. An opaque glass chamber was designed and fabricated for testing the sensors at different ambients. The chamber was further wrapped with a dark adhesive tape to prevent interference from any stray light. The chamber has inlet and outlet stopcocks for exposing it to ambient air or for sweeping the carrier gas and an injection port for the specific gas to be tested. Fig. 4 shows the block diagram and the photograph of the gas testing facility.

Testing and specificity studies

Known amounts of various gases (NH₃, H₂S, SO₂, CO, H₂ and CH₄) from small canisters

were injected into the chamber without any carrier gas flow, using gas tight syringes through rubber septum. The chamber was kept closed completely till the sensor response saturated and then the stop cocks were opened for recovery, by exposing to atmosphere. The room temperature sensitivity of the ultrathin SnO₂ films towards ammonia gas was studied by measuring the change in conductivity with time using an electrometer interfaced to a personal computer. Typical time response to ammonia gas at room temperature is shown in Fig. 5(i). The response time was less than 1 min and 90% recovery took place within half-an-hour. The lowest sensitivity observed (~ 3 ppm) is comparable to the requirement for the air quality monitoring (50 ppm for 2 h exposure). Repeated measurements were carried out on a single device over a period of 1 year and it showed the same response to ammonia indicating the stability and reproducibility of the sensor (Fig. 5(ii)). It was found that the response and recovery times were slower after one year. The reason for the slow recovery after a year could be due to exposure of the unpackaged sensor to ambient over a long time

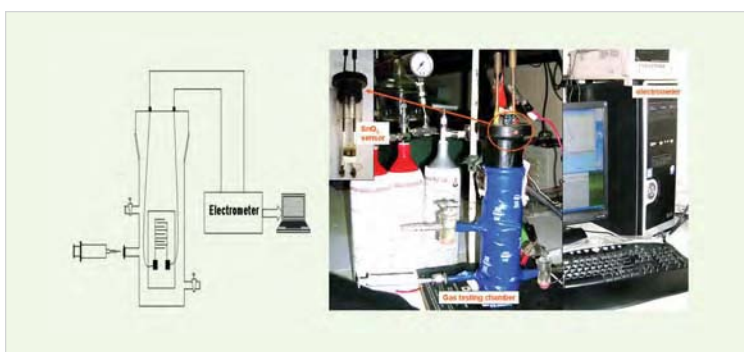


Fig. 4: Block diagram and the photograph of the gas testing facility

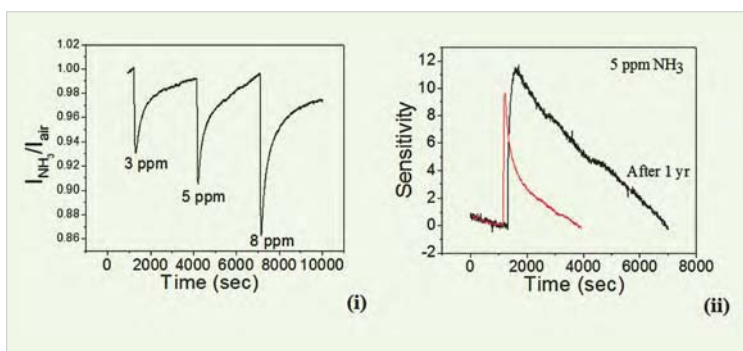


Fig. 5: (i) Typical response ($I_{\text{NH}_3}/I_{\text{air}}$) curve of SnO₂ with ammonia (ii) Sensitivity ($(R_{\text{NH}_3} - R_{\text{air}}) \times 100 / R_{\text{air}}$) plots of freshly prepared and one year old SnO₂ sensor.

Gas sensing mechanism

As already mentioned the surface of nonstoichiometric SnO_{2-x} chemisorbs oxygen forming an electric double layer, through partial sharing of conduction band electrons. The response of this oxygen adsorbed surface to different gases depends on their electrochemical activities. Strong reducing gases will uproot the adsorbed oxygen

layer for their own oxidation and in that process SnO_{2-x} surface gets back its shared band electrons as well as conductivity. Presence of strong oxidizing gases on the other hand results in transformation of the double layer towards stoichiometric SnO_2 , decreasing the electrical conductivity. Thus strongly reducing / oxidizing gases bring about irreversible changes in the surface properties and it requires either air flow or proper heat treatment to gain back the sensing property. Interestingly, interaction of ammonia with the ultrathin film has caused a

decrease in conductivity as shown in Fig. 5. The sensing mechanism of NH_3 is schematically shown in Fig. 6. NH_3 which is a mild reducing gas, is a polar molecule containing partial positive charge on its H atoms (Fig. 6). When NH_3 gas is injected into the chamber, it settles on the surface double layer through polar interaction (Fig. 6) and in this process reduces the conduction band electrons of SnO_{2-x} , thereby reducing the conductivity. As the polar interaction is weak, NH_3 molecules undergo instant detachment (disperse) from the double layer during the recovery phase. This makes the sensor unique and specific to ammonia at room temperature.

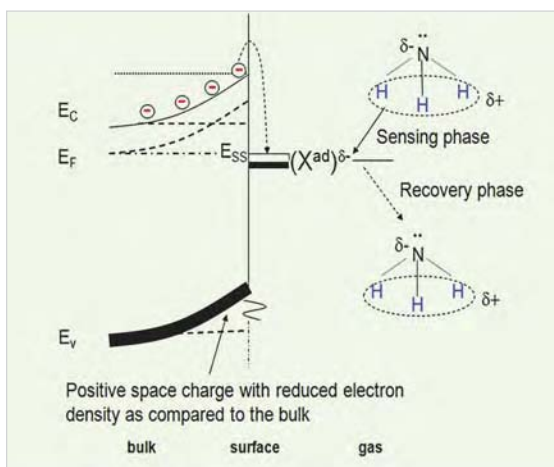


Fig. 6: Schematic band diagram indicating the energy levels on the surface of SnO_2 thin film in presence of surface adsorbed species and the target gas NH_3 ; E_c , E_f , E_v , E_{ss} : energy levels of conduction band, Fermi level, valence band and surface states respectively. $(X^{ad})^\delta$ -negatively charged surface adsorbed species.

Specificity

As for other gases like CO , CH_4 and H_2 which are not polar, they do not show any effect on the SnO_2 film (Fig. 7(i)). In case of H_2S gas, reduction reaction dominates on the SnO_2 surface forming a new species making the response (increase in current) and recovery slower. While testing with a gas mixture of NH_3 (10 ppm) and H_2S (1 ppm) (Fig. 7(ii)) it was observed that current decreased initially due to ammonia gas (fast response, marked as 1) showing immediate response with ammonia. Subsequently, the current increased slowly due

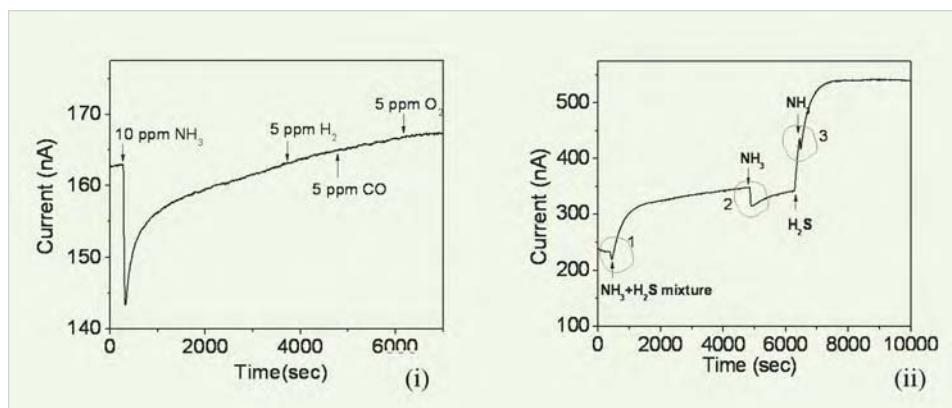


Fig.7: (i) Response of the sensor with NH_3 , H_2 , CO and O_2 gases (ii) Response with NH_3 and H_2S . Circle indicates NH_3 response with decrease in current.

Table 1: Specifications of ultrathin SnO₂ sensor

Property	Value	
Drift in base current	2-3 %	
Sensitivity $S = ((R_{\text{NH}_3} - R_{\text{air}}) \times 100) / R_{\text{air}}$	10-14 % for 5 ppm of NH ₃	
Response time	40 sec (for 5 ppm NH ₃)	
Recovery time (after opening of stopcocks, without any carrier gas flow)	30 mins for 90 % recovery	
Reproducibility after a year	Sensitivity intact	
	Response time	200 sec (5 ppm of NH ₃)
	Recovery time	1 hr (5 ppm of NH ₃)
Specificity	Specific to NH ₃ in presence of other reducing gases (H ₂ S, SO ₂ , CO, H ₂ , CH ₄)	

to the presence of H₂S gas (slow response). After the saturation of current with H₂S gas, ammonia was injected again (marked as 2) and its characteristic response was observed. Even in the presence of H₂S gas, subsequent ammonia injection showed similar response (marked as 3) as in the earlier case. These studies indicated the specificity of the SnO₂ sensor towards ammonia gas even in the presence of other reducing gas like H₂S. Table 1 summarizes the specific properties of SnO₂ based room temperature NH₃ sensor.

Conclusions

It has been demonstrated that ultra thin SnO₂ films fabricated from the thermal decomposition of LB film precursor, exhibit room temperature gas sensitivity comparable to that required for air quality monitoring. The sensor is specific to NH₃ gas at room temperature and shows fast response and recovery without any carrier gas flow. The stability studies indicated that these sensors are stable at least for a year with no significant change in sensitivity. The present study also shows the applicability of the alternative LB technique for the formation of

ultrathin oxide film with controlled thickness, which is useful for many device applications. The entire fabrication process is cost effective.

Acknowledgements

Authors are thankful to Dr. D. Das, Head, Chemistry Division, BARC, for his constant encouragement, fruitful discussion and constructive suggestions during the course of the work.

References

1. N. S. Ramgir, I. S. Mulla, K. P. Vijayamohanan, *Sens. & Actuat, B, Chem.* 107 (2005) 708-715.
2. W. Gopel, K.D. Schierbaum, *Sens. & Actuat, B, Chem.* 26 (1995) 1-12.
3. Sipra Choudhury, C. A. Betty, K.G. Girija, S. K. Kulshreshtha, *Appl. Phys. Lett.* 89 (2006) 071914-16
4. Sipra Choudhury, C. A. Betty, K. G. Girija, *Thin Solid Films* 517 (2008) 923-928.

Development of Online Radon and Thoron Monitoring Systems for Occupational and General Environments

J.J. Gaware, B.K. Sahoo, B.K. Sapra, Y.S. Mayya

Radiological Physics and Advisory Division

Abstract

Online radon and thoron monitors have been developed using ZnS(Ag) detector for continuous monitoring of concentrations in occupational and general environments. Their performance has been tested successfully both in laboratory and field conditions. Special features of these monitors include low cost, high sensitivity and non-interference of humidity and trace gases. The capability of these radon monitors for networked radon monitoring in U mines and in the U-tailings pond has been demonstrated. The thoron monitor is designed for stack monitoring of thoron release in a thorium processing facility. Being highly sensitive, these monitors can also be used for radon/thoron monitoring in dwellings, radon exhalation measurements, radon concentration in water samples and thoron emission measurements from monazite sands in High Background Radiation Areas.

Introduction

Unlike time-integrated monitoring of radon and thoron which is mainly limited to dosimetric applications, continuous online monitoring yields insight into spatio-temporal correlations, build-up in confined spaces, hourly variations induced by pressure and temperature variations, atmospheric transport, extreme excursions, duration of specific highs and lows etc. While the increased computational capabilities on environmental modeling have given rise to greater needs for real time data, the corresponding developments in networking and data transmissions have made it possible to achieve large scale simultaneous measurements. Such facilities are being increasingly developed as part of systems for earthquake predictions, in uranium mining, environmental monitoring and geophysical research.

Apart from these general applications, monitoring radon concentrations in Uranium mining and thorium processing facilities is important to evolve effective strategies to reduce radiation doses to occupational workers. With this in view, automatic radon and thoron monitors have been developed as described below.

Description of systems

Online Radon Monitor

Traditionally, the Lucas scintillation cell is used for one point sampling of radon (Lucas, 1957; Abbady et.al., 2004). The counting is carried out after a delay of 3 hrs, allowing for the decay products to achieve radioactive equilibrium with radon. The same Lucas cell may be used for continuous radon measurements with the help of an algorithm for calculation of radon concentration for each sampling time interval. The algorithm accounts for the

fractions of radon decay products contributing to the total counts formed by radon in the current interval and in its preceding intervals. This innovative algorithm for correlating the counts with the radon concentration has been developed in-house, based on the theoretical growth and decay equations of radon decay products. Using this algorithm, two versions of radon monitor have been developed. The portable version called SRM (Scintillation Radon Monitor), utilizes a ZnS:Ag based scintillation cell for measurement of alpha from radon and its decay products. The other version named as ECAS (Electrostatic Collection and Alpha Scintillation) is developed using an electrostatic chamber for collection of charged decay products of radon on the ZnS:Ag surface. The details of these two versions are described below.

Portable Radon Monitor - SRM

The schematic of the microprocessor based SRM and its photograph are shown in Figs.1a & 1b respectively. Radon is sampled into the scintillation cell (150 cc) through a “progeny filter” and “thoron discriminator” eliminating radon progenies and thoron. The thoron discriminator based on “diffusion-time delay” does not allow the short lived thoron ^{220}Rn (half life 55.6 sec) to pass thorough. The alpha

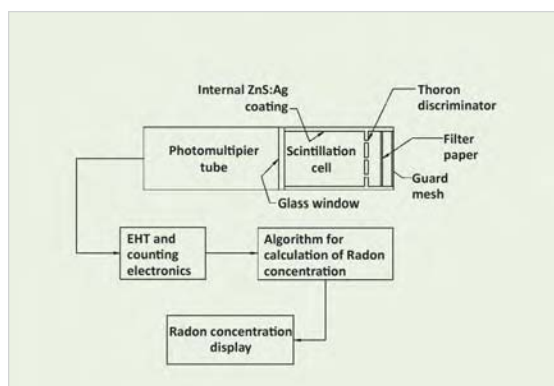


Fig. 1a: Schematic diagram for Portable Radon Monitor (SRM)

scintillations from radon and its decay products formed inside the cell are continuously counted for a user-programmable counting period by the PMT and the associated counting electronics. The alpha counts obtained are processed by a microprocessor unit as per the developed algorithm to display the concentration of radon.

Considering the limitations on the range of the alpha particles (~ 6 cm), the dimensions of the scintillation cell were optimized to achieve high sensitivity (1.2 cph/Bqm $^{-3}$) with lower detector volume (150 cc). The low detector volume, delivering very high sensitivity per unit activity of radon (6000 cph/Bq), is very useful for measurements of mass exhalation and surface exhalation of radon from various naturally occurring radioactive materials

High Sensitivity Radon Monitor - ECAS

The low range of the alpha particles (~ 6 cm), makes it difficult to enhance the sensitivity of the SRM monitor just by increasing the dimensions (or volume) of the scintillation cell. Hence, an electrostatic collection technique for charged decay products of radon, namely $^{218}\text{Po}^+$ and $^{214}\text{Pb}^+$ ions, on the ZnS:Ag scintillator has been used. The schematic and the photograph of ECAS are shown in Figs.2a & 2b respectively. As in SRM, the sampling of radon into the



Fig. 1b: Photograph of Portable Radon Monitor (SRM)

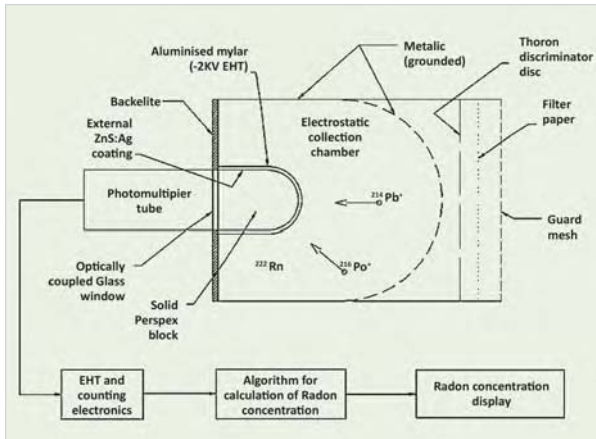


Fig. 2a: Schematic diagram for high sensitivity radon monitor (ECAS)

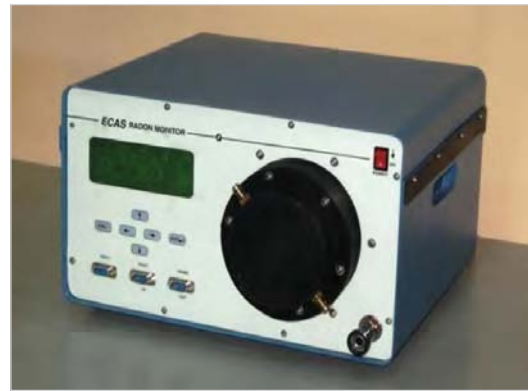


Fig. 2b: Photograph of high sensitivity radon monitor (ECAS)

detector volume (1000 cc) is carried out by diffusion through “progeny filter” and “thoron discriminator” in succession. The electric field for various detector geometries and dimensions were modeled using commercial software and the optimal field with this simple-to-fabricate cathode and anode design was obtained. Accordingly, an electrical potential of -2 KV is applied to an aluminized mylar ($12\mu\text{m}$ thickness) covering the ZnS:Ag scintillator coated on the cathode which is a solid perspex cylindrical block with a hemispherical head. The alpha scintillations produced by ^{222}Rn , ^{218}Po and ^{214}Po are detected by the PMT and the associated counting electronics. The alpha counts obtained are processed by a microprocessor unit to display the concentration of radon.

Online Thoron Monitor

The indigenously developed microprocessor based thoron monitor consists of two Lucas scintillation cells (LSCs) which are coupled to a separate photomultiplier tube with associated pulse preamplifier and scalar. Its schematic diagram and photograph are shown in Figs.3a & 3b respectively. The LSC is a 2" dia and 3" height cell built in S.S. 316 material with inbuilt two levels of radon-thoron progeny pre- filters for reducing the background contamination. The flow to either LSC is switched by microprocessor

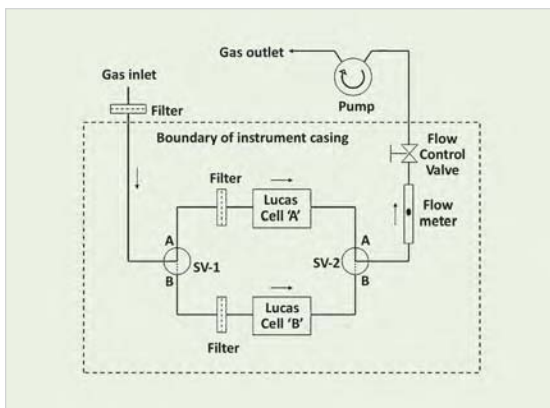


Fig. 3a: Schematic diagram for online thoron monitor



Fig. 3b: Photograph of online thoron monitor

at the intervals specified through programmable parameters. During each interval, while one cell counts the background, the other cell measures counts due to both thoron and the background activity. The unit automatically calculates and logs the thoron concentration data in the memory.

Performance evaluation

Various tests were carried out under controlled conditions in a chamber to evaluate the performance of the monitors. The first set of experiments was carried out to compare the measurements of online radon monitors against the commercially available system AlphaGUARD. A fair agreement was seen between ECAS, SRM and AlphaGUARD as shown in Fig. 4. Similarly, the measurements with the indigenous thoron gas monitor was compared with that obtained with the commercial unit RAD-7 (Fig. 5). Since the background is high at higher thoron concentrations, the thoron monitor is tested upto 2 MBq/m³. For both the monitors, the variations were within 3%.

To evaluate the response time of SRM radon monitor and also to study the effectiveness of algorithm based calculation, the measurements of radon counts and concentration for sudden

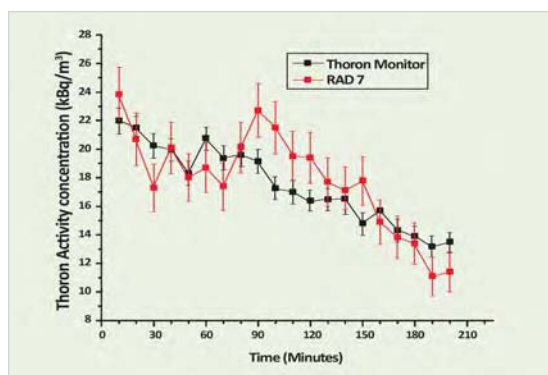


Fig. 5: Comparison of measurements of Thoron monitor with RAD7

rise and fall of radon was carried out which is shown in Fig. 6. The radon concentration of the order of 10 KBq m⁻³ was suddenly introduced inside a closed chamber and after 3 hrs, it was suddenly brought down to 100 Bq m⁻³ (a factor of 100). The gross counts show a slow rise due to time taken to build-up and a slow fall due to the presence of residue activity. However, the algorithm used for the estimation of radon concentration as measured by SRM corrects for these delays and depicts the sharp changes in the concentration as expected. To demonstrate the capability of ECAS to operate in high humidity conditions measurements were carried out by varying the humidity as shown in Fig.7. As may be seen, the effect of humidity does not arise as the electrostatic voltage is not utilized for collection of radon progenies

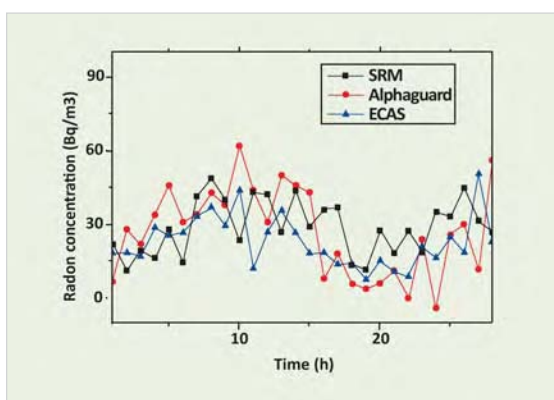


Fig. 4: Comparison of radon measurements by SRM and ECAS against Alphaguard

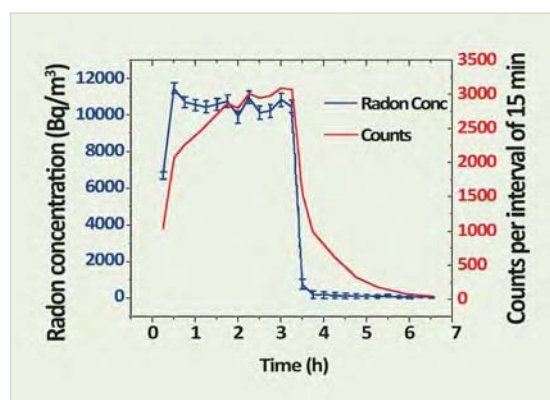


Fig. 6: Response of SRM radon monitor to sudden variations in radon concentration

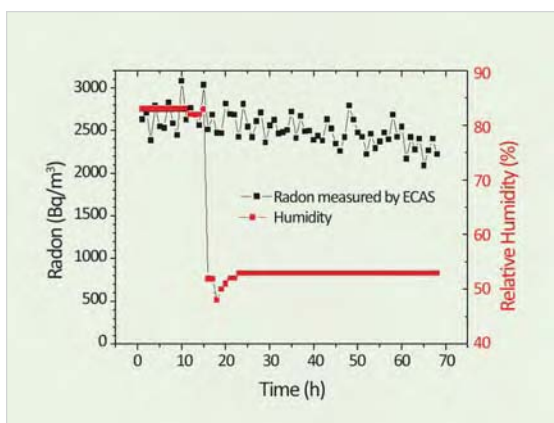


Fig. 7: Radon concentration measurements with varying humidity conditions

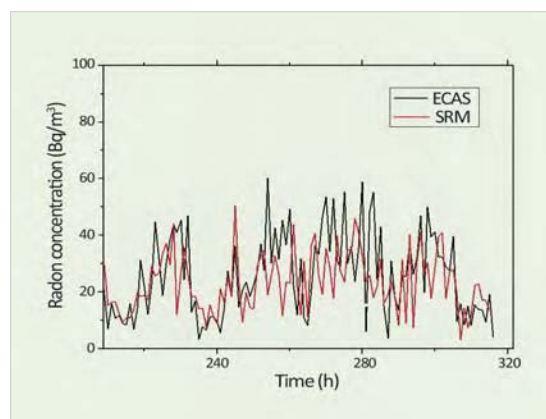


Fig. 8: Ambient radon measurements by ECAS and SRM for a period of about two weeks

To assess the long term measurement capability of SRM and ECAS radon monitor, they were operated continuously in a room for about two weeks without any manual attendance. Both the instruments performed successfully with agreements in radon concentration as seen by the trends given in Fig. 8.

Additional tests were also carried out in controlled conditions to obtain technical specifications of radon and thoron monitors. These specifications are summarized in Table 1.

Table 1: Technical Specifications of online radon/thoron monitor

Parameters	Online Radon Monitor	Online Thoron monitor
Sensitivity	ECAS: 2.8 cph/(Bq/m ³) SRM: 1.2 cph/(Bq/m ³)	0.7 cph/(Bq/m ³)
MDL	ECAS: 8 Bq/m ³ at 95% confidence, 1 hr counting SRM: 14 Bq/m ³ at 95% confidence, 1 hr counting	15 Bq/m ³ at 95% confidence, 1 hr counting
Upper Detection Limit	50 MBq/m ³	50 MBq/m ³
Cycle time	15 / 30 / 60 min – Fast mode 1 / 2 / 3 h – Sensitive mode	10 / 30 / 60 min
Radon Response time	20 min for 95% of radon in air	10 min for 95% of thoron in air
Thoron Interference	< 5% using thoron discriminator	Not applicable
Humidity and Trace gas effect	<5% in ambient environment (20% to 60% RH) and <10% in highly humid environment (60% to 95% RH) for ECAS. Negligible for SRM.	Negligible

Applications of radon monitors

The features such as uninterrupted online operation, high sensitivity and free from humidity / trace gas interference open up diverse applications in radon and thoron studies. These include calibration of passive detector systems, indoor/outdoor radon monitoring, network based online radon monitoring in workplaces such as underground uranium mines, radon emission studies from soil/water/building materials, field survey and site monitoring such as uranium tailings pond. Some of the potential applications have been demonstrated below.

Measurement of radon emission from soil and building materials.

Soil in the earth's crust is the major source of radon emission into the environment. We have demonstrated the use of ECAS for measuring the rate of radon emission from soil. The "accumulator" technique has been used for this. The soil area of interest is covered with the accumulator and the radon build up in it monitored using ECAS connected in a closed loop fashion with an external pump. The buildup data is fitted to an appropriate model to extract the radon emission rate from soil. The experiment was conducted in an open ground (Fig. 9). The



Fig. 9: Measurement of radon emission from soil

accumulator technique of Sahoo and Mayya (2010) was followed to measure the radon emission rate from soil which was found to be $80 \text{ Bq m}^{-2} \text{ h}^{-1}$. This was close to the value obtained using RAD-7. Knowing that building materials are the second most importance source of radon, we used ECAS to measure the radon emission from cement samples (Fig. 10) using



Fig. 10: Measurement of radon emission from a cement sample

the mass exhalation measurement procedure of Sahoo et. al. (2007). The emission rate was found to be $7.2 \text{ mBq kg}^{-1} \text{ h}^{-1}$ which falls within the range reported by Sahoo et al., 2007.

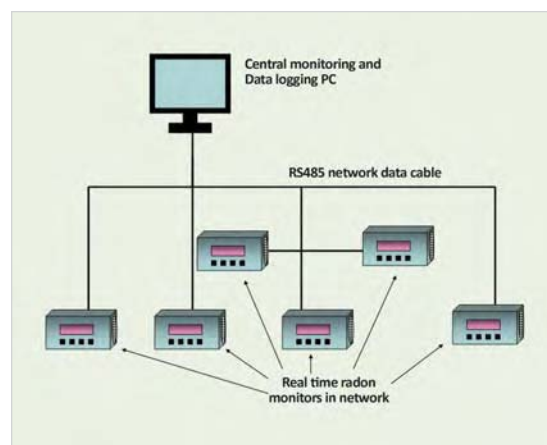


Fig. 11: Schematic diagram of Radon monitoring network at Turamdih U Mines

Networking in Uranium mines at Turamdih - field trial

The networking capability with fast response of ECAS is useful for monitoring uranium mines and tailings pond, with multiple such units networked to give real-time spatial profiles of radon. In this context, few online monitors were installed inside the uranium mines (Fig.11) at the locations where the concentration of radon is expected to be high. Results of the measurements are shown in Fig.12.

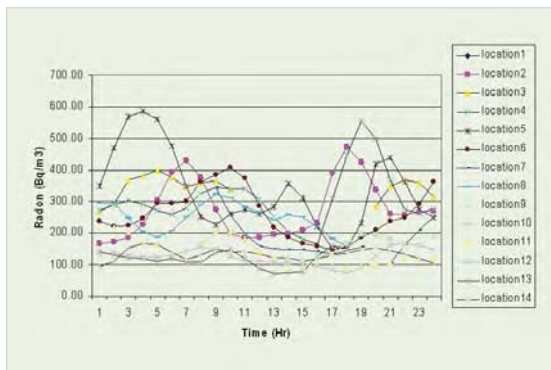


Fig. 12: Radon levels monitored at various locations inside Uranium mines

Summary and Conclusions

Different versions of online radon and thoron monitors have been developed using ZnS(Ag) detector for applications in front end nuclear fuel cycle. Special features of these monitors include low cost, high sensitivity and non- interference of humidity and trace gases. The performance of these monitors were tested successfully both in laboratory and field conditions. They find wide applications for networked based radon monitoring in U mines, tailings pond region and stack monitoring of thoron release in a thorium processing facility. Being highly sensitive, they can also be used for ambient measurements such as radon/thoron monitoring in dwellings, radon exhalation measurements, thoron emission measurements from monazite sands etc. These

indigenous monitors will serve as import substitutes for the Indian radon/thoron research programmes.

Acknowledgements

The authors would like to thank Mr.. H.S. Kushwaha, Ex-Director, HS&EG and Dr. A.K. Ghosh, Director, HS&EG, BARC, for their constant encouragement and support towards this work.

References

1. Abbady A, Abbady AG, Michel R., Indoor radon measurement with the Lucas cell technique, *Appl Radiat Isot.*, 61(6) (2004):1469-1475.
2. Lucas F.H. Improved low-level alpha-scintillation counter for radon. *Rev. of Sci. Inst.*, 28 (1957): 680-683.
3. Sahoo BK, Mayya YS. Two dimensional diffusion theory of trace gas buildup in soil chambers for flux measurements. *Agric. and Forest Meteorol.* 150 (2010):1211-1224.
4. Sahoo BK, Nathwani D, Eappen KP, Ramachandran TV, Gaware JJ, Mayya YS. Estimation of radon emanation factor in Indian building materials, *Rad. Meas.* 42 (2007): 1422-1425.

Formal Model Based Methodology for Developing Software for Nuclear Applications

A. Wakankar, R. Mitra , A.K. Bhattacharjee, S.V. Shrikhande,
S.D. Dhodapkar, B.B. Biswas and R.K. Patil
Reactor Control Division

Abstract

The approach used in model based design is to build the model of the system in graphical/textual language. In older model based design approach, the correctness of the model is usually established by simulation. Simulation which is analogous to testing, cannot guarantee that the design meets the system requirements under all possible scenarios. This is however possible if the modeling language is based on formal semantics so that the developed model can be subjected to formal verification of properties based on specification. The verified model can then be translated into an implementation through reliable/verified code generator thereby reducing the necessity of low level testing. Such a methodology is admissible as per guidelines of IEC60880 standard applicable to software used in computer based systems performing category A functions in nuclear power plant and would also be acceptable for category B functions.

In this article, we present our experience in implementation and formal verification of important controllers used in the process control system of a nuclear reactor. We have used the SCADE (Safety Critical System Analysis & Design Environment) environment to model the controllers. The modeling language used in SCADE is based on the synchronous dataflow model of computation. A set of safety properties has been verified using formal verification technique.

Introduction

The approach used in model based design is to build the model of application in some modeling language and then obtain the implementation in a programming language automatically using code generator. In older model based approach (e.g. UML tools [1]), the correctness of the model is mainly established by simulation. However simulation cannot guarantee that the design meets the system requirements under all possible scenarios. This is possible only if the modeling language is based on formal semantics and the model can be subjected to formal verification of system properties, which are derived from system requirements. Verification

of these properties establishes that the model meets the system requirements. Such a model driven design methodology where the modeling language has formal semantics and environment supports formal verification of properties is termed here as Formal Model Based Design Approach [2].

The advantage of this approach is that, any change in the requirement can be directly introduced in the model and verified (both via simulation and formal verification) before code is generated automatically, thereby keeping the implementation in sync with the design. This is a significant advantage in implementing change requests.

Such methodology for the development of software used in safety class applications conforms closely to the design guidelines recommended by IEC60880. In fact since it is possible to rigorously verify safety properties, the design process can meet most of the guidelines in appendix E of IEC60880. Since use of formal model based technique represented methodology change, it was decided to carry out implementation for two important controllers for which earlier implementation existed for comparative purposes. SCADE [5], a model based design environment was chosen for this purpose. SCADE supports a graphical modeling language having an underlying formal semantics defined on synchronous dataflow model of computation. The SCADE environment also supports model simulation, model test coverage (MTC) analyzer, formal verification tool and certified code generator. It allows model verification through interactive simulation and formal verification. Another important aspect is that the SCADE models are built using graphical notation that is easily understood, thus greatly helping to simplify review of models by control engineers.

Two controllers viz Steam Generator Pressure Controller (SGPC) and Primary Heat Transport Pressure Controller (PHTPC) were selected for implementation. These controllers were earlier implemented using conventional software development techniques and are in actual use. In that way it was possible for us to compare the effectiveness of the new technique. The complete development process was followed which included modeling, simulation, test coverage measurement and code generation. This was followed by testing in target hardware with I/O simulation. For the verification of safety properties the SCADE Design Verifier was used. Two controllers were implemented using SCADE but only SGPC controller is described herein.

Background

Process Control Systems in Nuclear Reactor

The objective of SGPCS (Steam Generator Pressure Control System) [8, 9] is to regulate the steam generator (SG) pressure by controlling the total amount of steam drawn from the SG. The heat input to the SG through Primary Heat Transport system is a function of reactor power, which is controlled independently. When the energy in the steam drawn from SG equals the energy released from reactor fuel into the primary coolant, the primary fluid temperature and steam temperature (and hence the pressure) are maintained at steady values. The steam pressure regulation is achieved by controlling the valves in various steam lines taking steam to either the turbine (turbine governor valves TGVs) or dumping into condenser (condenser steam dump valves CSDVs) or discharging to atmosphere (atmospheric steam discharge valves ASDVs). So the objective of the SGPC system is to generate the control signals for valves specified above. The control signal is generated by applying PID control algorithm to the error signal calculated based on the difference between measured SG pressure and operational pressure setpoint (OPSP). The operational pressure setpoint is function of reactor power and is calculated using no load setpoint (NLSP) and DT, the measured differential temperature across SG, which is a measure of reactor power. The main control signal is generated by applying PID control algorithm to the error, which is then split into three ranges to derive control signals for the three types of actuating valves i.e. TGVs, CSDVs and ASDVs. Since these controllers perform critical functions, the input measurements are triplicated /quadruplicated to provide redundancy.

SCADE Specification Language

The SCADE [5, 6] modeling notation supports Dataflow Equation and Safe State Machine for modeling the system. A dataflow equation describes the logical relationship between input and output variables. Safe state machine describes the control flow in the system in terms of state transitions. Set of dataflow equations are evaluated in parallel unless there is a data dependency between them. Internally the SCADE models are represented in SCADE textual language. SCADE textual language is based on the dataflow formalism, which is similar to the Synchronous dataflow language Lustre [4].

Synchronous languages [3] are based on synchrony hypothesis, which assumes that the program is able to react to an external event, before any further event occurs. In dataflow language a program is described as network of operators transforming flows of data. SCADE model is graphically represented as network of operators. For example a basic counter that counts up from 0 can be expressed in SCADE textual language as

$$N = 0 \rightarrow \text{pre}(N) + 1 \dots\dots\dots(1)$$

In above equation N is a variable that stores the value of counter at a given instance of time. The operator \rightarrow is called the “followed by” operator and it is used for initialization. Operator “pre” is used to refer to the value of variable at previous instant of time. Therefore the above equation specifies that the initial value of variable N is 0 and thereafter its value is one more than the previous value.

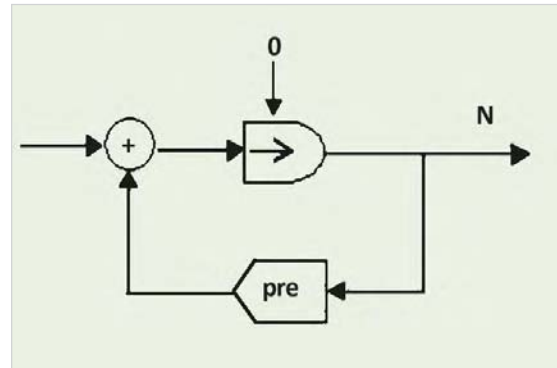


Fig. 1: SCADE Operator Diagram

SCADE model corresponding to above equation is shown in Fig.1. A network of operators in SCADE can be encapsulated as a new reusable operator that is called a node or SCADE operator. The requirements of the system to be implemented are mapped in the form of network of SCADE operators, where each operator provides a specific functionality independently or by interaction with the other SCADE operators.

SCADE Suite contains an editor for modeling the system behavior, a SCADE model simulator for validating the model with the help of test cases, a SCADE MTC module for accessing the coverage of the model during simulation (based on MC/DC structural coverage criteria) and a SCADE Design Verifier to apply formal verification technique for proving important properties of developed SCADE model.

SCADE Design Verifier supports formal verification based on model checking technique. The verification engine supports two kinds of verification; *debug mode*, which involves bounded model checking [10] and *proof mode* involving exhaustive verification. A property that is shown to be true in debug mode (bounded by

given depth) should not be assumed to be true under all possible cycles of execution. The proof strategy can take enormous amount of time (may not terminate in a bounded time) if the property is not verifiable within certain search depth because the system may have very large state space. The verification interface provides strategy options for terminating the search if the verification is not successful within a specified amount of time. It is to be noted that the property verifications reported in the later part of the paper were done using the *proof mode*.

Development of the Model for SGPCS in SCADE

The processing logic of the SGPCS can be categorized as Signal Processing Logic and Control Logic

This is shown schematically in Fig. 2. For all the important processes parameters, triplicate or quadruplicate measurements are provided. Signal processing logic performs the validation of input signals and generation of “representative” (good) signal for each input parameter from multiple measurements rejecting where necessary any faulty measurements, to ensure reliable operation even in case of some sensor failures. Control logic involves the implementation of process control algorithm for SGPC system. The “representative” signals from signal processing logic are the inputs to the control logic and it generates the required control signal for Turbine Governor Valves (TGVs), Condenser Steam Dump Valves (CSDVs) and Atmospheric Steam Discharge Valves (ASDVs). The formal model has been developed in SCADE only for the Application Control Logic since this component could be cleanly substituted in old implementation without any other modification.

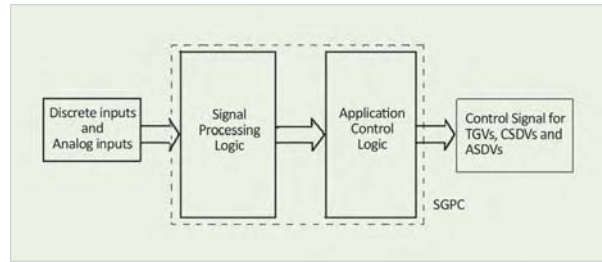


Fig. 2: SGPCS Inputs and Outputs

The equations expressing relationship between output and input variables were grouped and implemented graphically in SCADE as different nodes, according to the functionality they provide. In this way the SCADE model is modularized and these modules can be reused in other implementation. The representative signals for all the discrete and analog inputs that are used in the model are read from the interface of the signal processing logic already implemented in the existing code.

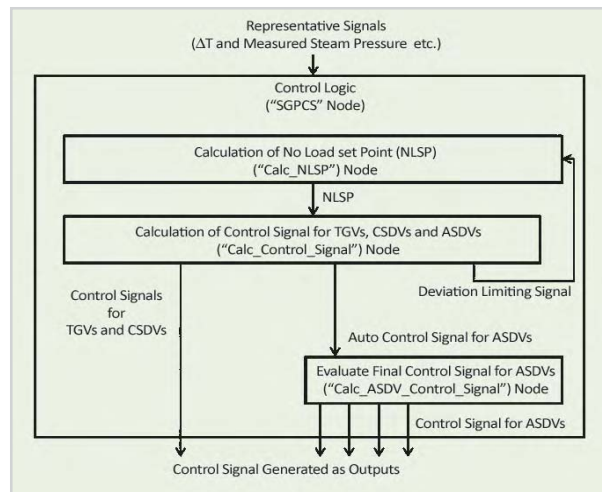


Fig. 3: SCADE Nodes and Data Flow

Control Logic is divided into nodes. The nodes, which generate actual control signals are Calc_NLSP, Calc_Control_Signal and Calc_ASDV_Control_Signal. The function of these nodes is to generate “No Load Set Point (NLSP)”, “Control Signal for TGVs and CSDVs” and “Control signal for ASDVs” respectively as shown in Fig. 3.

Calc_Control_Signal is the most complicated node because this node implements the algorithm for computation of pressure set point (OPSP) for SG and calculates the control signal by applying PID control algorithm to the error signal. The brief overview of node Calc_Control_Signal is depicted in Fig. 4.

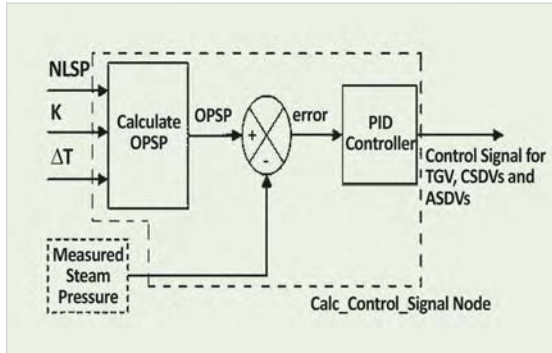


Fig. 4: Schematic of SCADE Node Calc Control Signal

The lower level nodes realize the control functionalities like PID control within Calc_Control_Signal, lookup tables and range conversion algorithms. Fig. 5 shows the hierarchical architecture of the SCADE model of SGPCS, along with the coupling among nodes and number of instances of each node.

Validation of SGPCS model

The validation of SGPCS model is done by simulating the SCADE model. We have to apply a sequence of input vectors to test a given system behavior. The trend of outputs with the applied input sequence is observed and compared with the expected outputs, for analyzing the correctness of the model. Each test sequence that may expand over several cycles is stored as a separate scenario file. The scenario file stores the value of all the input vectors applied during each cycle. The scenario files are useful to automatically regenerate the previously conducted test whenever required.

To assess how thoroughly the behavior of the

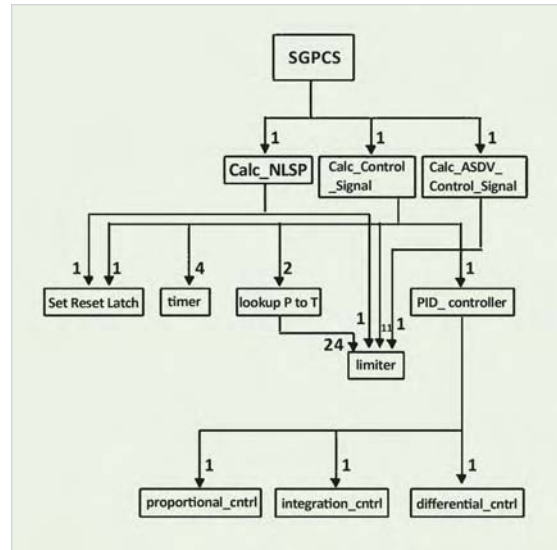


Fig. 5: Hierarchical architecture of SCADE model of SGPCS

model is simulated, we have used Model Test Coverage (MTC). MTC is a SCADE Suite module, which allows measuring the coverage of model during model simulation activity. SCADE MTC analyzer uses MC/DC [7] structural coverage criteria to assess the model coverage. The MTC is done by using the scenario files stored during the model simulation. The use of scenario files ensures that the same test cases are applied during simulation and MTC. Hence the coverage results observed after MTC shows that how extensively the behavior of the model was simulated and points out the part of the model that was not covered during model simulation. We can then design new test cases for covering those parts of the model that are not covered. By applying test cases as per the previously prepared test plan, we could achieve 97 percent model coverage.

From the analysis of the operators that were not tested using the test plan, we designed new test cases for increasing the model coverage. An example for derivation of such a test case can be illustrated using the Fig.6. Each operator in the figure is labeled with an instance number to distinguish between two instances of same

operator. So to identify each operator uniquely during illustration, we have used operator name followed by its instance number e.g. the AND operator labeled with instance number 2 will be depicted as AND2. Similarly the inputs of each operator are identified as I1, I2...In, depicting 1st, 2nd ... nth input respectively. In the figure below MTC shows that the operator AND2 is not covered completely. According to the MC/DC criteria the three input AND gate, having inputs I1, I2 and I3 is said to be covered completely if the following conditions are simulated.

- I1, I2 and I3 are true
- Only I1 is false
- Only I2 is false
- Only I3 is false

The coverage analysis shows that, for the operator AND2 the condition “Only I2 is false” was not simulated. From the Fig.6 it could be determined that to simulate this condition, we should have an input combination where NOT(ASDV_auto) is true, NOT(ASDV_HC) is true, NOT(ASDV_CM_raise) is false, NOT(ASDV_auto) is true, NOT(ASDV_HC) is true, ASDV_CM_lower is true, pre F is true, Rm¹ ST is true, pre F is true.

is false and ASDV_CM_raise is true. This derived input test vector is added to the test plan to increase the model coverage.

We have also observed that some conditions required to completely cover the operator according to MC/DC criteria were physically infeasible. Fig.7 shows one such condition. The MTC in this figure shows that the operator AND6 is not covered because the condition “only I1 is false” was not simulated. To simulate this condition, input I1 for operator AND6 should be false keeping inputs I2 and I3 as true. I2 for the AND6 is output of operator timer1. The output of timer1 operator becomes true only if input is true for specified time interval or more; otherwise its output is false. So it can be determined that if I1 is false then output of timer1 will be false and hence I2 will also be false i.e. whenever I1 is false, I2 will also be false. So we cannot design test case, which simulates the condition “only I1 false” for the operator AND6.

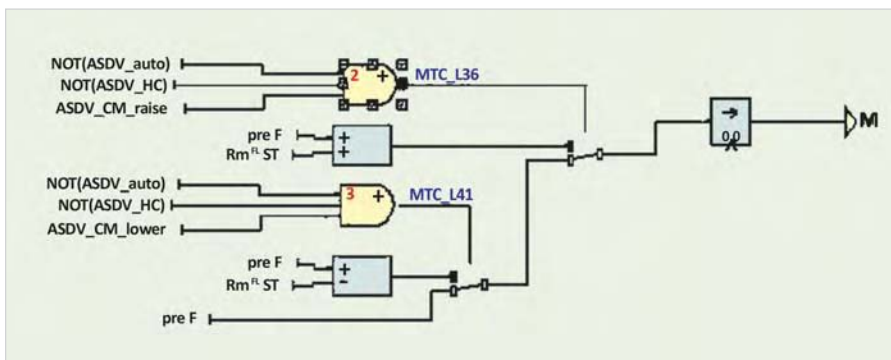


Fig. 6: Derivation of Test Case from the Result of MTC

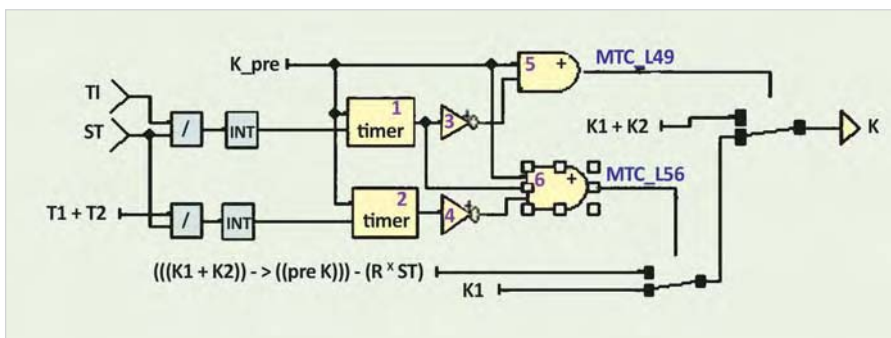


Fig. 7: Part of Calc_Control_Signal node

Infeasible scenarios as described above had to be left out and hence it was possible to achieve 99.8 percent model coverage.

Formal Verification of Requirements of SGPCS

The verification of the SGPCS model was carried out by using the formal verification technique called model checking. It involves expressing a system requirement as a property and checking whether property is satisfied by the model. Each of the properties to be verified was modeled as an “observer node” using built-in SCADE verification operators. The composition of “observer node” with the system model was used for model checking using the SCADE Design Verifier.

Some of the important system properties of SGPCS that were formalized and verified are explained below. Each property is first stated in English as it appears in specification followed by brief explanation. Later the property is stated formally using SCADE notation and explanation is provided whenever required.

Property1

If manual_crash_cool or auto_crash_cool signal is true then No Load Set Point (NLSP) should decrease till lower saturation limit (100.0) is reached.

The signals **manual_crash_cool** and **auto_crash_cool** are two discrete inputs, which are used to maneuver the pressure setpoint (NLSP) during some emergency condition. If at least one of these inputs is true then NLSP is decreased till the limiter clamps the value of NLSP to 100.0

Formal Specification of the property1 in SCADE is shown in Fig. 8. In figure, the block “verif::implies” implements the mathematical implication (p!q). The first input denotes ‘p’ and second input denotes ‘q’. The output of the block is true if (p!q) holds. The output of this block is assigned to the Boolean output property1.

Property 2

If NLSP_lower and NLSP_raise both signals are true then NLSP should decrease till lower limit (100.0) is reached.

The signals **NLSP_lower** and **NLSP_raise** are discrete inputs used to lower and raise the value of NLSP respectively, however if both the signals are true simultaneously then **NLSP_lower** signal must have a higher priority over **NLSP_raise**.

Formal Specification of the property2 is shown in Fig. 9.

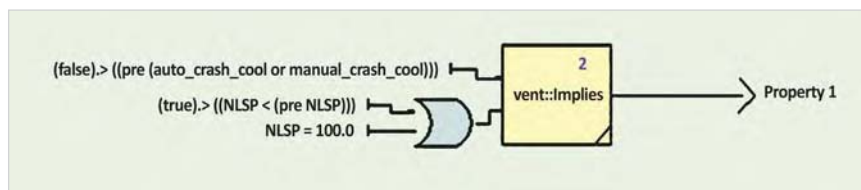


Fig. 8: SCADE Observer for Property1

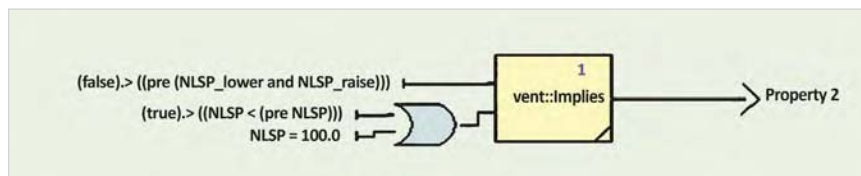


Fig. 9: SCADE Observer for Property2

Property3

If the *loss_of_electric_load* or *turbine_trip* signal is true and reactor power exceeds 20% Full Power then Anticipatory Action (AA) should start and should get completed in time $T1+T2$, where $T1$ and $T2$ are predefined constants. AA lowers the operational set point (OPSP) in proportion to reactor power based on the following equation.

$$OPSP = NLSP - K *DT \dots\dots\dots(2)$$

The variation of K before, during and after AA is shown in Fig.10, where $K1$ and $K2$ are positive constants.

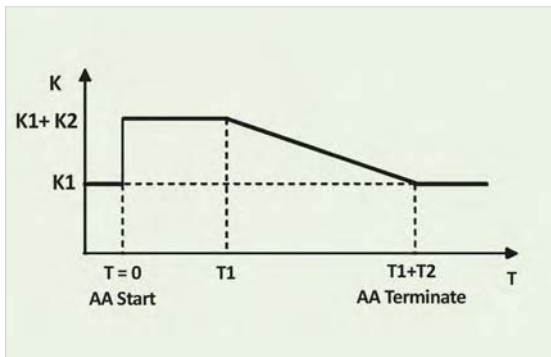


Fig.10: Timing diagram for Anticipatory Action

The signals **loss_of_electrical_load** and **turbine_trip** are the discrete inputs to the SGPC model, which decide the condition for start and termination of AA

In SCADE, the time is measured in terms of number of execution cycles. The number of execution cycles in time $T1+T2$ can be determined by dividing time $T1+T2$ by sampling time (0.175 sec). The value of $T1$ and $T2$ is 1 and 2 respectively. Hence the number of execution cycles is $(1+2)/0.175 = 17.14 = 17$. However Fig.10 shows that the value of K at the first and last cycles is equal to $K1$. Therefore the number of cycles during which AA will be present is two less than the calculated number of cycles in time $(T1+T2)$. Hence AA should appear for $(17-2) =15$ cycles”.

Formal Specification of the property3 in SCADE is shown in Fig.11. In figure the block $\text{if_else}(C1, I1, I2, O1)$ specifies an if-else condition as “ $O1 = \text{if } C1 \text{ then } I1 \text{ else } I2$ ”. The block `verify::AfterNthTick` is used to express that the output equals input, except for the first N ($N=1$) cycles during which the output is true. The block `verify::AtLeastNTicks` express that the output equals the input as soon as the input is true for $N=15$ cycles, before that the output is false. Similarly the block `verify::HasNeverBeenTrue` is used to express that the output becomes false as soon as its input becomes true for the first time, after this cycle the output remains false.

Property 4

Anticipatory action is discontinued after a reactor trip or when both initiating conditions i.e.

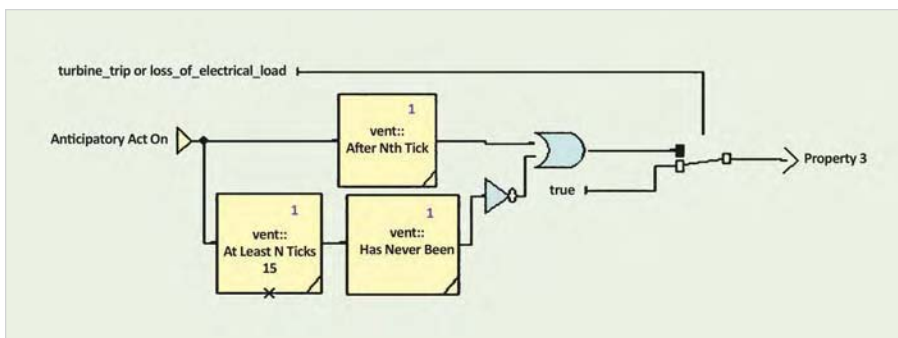


Fig.11: SCADE Observer for Property3

loss_of_electrical_load and *turbine_trip* are not true.

This property specifies the condition for the termination of anticipatory action. Thus if required condition for anticipatory action does not exist or if it disappears then anticipatory action will terminate.

The formal specification of the property4 in SCADE is shown in Fig.12.

Property5

If ASDV is in computer manual mode (i.e. ASDV is neither in auto mode nor in hand controller mode) and

- a) *ASDV_CM_raise is true and ASDV_CM_lower is false then ASDV_control_signal will increase.*
- b) *ASDV_CM_raise and ASDV_CM_lower both are true then ASDV_control_signal will remain unchanged.*
- c) *ASDV_CM_raise is false and ASDV_CM_lower is true then ASDV_control_signal will decrease.*

The final control signal for ASDVs is calculated based on the mode of operation. ASDVs can be in one of the three modes: *auto*, *hand control* or *computer manual*, which are selected from a three-position switch. Hence in the model the

mode is determined by two input variables **ASDV_auto** and **ASDV_HC**. If input **ASDV_auto** is true then mode is auto, if input **ASDV_HC** is true then mode is hand controller and if both inputs are false then mode is computer manual. Inputs **ASDV_CM_raise** and **ASDV_CM_lower** are used to raise and lower the **ASDV_control_signal** respectively.

The formal specification of the property5 in SCADE is shown in Fig. 13. The property could not be proved and a counter example was generated. The property could not be proved because the specification does not place any restriction on mode of ASDV in the instant before coming to computer manual mode. Therefore if in the previous instant the mode was other than computer manual the control signal values before and after mode change do not conform to the property specification. The model was later corrected to implement the bumpless transfer functionality.

The time required for verification of these properties was found to be less than 10 seconds on a XEON Server with 4GB RAM.

Code Generation and Integration

SCADE environment provides IEC61508 SIL3 certified automatic code generator (KCG). The verified model was used to generate the C code automatically. The use of certified code

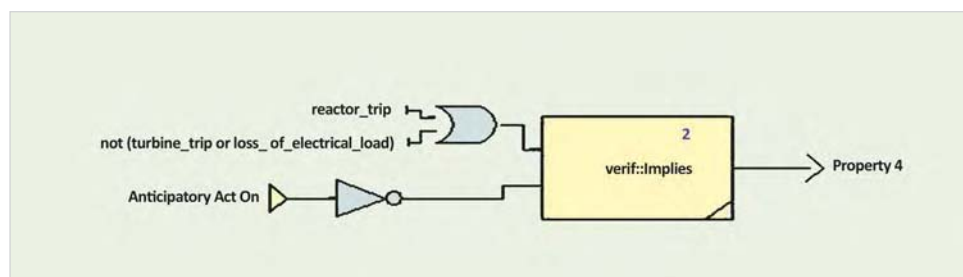


Fig.12: SCADE Observer for Property4

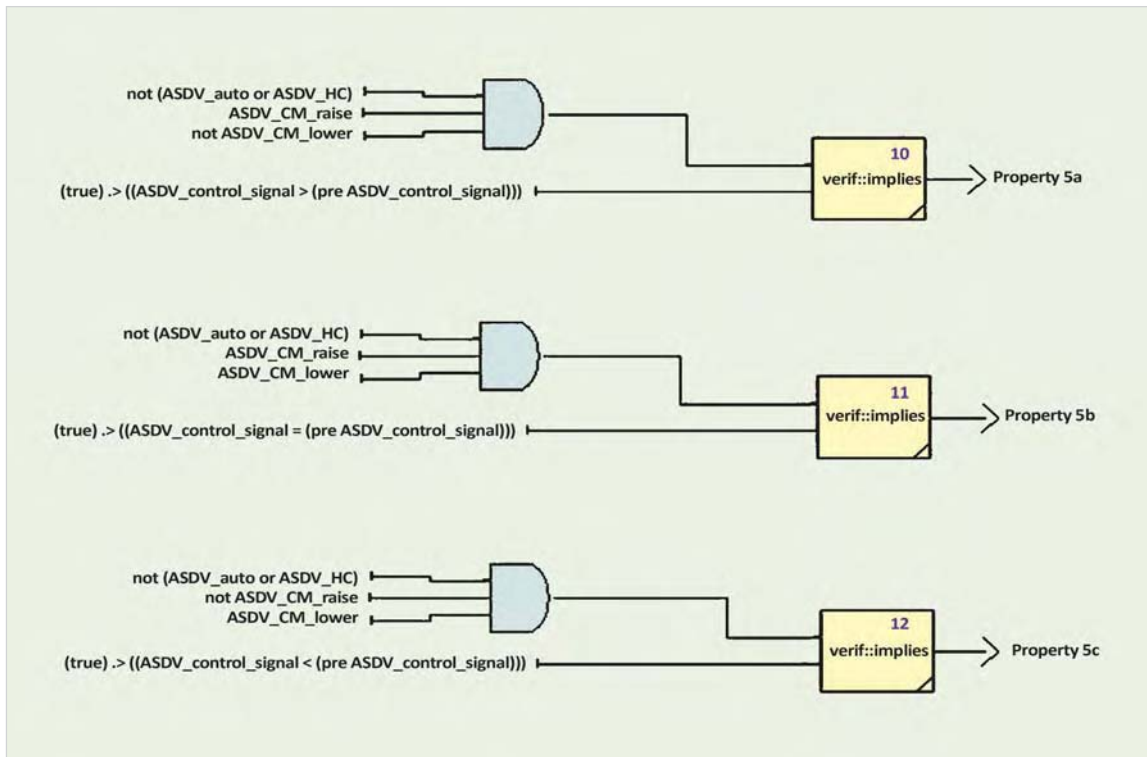


Fig.13: SCADE Observers for Property5a, Property5b and Property5c

generator ensures that every specification in the model is correctly reflected in the code, which eliminates the need for unit testing.

The SGPC module developed using SCADE was integrated with prototype system in the lab. This was done by replacing old handwritten SGPC code by the one developed with SCADE.

Two identical hardware based controller setups were available. One was loaded with the old handwritten SGPC code. This implementation is in use for several years. The other controller was loaded with automatically generated code from the SCADE model. There was no discrepancy observed in the output of these two systems during testing.

The final size of the executable generated was ~163 KB whereas the size of old executable was ~167 KB, which was comparable.

Conclusion and Future work

This methodology is suitable for the systems whose output behavior involves cyclic executions of *read, compute and output*. Software based controllers used in embedded control applications typically fall in this class of systems. It has been our experience that it is quite easy to adopt the methodology in the design life cycle of such software and comply with the recommended practices of IEC60880. This is because the SCADE environment supports a formal language and has tool support for testing the model conforming to MC/DC structural coverage and formal verification. The availability of IEC 61508 SIL3 certified code generator has reduced the code generation effort to a *push button* and there is no effort required for low level testing. It must be emphasized that once the model is validated and code is generated from the model, it is not recommended to do any manual changes

in the generated code. The availability of certified code generator is a great advantage over the other traditional development methodologies (e.g. UML) involving modeling language having less formal semantic foundation. The lack of semantics in such modeling language hinders complete automated code generation and hence no certifiable code generation is possible for the entire modeling language.

During formal verification, it was observed that most of the time was spent on reviewing property expressed in SCADE with corresponding English specification. Although the tool supports an easy to use interface to the back end verification engine, the user is expected to know the limitations of formal verification of systems involving integer, real and nonlinear arithmetic.

SCADE supports predefined operators for specifying verification conditions. However formal logics such as LTL are more expressive and it is possible to express properties much more succinctly in these notations. For example, the property 3, in section V.C, could have been specified as $(s \rightarrow (p \mathbf{U}_{15} q))$, where s is the initiating event (turbine trip or loss of electrical power), p is the Boolean condition for anticipatory action and q is the Boolean condition signifying the end of anticipatory action. The sub-expression $p \mathbf{U}_{15} q$ in the verification condition demands that p is true for 15 ticks and henceforth q is true and the complete property states that if s is true and remains true then p shall remain true for 15 ticks and subsequently q shall remain true. It is felt that such properties are difficult to express using standard SCADE blocks. SCADE does not support a tool that can translate specifications in such logic as explained above into equivalent SCADE property observers. We are now working on to develop such a property synthesis tool and integrate in the SCADE environment.

Acknowledgements

We are thankful to Shri G.P. Srivastava, Director E&I Group for his encouragement during this work. We are thankful to Shri C.K. Pithwa, Head, ED (earlier Head, CCDS, RCnD), for providing us the initial specification of SGPCS from which the formal model has been developed. Thanks are also due to Mrs. Ratna Bhamra for helping us to understand the initial specifications.

References

1. Unified Modeling Language <http://www.omg.org/technology/documents/formal/uml.htm>.
2. A. Wakankar et. al., Formal Model Based Methodology for Developing controllers for Nuclear Applications, Proceedings of 20th IEEE International Symposium on Software Reliability Engineering (ISSRE-2009), Mysore, India.
3. N. Halbwachs, Synchronous programming of reactive systems. Kluwer Academic Pub, 1993.
4. N. Halbwachs, P. Caspi, P. Raymond and D. Pilaud, The synchronous dataflow programming language Lustre. Proceedings of the IEEE, vol. 79(9). September 1991.
5. SCADE Tool <http://www.esterel-technologies.com/>.
6. SCADE Language Reference Manual, Ver 6.1, Esterel Technologies Ltd., France
7. SCADE User Manual, Ver 6.1, Esterel Technologies Ltd., France
8. S. Glasstone and A. Sesonske Nuclear Reactor Engineering, Chapman & Hall, New York.
9. Software Requirement Specification for DPHS-PCS Rev 2 USI 63000 Internal Document RCnD, BARC, Feb. 2005
10. A. Biere, et.al., *Bounded Model Checking* Vol. 58, Advances in Computers, 2003 (Academic Press).

Development of Digital Radiotherapy Simulator: A Device for Tumour Localization, Radiotherapy Planning and Verification

D.C. Kar, R. Sahu, K. Jayarajan, D.D. Ray and Manjit Singh

Division of Remote Handling and Robotics

Abstract

Radiation therapy is one of the established modes of cancer treatment. For the safe and effective radiation therapy, it is necessary to plan and deliver the radiation beam accurately. Radiotherapy Simulator helps in identifying the organs at risk and in localising the cancer-affected tissues. For teletherapy, the Simulator would also help in choosing the right radiation beam and aiming it at the target. Although, radiotherapy simulator is an essential tool for improving the quality of teletherapy, there is acute shortage of such machines in our country due to the high cost of the imported units and the lack of indigenous technology. In fact, many cancer hospitals with teletherapy units do not have radiotherapy simulator. Considering the growing incidence of cancer and the need for such devices, Bhabha Atomic Research Centre (BARC), Mumbai has recently developed a Radiotherapy Simulator. This article briefly describes some of the features of the indigenous Radiotherapy Simulator.

Introduction

Cancer is a major health concern in our country, and majority of the patients require radiotherapy during the course of treatment. Radiotherapy simulator is a machine that helps in radiotherapy planning, prior to the treatment delivery. It helps to diagnose the physical extent of the tumour and its relation to the surrounding tissues for proper selection of the size and orientation of the radiotherapy beams. It also helps to plan the treatment, to protect the critical organs adjacent to the tumour to be treated. The capability of a simulator for real-time review of the images and their analysis helps in accurate planning and verification in a short time. Advances in acquisition, storage and transfer of images have dramatically improved the image quality leading

to improved performances in radiation therapy planning [1].

In India, there is wide gap between the demand and availability of radiotherapy facilities [2]. Among the few centres with teletherapy facilities, many do not have radiotherapy simulator for accurate delivery of radiation therapy. They generally depend on conventional radiography units for tumour localization.

In the conventional form, a radiotherapy simulator is similar to an isocentric external beam therapy machine. It can reproduce the geometric movements of (external beam) radiotherapy machines. However, unlike a teletherapy machine that delivers high-energy radiation beams for treatment, a radiotherapy simulator

uses diagnostic X-ray beams for imaging, either in radiography or fluoroscopy mode. Unlike the complex CT-Simulators, which performs virtual simulations, radiotherapy simulators are less expensive, and easy to operate and maintain [3]. The conventional design of Radiotherapy Simulator does not pose any restriction on the size of the patient.

Considering the growing requirement for such machines in our country, BARC has initiated the development of radiotherapy simulator. The development is successful and the first indigenous



Fig. 1: Indigenous Radiotherapy Simulator installed at Indian Red Cross Society Hospital, Nellore, AP

unit is installed in Indian Red Cross Society Hospital, Nellore, Andhra Pradesh (Fig. 1). This article describes the development in brief.

Brief Description of the Unit

Major sub-systems in the radiotherapy simulator are gantry, collimator, X-ray tube, imaging unit, patient support/positioning system, and remote control console. The schematic layout of the machine is shown in Fig. 2.

Gantry

The Gantry consists of a C-arm, which can rotate about the longitudinal axis passing through the isocentre. One end of the C-arm holds the

collimator subassembly and the X-ray tube. The imaging subsystem is mounted on the other end of the C-arm. The collimator sub-assembly can move radially closer to or away from the isocenter to change the focus to axis distance (FAD). This helps the simulator to adapt with teletherapy machines of different source to axis distances. The image intensifier arm also can move radially closer to or away from the isocenter. This helps in capturing images with varying magnifications and avoiding collision between the image intensifier and the couch, during continuous gantry rotation.

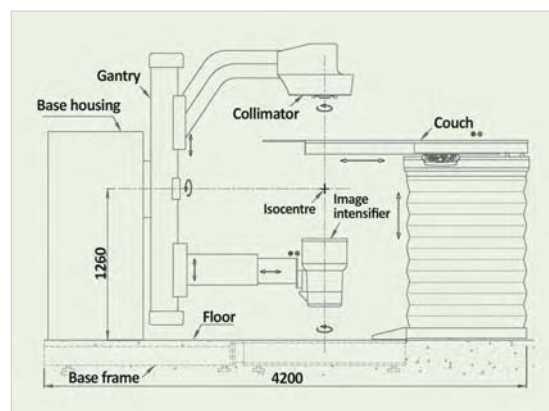


Fig. 2: Schematic layout of the Radiotherapy Simulator

Collimator

The aperture control mechanism or the collimator provides a rectangular opening of the X-ray beam. Each side is independently controlled to generate an arbitrary rectangular radiation field. Both pairs of the jaws can be moved in symmetric as well as asymmetric mode. The collimator is designed with over-travel to suit the latest radiation therapy units. Four independently actuated delineator wires are provided to define the tumour boundary within the radiation field (Fig. 3). The collimator assembly can also be rotated about an axis orthogonal to the gantry rotation axis, passing through the centre of the X-ray beam.

To visualize the projection of the X-ray field on the patient's skin, a field light projection mechanism is used. An optical distance indicator (ODI) system is also mounted on the collimator to facilitate measurement of focus to skin distance by projecting an optical scale on patient's body.

X-ray Tube

The X-ray Tube is of rotating anode type with dual focal spots (0.4mm, 0.8mm) for sharper image. It has high heat storage capacity for

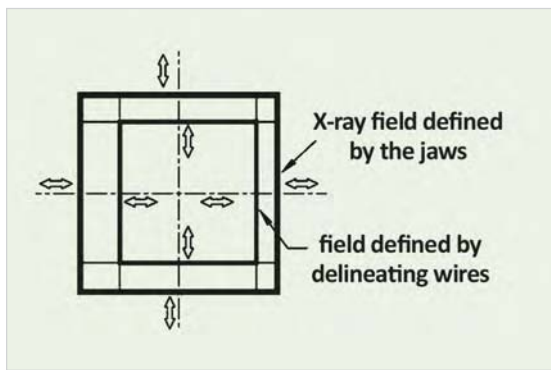


Fig. 3: Schematic layout of the collimated field

uninterrupted usage. 15° anode angle is adequate to cover X-ray field sizes required for radiotherapy simulation applications.

Imaging Sub-system

The imaging subsystem consists of a 12" tri-field image intensifier coupled with 1024 x 1024 - pixel CCD camera system. It provides sharp digital images in fluoroscopy as well as radiography mode. It is interfaced with microprocessor-controlled HF generator for quick image processing. Automatic exposure control ensures uniformity in dose per image. The camera-lens assembly captures the images and passes in digital form. The image intensifier support arm has two orthogonal (lateral and longitudinal) motorized motions for remote and interactive positioning of the image intensifier at the region of interest.

Couch

The patient support/positioning system or couch is a pit-mounted, isocentric platform with four independently actuated motions: vertical linear, lateral linear, longitudinal linear, and isocentric rotation. It has a radio-transparent thin sheet of carbon-fibre composite mounted on the top. The couch platform can be lowered to a level convenient for the patient to lie down. Two keypads (Fig. 4) are mounted on either side of the couch at convenient locations for interactive patient setup. All the motions of the gantry, collimator, and the image intensifier support arm can be controlled through these keypads as well as from the remote control console. The values of important positioning parameters are displayed on the wall-mounted display monitor. The patient remains immobilized during simulation with the help of restraining straps,



Fig. 4: Keypad located on the sides of the couch

blocks, masks etc to minimize patient's motion during simulation. This couch also has the provision for the use of indexed positioning devices for fast and accurate reproduction of a setup.

Control Console

The control console is located at a remote location outside the simulator room. After immobilizing the patient on the simulator couch, the operator leaves the room, and operates the machine from this console. The control console consists of a desktop computer, a mouse,

a physical key switch, and two buttons for activating the X-ray beam. One more desktop computer is used for display and storage of the acquired images. The operator can control all the unit motions, viz. gantry, collimator, imaging arm and the couch, through the graphical user interface as shown in Fig. 5. The digital readouts for all the motions remain displayed on the console. For imaging, the operator can select one of the two modes : *fluoroscopy* or *radiography*. In fluoroscopy mode, the live images of any moving organ can be viewed. This mode can also be used while one or more unit motions are active, for determining appropriate beam (for therapy) directions. Static anatomical images can be captured in the radiography mode. For either of these modes, the operator can select the exposure parameters, such as kV, mA and mAs.

Important features viz. automatic correction of image distortion, last image hold, MLC (multi leaf collimator) overlay, DICOM (digital image communications in medicine) compatibility, storage and management of acquired images, annotations, image manipulation and viewing tools, printing etc. are implemented for the convenience of the user as well as smooth workflow.

Auxiliary sub-systems

Patient Positioning Lasers

Accurate patient positioning is essential for effective treatment simulation. The laser system consists of three linear red diode lasers: two in cross planes and one in sagittal plane. It is similar to the laser system used for teletherapy machines. The projections of these lasers mark the isocentre, which serves as the reference for

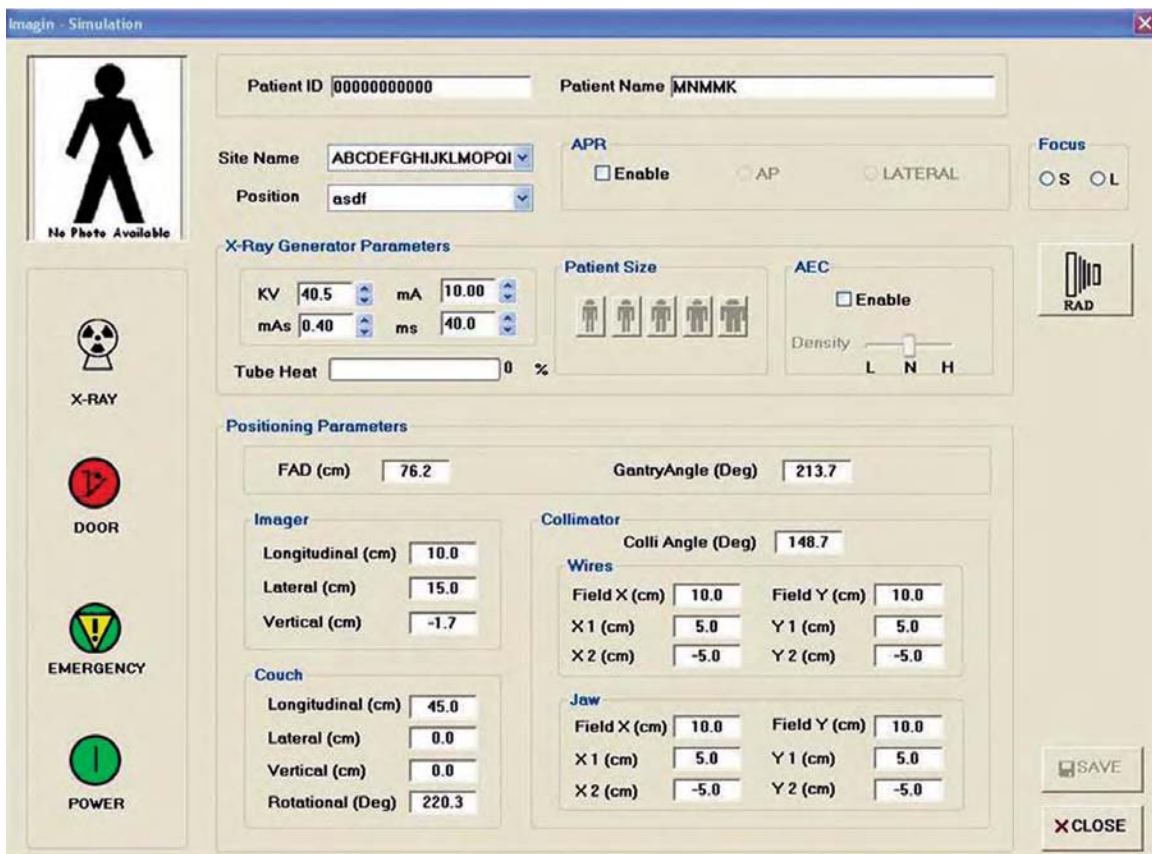


Fig. 5: Graphical user interface at the control console

various setup parameters in order to reproduce exact positions on treatment machines.

Safety Interlocks and Emergency Stop Buttons

Many safety interlocks are provided to protect the patient and the operators from unwanted exposure to radiation. These include door interlock of the treatment room (to prevent exposure by accidental opening of door), external mains power supply interlock and emergency interlock (due to fault in any of the unit motions). Emergency stop buttons are installed in the base housing, couch, door, control console and on the passage wall inside the room.

Visual Monitoring

Radiotherapy simulation requires special rooms with adequate shielding to protect the operating personals, the public as well as the environment from the harmful effects of ionizing radiation. During simulation, the patient is monitored continuously from the control console through the lead-glass window.

Wall Mounted Display

A monitor in the treatment room displays important parameters related to the machine. Whenever an authorized user logs into the system, system parameters like FAD, image intensifier distance, gantry rotation angle, collimator rotation angle, positions of the collimator blades, delineator wires, couch longitudinal, lateral, vertical and isocentric rotation etc. are displayed in the monitor.

Technical Specifications

Gantry Rotation	
At FAD=100cm (°)	± 185
Isocenter height (cm)	128
Max. Speed (rpm)	1
Auto stops (at deg)	± 90 & ± 180
Anti-collision	Logic
Focus to Axis Distance (FAD)	
Range (cm)	80-120
Auto stop at FAD(cm)	80,100,120
Max. Speed (cm/min)	100
Collimator	
Rotation (deg)	± 95
Max. Speed (rpm)	1.0
X-ray field (delineators)	
Field size (cm x cm)	45 x 45 (max.)
Jaw motions	Independent
Max. overtravel (cm)	20
X-ray field (shielding jaws)	
Field size (cm x cm)	0.5 x 0.5 to 50 x 50
Independent jaw motion	Yes
Over travel (cm)	20
Pairing delineators	Yes
FAD tracking	Yes
Image Intensifier Arm	
Support Arm Motions	
Longitudinal (cm)	±20
Lateral (cm)	±20
Radial (cm)	0 to 60
Auto recenter	Yes
Max. speed (cm/sec)	2.5
Anti-collision	Logic
X-Ray Generator	
Power (KW)	65
KV Peak (KVp)	
Fluroscopy	40-125
Radiography	40-150
Milli Amperage (mA)	

Fluoroscopy	1-20
Radiography	1-800
Power Supply	400VAC, 3phase

X-Ray Tube

Focal Spot Size (mm)	0.4, 0.8
Target Angle (deg)	15
Heat Storage Capacity (KJ)	280

Image Intensifier

Tri-Field (max dia., mm)	290
Contrast Ratio	13:1
Conversion Factor	240 ((cd/m ²)/(mR/s))
Central Resolution(lp/cm)	44

Couch

Motions	
Vertical(cm, from floor)	68-135
Vertical speed (cm/min)	60, 110
Longitudinal (cm)	90
Longitudinal speed(cm/min)	35, 200
Lateral (cm)	±20
Lateral speed (cm/min)	35, 200
Isocentric Rotation (deg)	±95
Anti-collision	Logic
Auto Setup	Yes
Table top	
Carbon fibre	Yes
Transmission (mm,eq.Al)	1.0
Deflection (mm, at 90 Kg)	<2.0
Load capacity (Kg)	135

Software

PC operating System	WinXP/2000
Storage of digital images	Yes
Network Mode	DICOM
Calibration facility	Yes
MLC overlay on image	Yes
Image processing tools	Yes

Quality Assurances and Regulatory Compliances

Radiotherapy simulator has major influence on the overall performance of the radiation therapy process. Although not used directly for the dose delivery, its role is important in determining the target location, treatment planning and spatial accuracy in dose delivery. As the simulator has many features of therapy machine and diagnostic radiology unit, it has to conform to requirements of both the applications.

The unit is tested and is found to be conforming to the International Electrotechnical Commission (IEC) Standards [4-6]. The machine will be used clinically, after the clearance by Atomic Energy Regulatory Board (AERB).

Conclusion

The technology for our indigenous radiotherapy simulator is developed successfully. The first machine is installed in Indian Red Cross Society Hospital, Nellore, Andhra Pradesh. This computer-controlled machine is simple and user-friendly. Other features of the machine, such as filmless operations and ease of transfer and storage of digital images can streamline the workflow and improve overall performances of the department. The indigenous machine is less expensive, compared to imported simulators. Therefore, smaller radiotherapy centres, especially those at remote places, will be able to afford this simulator, leading to safer and more effective radiation dose delivery.

References

1. Cho, P. S., Lindsley, K. L., Douglas, J. G., Stelzer, K. J., and Griffin, T. W. (1998), Digital Radiotherapy Simulator,

- Computerized Medical Imaging and Graphics*, Volume 22, pp.1-7.
2. Jayarajan K., Kar D.C., Sahu R and Singh Manjit, Bhabhatron: An Indigenous Telecobalt Machine for Cancer Treatment, *BARC Newsletter, Founder's Day Special Issue*, Issue No 297, October 2008, page 27-34.
 3. Suhag V., Kaushal, V., Yadav, R., and Das, B. P. (2006), Comparison of Simulator- CT versus simulator fluoroscopy versus surface marking based radiation treatment planning: A prospective study by three-dimensional evaluation, *Radiotherapy and Oncology*, Volume 78, pp.84-90.
 4. IEC 60601-1 – Medical Electrical Equipment- Part 1: General Requirements for Basic Safety and Essential Performance, Edition 3, 2004, *International Electrotechnical Commission*, Geneva
 5. IEC 60601-2-29 - Medical Electrical Equipment- Part 2: Particular Requirements for the Safety of Radiotherapy Simulators, Edition 2, 1999, *International Electrotechnical Commission*, Geneva
 6. IEC 61168- Radiotherapy Simulators- Functional Performance Characteristics, Edition 1, 1993, *International Electrotechnical Commission*, Geneva.

National Conference on Advances in Nuclear Technology (ADNUTECH 2010): a report

A two-day national conference on Advances in Nuclear Technology (ADNUTECH 2010), organized jointly by the Department of Atomic Energy (DAE) and the Indian National Academy of Engineering (INAE) was held during December 2-3, 2010 at the Nabhikiya Urja Bhavan, Anushakti Nagar, Trombay. The Conference was aimed at highlighting the recent advances in the field of nuclear technology in India, including nuclear power scenario, emerging reactor technologies, nuclear instrumentation, control & computing, nuclear fuels and materials, laser, plasma and accelerator technologies, applications of radioisotopes in agriculture and healthcare. The Conference hosted eminent experts and academicians from the field of

nuclear technology in the country, who had been invited to deliver talks during various plenary sessions. Ms/s NPCIL and WIL were the corporate sponsors of the Conference. The Conference was attended by about 400 scientists, engineers, academicians and technocrats.

Welcoming the galaxy of scientists and technocrats, Shri V. K. Mehra, Director, Reactor Projects Group & Convener, ADNUTECH-2010, stressed on the significance of synergy between R & D efforts at various centres of the DAE and the industry, especially in the wake of a global nuclear renaissance.

Dr. P. S. Goel, President INAE, also addressed



Dr. S.K. Jain, CMD, MDCIL inaugurating the technical exhibition at ADNUTECH. Dr. R.K. Sinha, Director, BARC (extreme left) can be seen along with other senior scientists.



Welcome address by Shri V. K. Mehra, Director, Reactor Projects Group & Convener ADNUTECH

the gathering. He said that the INAE aims at promoting developments in engineering and sciences for their application to problems of national importance. He added that developments in the field of nuclear technology have proven to be of immense benefit to the society and the Academy would continue to support efforts in this direction.

Dr. R.K. Sinha, Director, BARC, in his inaugural address, spoke about various R & D initiatives taken up by BARC. Dr. Sinha reiterated that scientists and engineers at BARC strive relentlessly to achieve the vision of Dr. Bhabha. He stressed on the need to develop cutting edge technologies so that we remain in the forefront. He also highlighted the need to develop technologies which address the needs of the society. He impressed upon the need to develop safe nuclear reactors in which security concerns have to be addressed in the design stage itself. The keynote address was delivered by the Chief Guest Dr. Kirit Parikh, Chairman, Integrated Research and Action for Development & former Member, Planning Commission. Dr. Parikh outlined the ways to achieve an equitable level of human development in India, taking into

account, the concerns about global climate changes and shrinking reserves of conventional energy resources.

Shri R. S. Yadav, Associate Director, Reactor Projects Group and Secretary, Organizing Committee ADNUTECH-2010, proposed the vote of thanks. He thanked all speakers, industry sponsors and DAE units for extending their whole-hearted support in organizing the event.

Later, a technical exhibition showcasing various technologies developed as part of various programmes of DAE was inaugurated by Dr. S. K. Jain, CMD, Nuclear Power Corporation of India Limited. Various industries participated in the exhibition and showcased their products.

The Conference concluded with a discussion on the key topic “Challenges for implementing Nuclear Power Programme.” The panel chaired by Shri V. K. Mehra, Director RPG & ESG, BARC also included Dr. S. K. Jain, CMD NPCIL, Dr. A. K. Suri, Director MG, BARC, Shri S. C. Chetal, Director, REG, IGCAR, Shri S. K. Chande, Vice-chairman AERB, Shri G.P. Srivastava, Director, E & I Group, Shri M. V. Kotwal, Sr. Ex VP & Director, L & T Ltd. and Shri Kaustubh Shukla, COO, Godrej Precision Engg. Ltd. Discussions were centered around achieving installed capacity of 63 GW_e of nuclear power by 2030 and the contribution of nuclear power. Panelists felt that a judicious mix of imported light water reactors and indigenous PHWRs, would be necessary to achieve the target. Contributions to be made by designers, vendors, utilities, regulatory authority to achieve the target, were also emphasized.

DAE-BRNS Workshop on “High Resolution Gamma Ray Spectrometry (HRGS-2010)”: a report

A two-day DAE-BRNS Workshop on “High Resolution Gamma Ray Spectrometry using HPGe detectors (HRGS-2010)” was organized by the Radiochemistry Division, BARC, Mumbai, during October 7-8, 2010. Gamma-ray spectrometry plays an important role at every stage of nuclear fuel cycle and is used extensively to quantify fission and activation products during operation of nuclear reactors and other fuel cycle facilities, environmental radioactivity near the site of nuclear fuel cycle facilities and also in R&D work in Radiochemical laboratories. With the advent of commercially available high volume as well as high-resolution HPGe detectors, gamma-ray spectrometry plays an increasingly vital role in detection, identification and estimation of gamma emitting radionuclides, in the programme related

to Production and Application of radioisotopes. For quantitative estimation of radionuclides, it is necessary to calibrate the detector for absolute detection efficiency as a function of gamma ray energy in a standard source-to-detector geometry. With an objective to bring uniformity in gamma ray spectrometric measurements carried out at various laboratories of DAE as well as academic institutes, an intercomparison exercise for the measurement of gamma-ray emission rates of ^{133}Ba and ^{152}Eu sources using HPGe detectors was conducted in 2002, by the Radiochemistry Division, BARC and this was followed by a two-day Workshop during June 19-20, 2003. It provided an opportunity for the participants, to assess the relative accuracy achieved by their individual laboratories and scope for further improvement.



On the dais (L-R): Dr. V.K. Manchanda, Chairman, HRGS-2010 and Head, Radiochemistry Division, BARC
Mr. G. Nageswara Rao, Director (O), NPCIL and Dr. S. Kailas, Director, Physics Group, BARC

It was observed that during the last seven years there was significant growth in the number of laboratories in various units of DAE, engaged in gamma spectrometric analysis of a variety of samples. Radiochemistry Division receives large number of requests from various DAE laboratories from all over the country for lectures, training and supply of calibration standards sources. With the main objective to get acquainted with recent progress made in gamma ray spectrometry, gamma spectrometric analysis using advanced software, efficiency calibration and also to bring uniformity in gamma ray spectrometric measurements in various labs, the present two-day BRNS sponsored Workshop was organized at Computer Division Auditorium, BARC, Mumbai. There was an overwhelming response from various units of DAE including BARC. A total of 127 delegates participated from various units/divisions of NPCIL, ESL, Health Physics units, IRE, AMD, BRIT, RMC, AFFF, IGCAR and BARC.

The Workshop was inaugurated on 7th October 2010. Dr. V.K. Manchanda, Chairman, HRGS-2010 and Head, Radiochemistry Division, BARC delivered the welcome address and explained the relevance of this workshop. He also gave a brief account of contribution of Radiochemistry Division for the said purpose over the years. Dr. S. Kailas, Director, Physics Group, BARC gave inaugural address and highlighted the importance of gamma-ray spectrometry in various activities in DAE and applauded the efforts of the members of RCD for organizing HRGS-2010. Shri G. Nageswara Rao, Director (O), NPCIL was the Chief Guest and in his remarks, he emphasized the need for accurate determination of radionuclides in nuclear power programme for which knowledge in latest developments in gamma ray spectrometry and expertise are very essential, for the scientists working at NPCIL. Dr. Sarbjit Singh, Convener, HRGS-2010,

Radiochemistry Division, BARC proposed the vote of thanks.

The Workshop consisted of six lectures including demonstration of analysis of gamma-ray spectra. The resource personnel were: Dr. A. Goswami – Interaction of gamma-ray with matter, Dr. B.S. Tomar- Detectors for gamma ray spectrometry, Dr. Sarbjit Singh – High resolution gamma –ray spectrometry, Shri S. Venkiteswaran – Instrumentation for gamma-ray spectrometry, Dr. R. Acharya – Analysis of Gamma-ray spectra and Dr. K. Sudarshan – Demonstration of gamma-ray spectra analysis with PHAST software. Each lecture was followed by discussion, in which sufficient time was given for clarifications. Lecture notes were provided to all the participants. The lecture notes contain Standard Operation Procedures (SOP) for high resolution gamma ray spectrometry, determination of detector resolution, energy and efficiency calibration and relevant nuclear data on gamma-ray standard sources.

The feedback and valedictory session was held on 8th October 2010, in which Dr. V. Venugopal, Director RC&IG was the chief guest. Written as well as verbal feedback was taken from the participants. Dr. Venugopal gave his remarks on HRGS-2010 and appreciated the effort of RCD for conducting this two-day workshop. Dr. Venugopal also distributed the participation certificates to the delegates. Dr. V. K. Manchanda, Chairman, HRGS-2010, thanked Director, RC&I Group as Chairman, RTAC, BRNS for support, all the resource persons for excellent technical programme and delegates for very active participation. Dr. Sarbjit Singh, Convener, HRGS-2010 briefed about the experience of the workshop and future work in this regard.

Workshop on Protection against Sabotage and Vital Area Identification: a report

IAEA-India National Workshop on “**Protection against Sabotage and Vital Area Identification**” (VAI) was organized at Mumbai during October 4 – 8, 2010. This was the first National workshop organized in India with IAEA on “*Protection against Sabotage and Vital Area Identification*”. The workshop was held at CTCRS building, AERB complex, Anushaktinagar, Mumbai.

The workshop was inaugurated by Shri S K Chande, Vice Chairman, Atomic Energy Regulatory Board (AERB), India. The workshop was attended by 33 participants from different DAE organizations. Participants were carefully chosen to represent various types of nuclear facilities like nuclear power plant, back end and front end fuel cycle facilities and regulatory bodies etc. A total of 16 faculty members were involved for deliberations lectures and for conducting workgroup exercises. There were 4 expert faculty members

from abroad: 2 from Sandia National Laboratory (SNL), USA, one from Lithuania and one IAEA staff member. 12 faculty members from India were involved in lecture presentation and as workgroup instructors.

The workshop duration was 5 days which included 19 lectures and 7 workgroup exercises. Topics covered in the workshop were Vital Area Identification process, Protection against sabotage, Policy Consideration for VAI, VAI process including logic development, Management and organization of VAI process. Workshop material was printed in three different sets providing lecture presentation, text and subgroup exercises. A Workshop CD containing all the presentations was also prepared. Workshop kit containing three printed books, a CD and other necessary materials were distributed to all participants and faculties.

The workshop was concluded on 8th October afternoon after a feedback session from the participants. Certificates were distributed to all participants by Shri G. P. Srivastava, Course Director, Shri Jose Rodriguez, IAEA, Shri Bruce Vernado, Mr. Bruce Berry from SNL, USA and Dr. Georgij Krivoshein from Lithuania.



Group of participants at the Workshop

Valedictory Function of the Health Physics Training Course 15th Batch: a report

The Health, Safety and Environment Group concluded its regular one-year training course for science graduates. These graduates were recruited for operational radiation protection and associated functions of the nuclear fuel cycle facilities. The valedictory function of this course was held at the auditorium of Radiation Protection Training & Information Centre on November 08, 2010. Dr. S. Kailas, Director, Physics Group was the chief guest for the function. Dr. A. K. Ghosh, Director, Health, Safety & Environment Group, Dr. D. N. Sharma, Associate Director, HS&EG, Mr. R. Bhattacharya, Secretary, AERB, Dr. P. K. Sarkar, Head, Health Physics Division and Mr. R. G. Purohit, Head, ORPRS, HPD were also present on the dais. The invitees included course coordinators, faculty members and senior officers of Health, Safety & Environment Group.

Dr. P. K. Sarkar welcomed the chief guest, dignitaries, invitees and the faculty. He presented a brief outline of the training course which was started in 1989 with the specific objective of developing trained manpower in the specialized discipline of radiological safety required for the nuclear fuel cycle facilities, including nuclear power plants. He observed that, Health Physics being a specialized discipline, a combination of different branches of science and engineering, is not offered as a regular course by any of the universities in India.

He remarked that over the years, the Health Physics training programme has undergone significant changes with respect to the syllabus, structure of the training programme, training methodology, assessment procedures etc. The

changes were based on the feedback received from the faculty and the trainees and under the expert guidance of the apex committee and was essentially required, to bring up this training to meet the growing needs of our department and maintaining our training programmes with international standards.

He expressed happiness over the fact that presently the Health Physics training programme was acknowledged by other Divisions of BARC and that HPD had extended guidance and assistance to others when it became mandatory in BARC that all recruitments of technical staff shall be through formal training schemes only.

He noted that a large number of faculty and senior officers were associated with the training programme and that Health Physics Division had received whole-hearted cooperation from a number of Officers in arranging the practicals and the On-the-Job Training at different facilities. He attributed the success of the training programme to the combined efforts of all Divisions of HS&EG. He congratulated all the 35 trainees for their excellent performance and welcomed the youngsters.

Dr. D. N. Sharma, Associate Director, HS&EG while addressing the gathering, congratulated the trainees for their hard work which has resulted in their excellent performance in the course and enabled them to score additional increments in the Scientific Assistant grade at the time of absorption. He called upon them to continue their studies and to get actively involved with the ongoing programmes of the department. On this occasion, he recalled his continuing association with the training programme for the past few

years from the process of selection of the trainees to their final absorption interview.

In his presidential address, Dr. A. K. Ghosh, Director, HS&EG observed that the objective of the training programme was to give the candidates an in - depth awareness on the systems, procedures and technical aspects. It was also required to prepare them to adopt a scientific approach to the tasks assigned, to inculcate an analytical attitude in solving problems and to develop the required skills in their respective field of work. He appreciated the structure of the training programme and the syllabus, covering a wide variety of subjects including basic sciences, nuclear engineering and nuclear fuel cycle facilities.

He also expressed his happiness at the encouragement received from the Atomic Energy Regulatory Board for this training course

through the ‘AERB awards to the merit holders’ which is given to the 1st and 2nd rank holders of each batch.

In the valedictory address, the Chief Guest, Dr. S. Kailas, Director, Physics Group stressed on the importance of formal training to make oneself understand the concepts of nuclear and radiological safety aspects and also to have a clear awareness of the systems. He appreciated the efforts of Health Physics Division to impart professional training to the graduates in this specialized discipline and to make them competent to shoulder the responsibility of ensuring radiological safety in the nuclear facilities. He also congratulated the Health Physics Division for their efforts in building up a full-fledged infrastructure for carrying out the training programmes uninterruptedly for the last 20 years. The function concluded with a vote of thanks by Mr. R.G. Purohit, Head, ORPRS,HPD.



Chief guest, Dr. S. Kailas addressing the gathering. Seated from left to right are Dr. P. K. Sarkar, Head, Health Physics Division, Dr. A. K. Ghosh, Director, HS&EG, Shri R. Bhattacharya, Secretary, AERB, Dr. D. N. Sharma, Associate Director, HS&EG and Shri R. G. Purohit, Head, ORPRS, HPD

National Science Day Celebrations at BARC

It was on 28th February 1928, that the great Indian Physicist Sir C.V. Raman discovered the Raman Effect, while working in the laboratory of the Indian Association for the Cultivation of Science, Kolkata. He received the Nobel Prize in Physics in 1930, for his work on the scattering of light and for the discovery of the effect named after him. This day is of great importance for the Indian scientific community and is celebrated all over the country every year, as National Science Day.

The Scientific Information Resource Division took the initiative of celebrating the National Science Day at BARC. It was celebrated on 28th February, 2011, at the Central Complex auditorium. As part of the programme, the following events were organized.

1. Fusion Engineering Exhibition: The International Thermonuclear Experimental Reactor (ITER) is one of the most ambitious programmes which was launched in 1985, to develop Fusion energy as a viable energy alternative and to harness it for peaceful purposes. India became a member of this international collaborative activity in 2005. A number of R&D projects are currently being carried out in various Divisions of BARC as well as in other DAE units. The exhibition gave a flavour of all these global activities through posters, publications and audio-visual presentations.
2. Homi Bhabha Pavilion: The life and the work of Dr Homi Jehangir Bhabha was portrayed through a series of posters. It



Dr. Srikumar Banerjee, Chairman, AEC inaugurating the Fusion Engineering Exhibition

was a fitting tribute to this great visionary on this day, who pioneered the development of nuclear energy in India and laid a firm foundation.

3. **BARC Technologies: R&D spinoffs:** Over the years, BARC has developed a large number of technologies, some of which have even been transferred to various private firms for industrial production. All these technologies were showcased in the form of posters. BARC Scientists and Engineers who were involved in the development of these technologies, were present on the occasion, to interact and explain the significance of these technologies.

All the three exhibitions of one month duration were inaugurated by Dr. Srikumar Banerjee,

Chairman, Atomic Energy Commission. Dr. Banerjee showed keen interest in the exhibits. Dr. K. Bhanumurthy, Head, SIRD extended a warm welcome to all the invitees and colleagues. Dr. A.K. Suri, Director Materials Group, BARC, introduced the Chief Guest, Shri S.K. Sharma, Former Chairman, AERB. Dr. Banerjee gave an invited talk on “Order and Chaos”. On this occasion, a compilation of R&D publications of Dr. Srikumar Banerjee, both in the form of hard copy volumes as well as a CD, (compiled by SIRD) was released by the Chief Guest. Shri R.K. Singh, Head, MR&PAS, SIRD gave a vote of thanks.

Dr. R.K. Sinha, Director, BARC also visited these exhibitions on the 4th of March, 2011 and appreciated the effort. About 600 scientists and engineers have visited these exhibitions so far.



Dr. R.K. Sinha, Director, BARC at the Fusion Engineering Exhibition, Dr. A.K. Suri, Director, Materials Group and Dr. K. Bhanumurthy, Head, SIRD can be seen with him.

BARC Scientists Honoured

Name of the Scientists: Mr. N.K. Goel, Virendra Kumar, Y.K. Bhardwaj and S.Sabharwal
Radiation Technology Development Division, Radiochemistry and Isotope Group

Title of the paper : “Radiation synthesized stimuli-responsive HEMA-co-MAETC hydrogels”

Award : Best Poster presentation award

Presented at : 3rd Asia Pacific Symposium on Radiation Chemistry (APSRC-2010) and
 DAE BRNS 10th Biennial Trombay Symposium on Radiation and Photochemistry (TSRP-2010)” held at Lonavla during September 14-17, 2010

Name of the Scientist : Mr. S.K. Lalwani, Electronics Division

Award : “NDT Achievement Award-2010” for his outstanding contributions
 to “R&D in NDT”

Awarded by : **Indian Society for Non-destructive Testing (ISNT), Mumbai chapter**

Name of the Scientist : Ms. Shagufta Shaikh, Medical Division

Title of the paper : “Bull’s Multirule Algorithm, An Excellent means of Internal Quality Control for Hematology
 Analyzers”

Award : Best Paper Award 2nd prize

Presented at : AIIMT 20th Congress of Bio-Medical Laboratory Science held at Tiruchirappali,
 Tamil Nadu during Dec. 18-19, 2010

Name of the Scientist : Dr. B.N. Jagatap

Outstanding Scientist & Head, Atomic & Molecular Physics Division

Honour : Elected unanimously as the President, Physical Sciences Section of the 99th Session of
 Indian Science Congress

: 99th session of Indian Science Congress will be held at Bhubaneshwar during
 January 03-07, 2012, to be jointly organized by Kalinga Institute of Industrial Technology
 (KIIT) and National Institute of Science Education and Research (NISER).

Name of the Scientist : Dr. H.S. Misra, Head, Molecular Genetics Section, Molecular Biology Division

Award : “B. S. Sarma Memorial Award- 2010” for his outstanding contributions in Biological
 Chemistry and Allied Sciences

Awarded at : 79th annual meeting of the society held at Indian Institute of Science, Bangaluru. organized
 by the Society of Biological Chemists of India.



Alexandrian Laurel

Edited & Published by :
Dr. K. Bhanumurthy,
Head, Scientific Information Resource Division,
Bhabha Atomic Research Centre, Trombay, Mumbai 400 085, India.
Computer Graphics & Layout : N. Kanagaraj and B. S. Chavan, SIRD, BARC
BARC Newsletter is also available at URL: <http://www.barc.gov.in>